



Programme opérationnel Interreg IVA
France-Espagne-Andorre 2007 – 2013



SISPyr

Sistema de Información Sísmica del Pirineo
Système d'Information Sismique des Pyrénées
Sistema d'Informació Sísmica dels Pirineus

Feasibility of a Pyrenean earthquake early warning system based on the SISPyr network

Action 5



IGC
Institut Geològic
de Catalunya



Géosciences pour une Terre durable

brgm



GOBIERNO
DE ESPAÑA

MINISTERIO
DE FOMENTO

Instituto
Geográfico Nacional



UNIVERSITAT POLITÈCNICA
DE CATALUNYA

Main contributor: BRGM

2012-05-25

Authors: Samuel AUCLAIR (5), Yolanda COLOM (1), Jose-Antonio JARA (6), Xavier GOULA (1), Anne LEMOINE (5)

Keywords:

Early-warning, real-time seismology, Pyrenees, France, Spain, Andorra, SISPy

-
1. IGC, Institut Geològic de Catalunya
 2. OMP, Université Paul Sabatier, Observatoire Midi-Pyrénées
 3. UPC, Universitat Politècnica de Catalunya
 4. IGN, Instituto Geografico Nacional
 5. BRGM, Bureau de Recherches Géologiques et Minières
 6. GEOCAT

© 2012 SISPYR project

Synopsis

The massif of Pyrenees, who results from compressive movement between Iberic and Eurasian tectonic plates and who marks out the natural border between France and Spain, presents a moderate seismicity responsible of many destructive earthquakes over history, which maximum magnitude could probably reach 6.5. Thus, Pyrenees constitute one of the Spanish and French areas where the seismic hazard is the most important, what have led to the progressive development of seismological networks around the massif. In this context, the SISPy Interreg project has as principal objective to allow the pooling of Pyrenean seismological data and to improve the massif coverage by the networks favouring the progressive transition to real-time data transfer technologies. In order to make profit of advantages offered by real-time seismology, the SISPy project also aims to assess the feasibility of a Pyrenean earthquake early warning system (EWS).

In a first time, we focused on “technical” feasibility aspects. Then, the SISPy seismic network had been first examined in order to assess its adaptability to early warning purposes. In particular, redundancy issues, network coverage, data processing and time latency of the existing real-time system have been analyzed. The main conclusion of the previous analysis is that the existing network and system could be the base of an EWS implementation for Pyrenees. Then different rapid magnitude determination methodologies have been tested (so called τ_c , τ_p^{max} and P_d/P_v methods) in order 1) to check their adaptability to the Pyrenean context and 2) to establish empirical relationships usable in Pyrenees. To that end, a waveform catalog had first been constituted, gathering more than 2.400 records from 193 Pyrenean seismic events. The analysis of these records has allowed us to bringing to light clear correlations between earthquakes’ reference magnitudes and four waveforms indicators calculated from first seconds of the P wave on the vertical component.

In a second time, we considered the question of the opportunity to put in place EWS in Pyrenees. As to do that, an analysis of theoretical performances of the system had been performed: this exercise allowed us to establish approximate levels, for different types of earthquakes, of expected warning delays in the Pyrenees, thus providing a basis to underlie a reflection on how appropriate such a system may be in the zone. Furthermore, this simplified approach can guide definition of potential uses of Pyrenean early-warnings, since they are closely dependent to the time separating warning arrival to the one of destructive seismic-waves. Finally, we carried through a survey bound to French Pyrenean potential end-users in order to evaluate their wishes in terms of earthquake early warning.

Contents

1. Introduction	15
2. State of the art	17
2.1. Concerning the concept of onsite and regional early warning systems ..	17
2.2. EWSs worldwide.....	19
2.3. Methodologies for rapid assessment of earthquake strength – empirical relations.....	23
2.3.1. Frequency content.....	24
2.3.2. Signal amplitude.....	28
2.3.3. Other methodologies for assessing magnitude in real time	31
2.4. Application to early warning.....	32
2.4.1. Spatial and temporal integration of the data	32
2.4.2. Combined methods	34
2.4.3. Integration into a probabilistic approach.....	34
3. Preliminary analysis.....	37
3.1. Adaptability of the SISPy seismic network to early warning purposes...	37
3.1.1. EWS description from a technical point of view	37
3.1.2. SISPy network and systems description	41
3.1.3. Existing systems evaluation	53
3.1.4. Discussion	68
3.2. Spatial analysis of the network	69
3.2.1. Consequences of real-time network coverage on early warning	69
3.2.2. System latency and effective network coverage.....	71
3.3. Theoretical performance analysis.....	77
3.3.1. Earthquake early warning scenarios	78

3.3.2.	Exploration of theoretical performance at regional scale.....	86
3.4.	Discussion	87
4.	Catalogue of Pyrenean waveforms	91
4.1.	Data selection	91
4.2.	Reference magnitude	92
4.3.	Catalogue.....	93
4.4.	Data pre-processing	94
4.4.1.	Correction for instrument response	94
4.4.2.	Picking P-wave arrival times	95
4.4.3.	Spectral analysis: a common frequency domain	95
5.	Methodology for calculating parameters τ_c , τ_P^{max} , P_d and P_v	96
5.1.	Computing proxy parameters	96
5.1.1.	Iterative integration.....	96
5.1.2.	Calculating parameter τ_c	97
5.1.3.	Calculating parameter τ_p	97
5.1.4.	Calculating parameters P_d and P_v	99
5.2.	Selection of the traces to be used	100
5.2.1.	Discriminating between P and S waves	100
5.2.2.	Selection based on epicentral distance	101
5.2.3.	Selection based on signal noise.....	102
5.3.	Data filtering	104
5.3.1.	The number of poles	105
5.3.2.	Bandwidth & SNR threshold for calculating proxy parameters	107
5.3.3.	On the effectiveness of filtering	109
5.4.	A review of the parameters used to calculate proxies	110
6.	Reference relations	113

6.1.	Establishing reference relations.....	113
6.1.1.	The τ_c method	113
6.1.2.	The τ_p method	116
6.1.3.	Results for the P_d and P_v methods	118
6.2.	The influence of variations in the analysis time-length	126
6.3.	A comparison with previously established relations.....	131
7.	Towards extending the range of validity of the reference relations.....	135
7.1.	On using relations from other regions for Pyrenean earthquakes.....	135
8.	Application to the April 2010 earthquake	137
9.	Utility of a Pyrenean EWS	143
9.1.	Using seismic early warning	143
9.1.1.	Automatic actions	144
9.1.2.	Semi-automatic actions	144
9.1.3.	Population warning	145
9.2.	End-users survey.....	145
9.2.1.	Survey's objectives.....	146
9.2.2.	Targeted public.....	146
9.2.3.	Questionnaire	149
9.2.4.	Survey teaching aid.....	150
9.2.5.	Results of the survey.....	150
9.2.6.	Discussion.....	157
10.	Conclusion	161
11.	Acknowledgements.....	163
12.	Bibliography	165

List of Illustrations

Figure 1 – Classification of EWSs according to their design and how they are used.	19
Figure 2 – Seismic hazard map of the world showing the regions equipped with seismic early warning systems that are either operational (in blue) or in test stage (in green) (from Allen <i>et al.</i> , 2009).	19
Figure 3 – The observed correlation between coefficient τ_P^{max} and magnitude for different earthquakes, and comparison with rupture duration (Olson and Allen, 2005).	23
Figure 4 – An example of the correlation observed between the parameter τ_c and magnitude (Kanamori, 2005).	25
Figure 5 – Illustration of the relation between the P_d parameter and earthquake magnitude and hypocentral distance for California records (Wu and Zhao, 2006).	28
Figure 6 – Mean error observed on the real-time estimation of magnitude using τ_P^{max} for data from California and Japan (Allen, 2007).	32
Figure 7 – a. Impact of the number of stations being used and the length of the window of analysis on correlations between moment magnitude and characteristic period τ_c . b. Mean error on magnitude determination versus the number of stations considered and the length of the P wave that was analyzed (Sokolov <i>et al.</i> , 2009).	33
Figure 8 – Location of seismological stations considered for the EWS analysis according to owner organization and type. Also shown is the area covered by the SISPyR project.....	45
Figure 9 – SISPyR network and sub-networks.....	47
Figure 10 – SISPyR network communication schema for IGC.....	47
Figure 11 – DAS2 simplified chain schema	50
Figure 12 – Picking exemple	51
Figure 13 – Binder stacking stage exemple.....	52
Figure 14 – Data communication latency	57

Figure 15 – SISPyR sub-networks map	58
Figure 16 – Redundant path communication schema.....	59
Figure 17 – DAS2 simplified first phase schema	60
Figure 18 – Percentage of « noises » and number of stations.....	63
Figure 19 – Number of events, detected events and percentage of detection	64
Figure 20 – Mapping D_n (distance to the n^{th} closest real-time station) for two, three and four stations, and locations of the real-time stations affiliated with SISPyR.	71
Figure 21 – Different components of warning time.	72
Figure 22 – Mapping extension of the blind zone in function of the epicentre location with an EWS using a minimum of 1, 2, 3 or 4 stations (from up to down) for magnitude assessment. Are also represented the SISPyR seismic real-time network as well as epicentral locations of the main Pyrenean earthquakes ($M \geq 5$ for the period 580 – 2003 / Source: ISARD catalogue).	75
Figure 23 – Distribution of the epicentres of the main Pyrenean earthquakes ($M \geq 5$ for the period 580 – 2003 / Source: ISARD catalogue) versus extension of the blind zone (D_{bz}) and lead time (T_l).	77
Figure 24 – Location of epicentres of historical earthquakes considered in early warning scenarios. Are also represented the real-time SISPyR network as well as the area covered by the SISPyR project.	78
Figure 25 – Observed intensities and epicentre of the 2 nd of February of 1428 earthquake (from Olivera et al, 2006).	79
Figure 26 – Comparison between isoseist curves corresponding to the 02/02/1428 earthquake and blind-zone extensions of a virtual Pyrenean EWS based on the current real-time SISPyR network.	80
Figure 27 – Assessment of the lead times T_l at the outer limit of isoseist VI corresponding to the 02/02/1428 earthquake.	81
Figure 28 – Comparison between isoseist curves corresponding to the 21/06/1660 earthquake and blind-zone extensions of a virtual Pyrenean EWS based on the current real-time SISPyR network.	82
Figure 29 – Comparison between isoseist curves corresponding to the 19/11/1923 earthquake and blind-zone extensions of a virtual Pyrenean EWS based on the current real-time SISPyR network.	84

Figure 30 – Comparison between isoseist curves corresponding to the 13/08/1967 earthquake and blind-zone extensions of a virtual Pyrenean EWS based on the current real-time SISPyR network.....	85
Figure 31 – Theoretical performance at regional scale of a Pyrenean EWS confronting past seismicity to theoretical blind zones extension. Configurations for which 50% (left) and 80% (right) of historical epicentres lead to positive lead times (i.e. blind zones smaller than isoseist $I=VI$) are indicated thanks to green colour gradation, while negative values are indicated thanks to red colour gradation.....	86
Figure 32 – Hypothesis of an earthquake occurring below a station belonging to a triangular-mesh network.	88
Figure 33 – Hypothesis of an earthquake occurring at different positions inside a triangular-mesh network. Numbers indicated close to each “best-cases” epicentres’ locations are related to the minimum number of stations used by the EWS.....	89
Figure 34 – Theoretical performance at regional scale of a Pyrenean EWS lying on a 30 km triangular-mesh network, for different epicentre configurations corresponding to Figure 33.....	89
Figure 35 – The linear relation observed between M_{LDG} and M_{IGN}	93
Figure 36 – Distribution of the catalogue data versus epicentral distance and recording type.....	94
Figure 37 – Distribution of the catalogue data versus reference magnitude and recording type.....	94
Figure 38 – Calculation of the parameter τ_p according to whether X_0 and D_0 are set at zero or at one.	98
Figure 39 – Variation of the parameter τ_p^{max} versus the chosen initialization interval. Calculations performed on the traces in the catalogue that satisfy the selection criteria.....	99
Figure 40 – An example of an “automatic” pick of the S wave based on a calculation of the theoretical time difference between P- and S-wave arrivals.	101
Figure 41 – Distribution of τ_c with magnitude versus the minimum signal-noise ratio (SNR) minimal retained. Calculations carried out with $T_{analysis} = 3$ s and a maximum epicentral distance of 100 km.....	103
Figure 42 – Distribution of τ_p^{max} with magnitude versus the minimum signal-noise ratio (SNR) minimal retained. Calculations carried out with $T_{analysis} = 3$ s and a maximum epicentral distance of 100 km.....	103

Figure 43 – Distribution of $P_d^{10,LDG}$ with magnitude versus the minimum signal-noise ratio (SNR) minimal retained. Calculations carried out with $T_{analysis} = 3$ s and a maximum epicentral distance of 100 km.....	104
Figure 44 – Distribution de $P_v^{10,LDG}$ with magnitude versus the minimum signal-noise ratio (SNR) minimal retained. Calculations carried out with $T_{analysis} = 3$ s and a maximum epicentral distance of 100 km.....	104
Figure 45 – The frequency response of a Butterworth filter of order n varying from 1 to 4 (source: Wikipedia).	106
Figure 46 – Distribution of τ_c with magnitude versus the order chosen for Butterworth filter. Calculations performed on traces from the catalogue that satisfy the selection criteria.	106
Figure 47 – Parametric analysis of low-pass cut-off frequency and SNR threshold impacts on correlation quality between M_{LDG} magnitude and proxy parameters. In each illustration, SNR/frequency couple giving best results is shown in red.....	108
Figure 48 – The distribution of τ_c with magnitude versus instrument type. Calculations performed on traces from the catalogue that satisfy the selection criteria.	110
Figure 49 – Distribution of the seismic signals that satisfied the selection filters versus magnitude and epicentral distance corresponding to calculation of parameters P_d/P_v with a 2s P-wave analysis time length.	111
Figure 50 – Map of earthquakes included in the catalogue and of corresponding recording seismological stations.	112
Figure 51 – A comparison between parameter τ_c and local magnitude calculated by LDG (A) and IGN (B) for Pyrenean earthquakes. The grey dots represent values of the parameter τ_c calculated in each station (analysis interval set at 3 s), which are averaged by 0.1 magnitude intervals (black dots).....	114
Figure 52 – Empirical relations linking the parameter τ_c (mean per event) with local magnitude calculated by LDG (A) and IGN (B) for Pyrenean earthquakes. Calculations carried out on the traces of the catalogue that satisfy the selection criteria (analysis interval set at 3 s). The straight line obtained by linear regression is shown in black, while the grey dashed lines indicate the confidence interval at 95 % for a new observation.....	115
Figure 53 – A comparison between parameter τ_p^{max} and local magnitude calculated by LDG (A) and IGN (B) for Pyrenean earthquakes. The grey dots represent values of the parameter τ_p^{max} calculated in each station (analysis interval set at 3 s), which are averaged by 0.1 magnitude intervals (black dots).	117

Figure 54 – Empirical relations linking the parameter τ_p^{max} (mean per event) with local magnitude calculated by LDG (A) and IGN (B) for Pyrenean earthquakes. Calculations carried out on the traces of the catalogue that satisfy the selection criteria (analysis interval set at 3 s). The straight line obtained by linear regression is shown in black, while the grey dashed lines indicate the confidence interval at 95 % for a new observation. 118

Figure 55 – Relation between Pd parameter and earthquake magnitude (LDG magnitude on fig. A and IGN magnitude on fig. B) and epicentral distance for Pyrenean records. 120

Figure 56 – A comparison between parameter P_d^{10} and local magnitude calculated by LDG (A) and IGN (B) for Pyrenean earthquakes. The grey dots represent values of the parameter P_d^{10} calculated in each station (analysis interval set at 3 s), which are averaged by 0.1 magnitude intervals (black dots). 121

Figure 57 – Empirical relations linking the parameter P_d^{10} (mean per event) with local magnitude calculated by LDG (A) and IGN (B) for Pyrenean earthquakes. Calculations carried out on the traces of the catalogue that satisfy the selection criteria (analysis interval set at 3 s). The straight line obtained by linear regression is shown in black, while the grey dashed lines indicate the confidence interval at 95 % for a new observation. 122

Figure 58 – Relation between Pv parameter and earthquake magnitude (LDG magnitude on fig. A and IGN magnitude on fig. B) and epicentral distance for Pyrenean records. 123

Figure 59 – A comparison between parameter P_v^{10} and local magnitude calculated by LDG (A) and IGN (B) for Pyrenean earthquakes. The grey dots represent values of the parameter P_v^{10} calculated in each station (analysis interval set at 3 s), which are averaged by 0.1 magnitude intervals (black dots). 124

Figure 60 – Empirical relations linking the parameter P_v^{10} (mean per event) with local magnitude calculated by LDG (A) and IGN (B) for Pyrenean earthquakes. Calculations carried out on the traces of the catalogue that satisfy the selection criteria (analysis interval set at 3 s). The straight line obtained by linear regression is shown in black, while the grey dashed lines indicate the confidence interval at 95 % for a new observation. 125

Figure 61 – Comparison between observations and predictions of $M_{LDG,IGN}$, using both τ_c and $P_{d,10}$ proxy parameters (SNR=60, analysis time-length = 3s). Each dot is associated to a single earthquake. Grey dashed lines indicate the ± 0.5 magnitude prediction domain. 130

Figure 62 – A comparison between the empirical relation linking the parameter τ_c with the magnitude determined in the framework of this study (M_{IGN} – analysis

interval 3 s) with other relations published in the literature. Relations mentioned with an asterisk symbol are related to a local magnitude definition.....	132
Figure 63 – Comparison between τ_c estimations from Pyrenean data (this study) and worldwide data (Kanamori, 2005).	132
Figure 64 – A comparison between the empirical relation linking the parameter τ_p^{max} with the magnitude determined in the framework of this study (M_{LDG} converted into M_w using the relation in Drouet (2005) – analysis interval 3 s) with other relations published in the literature. Relations mentioned with an asterisk symbol are related to a local magnitude definition.	133
Figure 65 – A comparison between the empirical relation linking the parameter P_d^{10} with the magnitude determined in the framework of this study (M_{IGN} – analysis interval 2/4 s) with other relations published in the literature.	134
Figure 66 – Comparison between the results obtained for parameter τ_c from Pyrenean data with the relation established by Zollo <i>et al.</i> (2010) using worldwide data linking the parameter τ_c to magnitude. Grey dots indicated different results got for Pyrenean data making use of different filters, while red dots represents data from central Italy, which belong to the data set used by Zollo <i>et al.</i> (2010) to establish their correlation (see insert down-right).	136
Figure 67 – Seismic traces for the 1 April 2010 earthquake that satisfied the selection criteria and real-time evolution of the magnitude estimated by means of the different methods that have been examined versus the reference LDG magnitude (red line). The P-wave onset pick is marked by a red triangle.....	139
Figure 68 – Screen-shot of the online questionnaire (in French) in which lies the SISPYR EWS survey.....	150

List of Tables

Table 1 – Table summarizing the main EWSs either existing or under development.	21
Table 2 – Main empirical relations linking τ_c with magnitude reported in the literature.....	26

Table 3 – Main empirical relations linking τ_P^{max} with magnitude reported in the literature. *Standard deviation on magnitude.....	27
Table 4 – Main empirical relations linking P_d with magnitude or PGV reported in the literature.....	30
Table 5 – Empirical relations linking P_v with magnitude or PGV reported in the literature.....	31
Table 6 – Main references to articles using a combination of indicators to assess the “os” earthquake’s destructive potential, this latter referring to an “onsite” EWS that does not require magnitude estimation.....	34
Table 7 – SISPyR stations list (based on existing information at report elaboration time) *Approximate coordinates because station is not yet installed. (1) Before named AVIS.	44
Table 8 – SISpyr subnetworks.....	46
Table 9 – Data latency for some of the EWS SISPyR stations	48
Table 10 – Recommended stations requirements check table. * Estimated latency values	55
Table 11 – Events selected for analysis showing differences between manual and automatic results.	66
Table 12 – Comparison between extension of each isoseist curve with extension of blind-zone corresponding to a EWS based on 1, 2, 3 or 4 stations (dash parts): scenario corresponding to the 1428 earthquake.....	80
Table 13 – Comparison between extension of each isoseist curve with extension of blind-zone corresponding to a EWS based on 1, 2 or 3-4 stations (dash parts): scenario corresponding to the 1660 earthquake.....	82
Table 14 – Comparison between extension of each isoseist curve with extension of blind-zone corresponding to a EWS based on 1, 2 or 3-4 stations (dash parts): scenario corresponding to the 1923 earthquake.....	84
Table 15 – Comparison between extension of each isoseist curve with extension of blind-zone corresponding to a EWS based on 1, 2 or 3-4 stations (dash parts): scenario corresponding to the 1967 earthquake.....	85
Table 16 – Distribution of traces included in the Action 5 catalogue with respect to instrument type.	92

Table 17 – A comparison between automatic and manual picks for the earthquake time histories contained in the Pyrenean catalogue.....	95
Table 18 – The characteristics of the main acquisition instruments in the Pyrenean seismic monitoring network (instrumental response provided by the manufacturers).	96
Table 19 – Minimum epicentral distance versus the time interval between P- and S-wave onsets. Calculation carried out with the hypotheses given in Table 7.....	101
Table 20 – Table summarizing the different types of processing applied to the signals so as to calculate the different parameters.	110
Table 21 – Summary of the empirical relations obtained for each parameter that was studied and for different analysis intervals, with a local magnitude LDG.	127
Table 22 – Summary of the empirical relations obtained for each parameter that was studied and for different analysis intervals, with a local magnitude IGN.	128
Table 23 – Table summarizing the data used in establishing the correlations presented in Table 21 and Table 22, and the associated ranges of validity in magnitude.	129
Table 24 – List of the different recordings available for estimating the magnitude for the Bigorre earthquake on 1 April 2010.	137
Table 25 – List of earthquakes included in the study catalogue.....	176
Table 26 – Questions of the questionnaire in which lies the SISPyR EWS survey	180

Appendix

APPENDIX A Constitution of the waveform catalogue	169
APPENDIX B Questionnaire of the end-users survey.....	177
APPENDIX C Survey teaching aid: brochure.....	183

1. Introduction

In 1868, Cooper laid the groundwork for a new tool intended to provide San Francisco with an “early” warning for the imminent arrival of destructive waves generated by an earthquake occurring some 100 km from the city. The physical basis behind the system conceived by Cooper was simple: strong ground motion is the result of shear, or “S”, waves and of the ensuing surface waves, seismic waves propagating more slowly than electromagnetic waves.

A little over a century later, Cooper’s concept was called on to create earthquake early warning systems (EWS) which provide warning just seconds after an earthquake occurs.

Although the current state of knowledge does not yet allow earthquakes to be predicted on a time scale compatible with mankind’s contingencies, the EWS principle nevertheless offers a valuable alternative for limiting the exposure of elements at stake to seismic hazard. As to the public, and subject to appropriate information and preparedness, early warning is potentially a useful tool allowing protective measures to be adopted that can afford a significant reduction in loss of human life. From an organizational standpoint, automatic measures to ensure safety may also be set up that may limit damage in the event of strong ground motion, in addition to secondary accidents.

This innovative tool was made possible thanks to the modernization of seismic monitoring systems and the development of “real-time” seismology. It actually is possible, henceforth, to have access, just seconds after an event, to information notably concerning its strength, location and effects. These data are of primary importance for players in emergency management, for they may enable them to achieve very quickly an overall view of the damage situation and to implement appropriate response strategies.

2. State of the art

Prior to emitting an early warning consecutive to an earthquake, one must first be capable of assessing its destructive potential so as to ascertain whether the warning is warranted. However, because damage caused by an earthquake results not only from ground motion but also from the vulnerability of the stakes, it is hard to assess these in real time. Thus the operation consists most often in estimating the ground motions induced by the earthquake.

Over recent years, a great deal of work has been conducted in the framework of EWS in a variety of countries (Japan, Mexico, Taiwan, the United States, Italy, Switzerland, Turkey, Romania...). Thus, it has notably been established that the first seconds of seismic waves are seemingly able to provide information on the event's ultimate magnitude, and accordingly on its strength, and this holds true over a wide range of magnitudes. In practice, the data-processing stage must be as brief as possible. Also, this latter consists, for a limited number of stations, in restricting the size of the analysis window so that P waves are analyzed (and in some instances a portion of the S waves). P waves are considered to be "information carriers" and S waves as "energy carriers" (Kanamori, 2005). Many different methods have thus been developed which vary quite widely both in the parameters considered (dominant frequency during the first seconds of the P wave, P-wave amplitude, envelope parameters...) and in the spatial analysis conducted (use of a single station or rather of an array).

2.1. *Concerning the concept of onsite and regional early warning systems*

EWS are distinguished according to 1) their design and 2) their application. Regarding the design of early warning systems, these may be based either on the earthquake recordings obtained in a single station or on those from an array of stations. In this latter case, with stations lying between the seismic source and the area to be warned and analyzing the wavefront, we refer to "front-detection" systems.

If, on the contrary, we are looking not at how the EWS operates but at its intended use, two different categories can once again be distinguished: systems seeking to warn a limited area which can be assimilated to a point at the scale considered (designated here as "specific EWS"), and systems meant to warn wider areas, or a "region".

Most specific EWSs are based on an analysis from a single seismic station, while regional warning systems rely exclusively on the front-detection principle.

This said, the above breakdown is not necessarily a hard-and-fast rule, as with so-called “hybrid” systems, which operate like a single-station EWS when only one seismic station has detected the earthquake, but like classical regional systems when recordings from several stations are retrieved (Figure 1).

The last category of EWS, “front-detection”, applying to specific installations, are marginal, since they require a seismic array specifically dedicated to a given installation. This approach is resorted to only in the context of critical facilities sited in highly seismic zones (nuclear reactors, storage facilities for hydrocarbons...).

From the point of view of the methods called on in processing the data triggering the early warning, the so-called “single-station” approach, using the record from a single station, differs considerably from the “front-detection” approach, which integrates the signals from different stations. Hence, since “single-station” EWSs furnish only a very limited view, they are not expected to measure the strength of the earthquake, and only those effects expected at the station itself are generally assessed. Conversely, in order to issue a widespread warning, regional EWSs must estimate the appropriateness of the warning, not only at each of the stations that acquired an earthquake record but also over the entire target area. To do so, regional EWSs proceed initially to determine the event’s location and assess its magnitude and then to ascertain whether the warning is justified or not (a simple magnitude threshold, an estimate of epicentral intensity, the preparation of shake-maps. etc.).

Kanamori (2005) proposes a simplified classification containing only two types of EWS:

- “Regional”: EWS’s based on a dense array of seismic stations extending over a seismogenic zone;
- “Onsite”: EWSs based either on a single station or on a small-scale network deployed in the vicinity of the target site, which is far from the seismogenic zone.

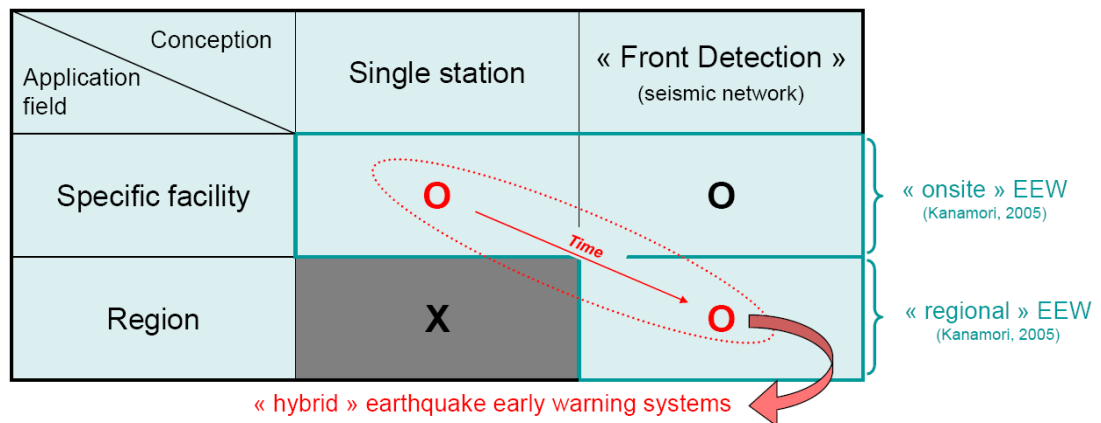


Figure 1 – Classification of EWSs according to their design and how they are used.

2.2. EWSs worldwide

In 2010, only five countries were equipped with operational EWSs effectively providing users with a warning. In addition to Japan and Mexico, which are exemplary in this field, the other countries included are Taiwan, Romania and Turkey.

While this number is still quite limited, many other early warning systems have been developed over recent years and currently have achieved the real-time test stage (cf. Figure 3), including two in Europe, Italy and Switzerland.

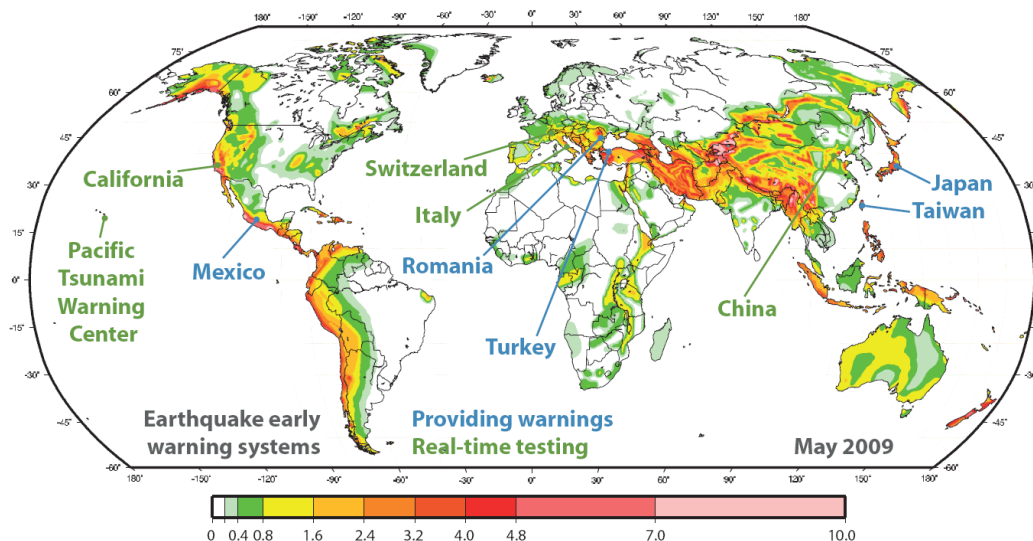


Figure 2 – Seismic hazard map of the world showing the regions equipped with seismic early warning systems that are either operational (in blue) or in test stage (in green) (from Allen *et al.*, 2009).

For further details on these systems, consult the recent article by Allen *et al.* published in 2009 in the volume of *Seismological Research Letters* devoted to EWSs, or to the report prepared at BRGM in 2008 (Auclair and Bertil, 2009).

A table summarizing EWSs either existing or under development in the world is presented in Table 1.

EEW type	EEW name		Area	Characteristic warning time (s)	Dsource/ target (km)	Network	Alert type	Main Réf.	Note	
Onsite Warning Systems	UrEDAS		Japan					Nakamura 1988		
	compact UrEDAS		Japan				Nakamura and Saita 2007b			
	FREQL		Japan				Nakamura and Saita 2007a			
Regional Warning Systems	Front Detection Systems	SASMEX	SAS	Mexico City (Mexico)	60	300/450	12 accelerometers along the coast of Guerrero	Public alert when $M \geq 6$ Restricted alert when $5 \leq M < 6$	Espinosa-Aranda et al. 1995/2009 Iglesias et al. 2007 Suárez et al. 2009	
			SASO	Oaxaca (Mexico)			36 seismic stations distributed across Oaxaca		Espinosa-Aranda et al. 2009	
		-		Bucharest (Romania)	20 / 25	160		Dedicated alert to nuclear plant	Böse et al. 2007 Ionescu et al. 2007	
		IERREWS		Istanbul (Turkey)	few seconds		10 seismic stations	Restricted alert (3 levels of warning)	Alcik et al. 2009 Erdik et al. 2003	Centralized EEW
		JMA EEW		Japan	few dizains of seconds		1000 seismic instruments	Public and restricted warning	www.jma.go.jp Horiuchi et al. 2005 Kamigaichi et al. 2009	
		ElarmS		California (USA)			600 seismic instruments (400 sites)	Members of the project	www.ElarmS.org Allen et al. 2009 Wurman et al 2007	
		Presto		southern Italy	15 to 30		28 stations (ISNet)		Weber et al. 2007	Probabilistic approach
		Virtual Seismologist		California (USA)			600 seismic instruments (400 sites)	Members of the project	Cua et Heaton 2007 Cua et al. 2009	Bayesian approach
		Virtual Seismologist*		Switzerland						
		PreSEIS*		California (USA) Istanbul (Turkey)				Böse et al. 2008 Köhler et al. 2009		
		SOSEWIN		Istanbul (Turkey)			20 seismic stations		Flemming et al. 2009	Decentralized EEW (analysis & alert)
		Taiwan EEW		Taiwan	20		102 accerometers	Restricted alert	Hsiao et al. 2009 Wu and Teng 2002	

* Not in use in real time

Table 1 – Table summarizing the main EWSs either existing or under development.

2.3. Methodologies for rapid assessment of earthquake strength – empirical relations

A great many methods have been developed to assess an earthquake's magnitude just a few seconds after the onset of rupture along the fault. In practice, these methods are based on empirical relations that link magnitude with various indicators calculated from the first seconds of seismic motion (cf. Figure 3): generally only the first few seconds of the P wave are analyzed, but increasingly often the S wave is called on in order to refine the early warning versus time.

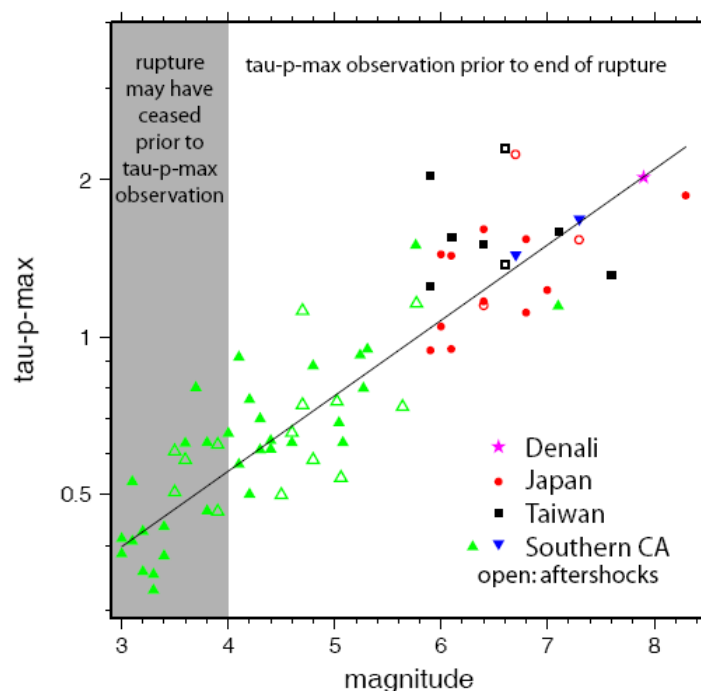


Figure 3 – The observed correlation between coefficient τ_P^{max} and magnitude for different earthquakes, and comparison with rupture duration (Olson and Allen, 2005).

Although empirically fairly robust, this principle for estimating magnitude before rupture has even terminated raises issues as to the deterministic nature of the rupture process, and consequently of magnitude. This issue has been subject to heated debate in the seismological community for quite a number of years and no-one has been able to bring forward a definitive answer. At least hypotheses have been able to be advanced in an attempt to explain the empirical correlations observed between magnitude and different indicators calculated from the first seconds of the seismic signal.

Thus, Zollo *et al.* (2006) explain that the fractures associated with the dynamics of high stress drops have a statistically increased probability of propagating over long distances and generating seismic ground motions with larger amplitudes, thereby justifying the use of amplitude parameters in the real-time determination of magnitude. In addition, small-magnitude earthquakes radiate higher-frequency energy than do larger earthquakes, which would thus enable the frequency content of the signal to be used to estimate magnitude.

Without being able to conclude as to the deterministic nature of earthquakes from a physical standpoint, we will subsequently concentrate on exploring the validity and the adaptability of this type of empirical relation to the Pyrenean context, which may make it possible to achieve protection against earthquake effects pragmatically. We will be listing hereinafter and describing succinctly the main methods that have been developed to date.

2.3.1. Frequency content

In assessing the strength of an earthquake, it is important to determine whether the rupture has ended or is still ongoing: this is generally “visible” from the frequency content of the first few seconds of the seismic signal. Seismic ground motions generated by earthquakes are typically richer in low frequencies when magnitude is greater. In view of this fact, methods endeavor to assess magnitude on the basis of frequency content.

Mean frequency: the τ_c method

One of the methods most commonly called on in the framework of EWS is τ_c . It is based on a calculation of the mean frequency f^m . Because the method is being used in real time, f^m is generally estimated in the time domain as the quotient between the amplitudes of the seismic signal, based on the Parseval theorem which establishes that the power of a signal $s(t)$ is the same whether the computation is carried out in the time or the frequency domain:

$$\int_{-\infty}^{\infty} s^2(t).dt = \int_{-\infty}^{\infty} |S(f)|^2.df \quad \text{Equation 1}$$

Thus, the dominant frequency f_p can be calculated as follows:

$$f^m = \sqrt{\frac{\int_0^{\infty} f^2 |U(f)|^2 df}{\int_0^{\infty} |U(f)|^2 df}} = \frac{1}{2\pi} \sqrt{\frac{\int_0^{\infty} \dot{u}^2(t).dt}{\int_0^{\infty} u^2(t).dt}} \quad \text{Equation 2}$$

where $U(f)$ is the Fourier transform of the seismic displacement $u(t)$ (vertical component).

Kanamori (2005) starts with the concept proposed by Nakamura in 1988 and modifies this relation by considering only a finite integration period τ_0 (generally $\tau_0 = 3$ s):

$$f_{Kanamori}^m = \frac{1}{\tau_c} = \frac{1}{2\pi} \sqrt{\frac{\int_0^{\tau_0} \dot{u}^2(t).dt}{\int_0^{\tau_0} u^2(t).dt}} \quad \text{Equation 3}$$

The parameter τ_c , calculated on the vertical component, represents the mean period of the initial portion of the P wave: it approximates the P wave pulse width. Its decimal logarithm generally seems to correlate linearly with the earthquake's magnitude.

With an analysis of 3 seconds of the P wave, this method yields good results up to a magnitude of 7.0, above which it appears to saturate (cf. Figure 4). When this analysis duration is shortened, saturation is observed at smaller magnitudes.

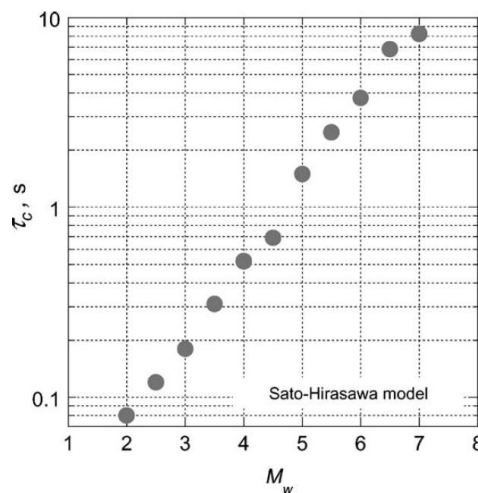


Figure 4 – An example of the correlation observed between the parameter τ_c and magnitude (Kanamori, 2005).

This methodology is used or has been tested in many EWSs that integrate it into the magnitude estimation process in different ways (cf. paragraph 3.4). The main relations that have been established are shown in Table 2, below.

Author	Instrument Type	D _{epi}	Region	M	Relation	Standard Deviation
Hsiao <i>et al.</i> (2009)	Acc.	< 40 km	Taiwan	4 - 7.3	Log(τ_c)=0.47xM _L -2.37	0.25
Shieh <i>et al.</i> (2008)	Acc.	< 70 km	Japan	6.0 - 8.3	$\tau_c=1.56 \times M_w - 7.76$	0.56
Sokolov <i>et al.</i> (2009)	Acc.	-	Japan, Taiwan	4.4 - 7.4	Log(τ_c)=0.293xM _w -1.644	0.15
Wu <i>et al.</i> (2007)	Acc. / BB	< 30 km	California	4.0 - 7.3	Log(τ_c)=0.237xM-1.462	0.09
Wu et Kanamori (2005a)	Acc.	< 21 km	Taiwan	5.1 - 7.6	Log(τ_c)=0.221xM _w -1.113	0.08
Wu et Kanamori (2008a)	Acc.	-	Monde (California, Japon, Taiwan)	4.1 - 8.3	Log(τ_c)=0.296xM _w -1.462	0.12
Wu et Kanamori (2008b)	Acc.	< 30 km	Japon	6.0 - 8.3	$\tau_c=1.68 \times M_w - 9.08$	0.52
Zollo <i>et al.</i> (2010)	Acc.	<60 km	World (Italy, Japan, Taiwan)	4.1 - 8.3	Log(τ_c)=0.21xM _w -1.19	0.25

Table 2 – Main empirical relations linking τ_c with magnitude reported in the literature.

Dominant frequency: the τ_P^{max} method

The τ_P^{max} method was introduced by Allen and Kanamori in 2003, reusing the concept proposed by Nakamura (1988). Like the parameter τ_c , τ_P^{max} seeks to characterize the signal's frequency content, but by using quite a different approach. Thus, while τ_c is calculated over a given time window (generally 3 seconds) and yields a mean frequency, τ_P is calculated in a continuous and recursive manner, making τ_P^{max} a parameter linked with dominant frequency.

Nakamura's original idea (1988) is to assess the dominant period τ_P recursively on the vertical component:

$$\tau_{P,i} = 2\pi \sqrt{\frac{\dot{U}_i}{\ddot{U}_i}} = 2\pi \sqrt{\frac{\alpha \dot{U}_{i-1} + \dot{u}_i^2}{\alpha \ddot{U}_{i-1} + \ddot{u}_i^2}} \quad \text{Equation 4}$$

where \dot{u}_i and \ddot{u}_i are ground velocity and acceleration and \dot{U}_i and \ddot{U}_i are ground velocity and acceleration smoothed by the quadratic mean. α is a smoothing constant ranging between 0.95 and 0.99 ($\alpha = 1 - dt$, dt being the signal's sample time step).

In practice, the maximum τ_P^{max} of the dominant period τ_P over the analysis window considered is retained, which is linked to the earthquake magnitude by means of an empirical log-linear relation.

In view of the fact that the high-frequency content of small-magnitude earthquakes is measured over a shorter time window, their magnitude can be assessed sooner than for strong events. In other words, a magnitude estimated using the τ_P parameter from one second of signal constitutes a lower limit. This estimation can be raised when the analysis is conducted over a longer time interval.

This methodology is called on or has been tested in many EWSs that integrate different approaches to the magnitude estimation process (cf. paragraph 3.4). The main relations that have been obtained are listed in Table 3.

In California, for example, this parameter was tested for the ElarmS system by Allen and Kanamori (2003), who established two separate relations according to the strength of the system: a relation allowing a “low” magnitude, noted m_l , to be estimated for “small” earthquakes ($M \leq 4.5$), and another, noted m_h , for stronger ones enabling a “high” magnitude to be estimated. Because the earthquake’s magnitude is not known initially, the system computes $m_l (\tau_{P,1s}^{max})$ one second after the event has been detected by the system (this value is updated one second later by calculating $m_l (\tau_{P,2s}^{max})$). If the value obtained for m_l exceeds 4.0, the system calculates m_h , retaining as final magnitude the mean between m_l and m_h .

Author	Instrument Type	D _{epi}	Region	M	Relation	Standard Deviation
Allen et Kanamori (2003)	BB	< 100 km	California	3.0 - 5.0	$m_{low}=6,3 \times \text{Log}(\tau_P^{max})+7,1$	0.30*
				5.0 - 7.3	$m_{high}=7,0 \times \text{Log}(\tau_P^{max})+5,9$	0.67*
Hsiao <i>et al.</i> (2009)	Acc	< 40 km	Taiwan	4.0 - 7.3	$\text{Log}(\tau_P^{max})=0,24Ml-1,51$	0.23
Olivieri et al (2008)	BB	< 100 km	Italy	2.5 - 6.0	$Ml=3.05 \times \text{Log}(\tau_P^{max})+4.3$	0.4*
Olson et Allen (2005)	Acc./BB	-	World (California, Japan, Taiwan, Alaska)	3.0 - 8.3	$\text{Log}(\tau_P^{max})=0.14 \times M-0.83$	0.54*
Shieh <i>et al.</i> (2008)	Acc	< 70 km	Japan	6.0 - 8.3	$\tau_P^{max}=0,45Mw-2.12$	0.18
Wurman <i>et al.</i> (2007)	Acc./BB	-	California	3.0 - 7.1	$M=5.22+6.66 \times \text{Log}(\tau_P^{max})$	-

Table 3 – Main empirical relations linking τ_P^{max} with magnitude reported in the literature.
*Standard deviation on magnitude.

Importantly, it should be noted here that unlike parameter τ_C , parameter τ_P^{max} is strongly influenced by the noise prior to the signal onset.

Wavelet analysis

Proceeding from the same principal as that underlain by the τ_c and τ_P^{max} methods, the wavelet method is based on a different means of calculation of the signal's dominant frequency purporting to be more stable and robust. Proposed by Simons *et al.* in 2006, this consists in working in the time as opposed to the frequency domain using a wavelet analysis.

Although promising, this method has yet to be tested on any EWS.

2.3.2. Signal amplitude

The maximum magnitude of the signal is likewise a good indicator of the force released by an earthquake (Figure 5) provided a distance parameter is factored in.

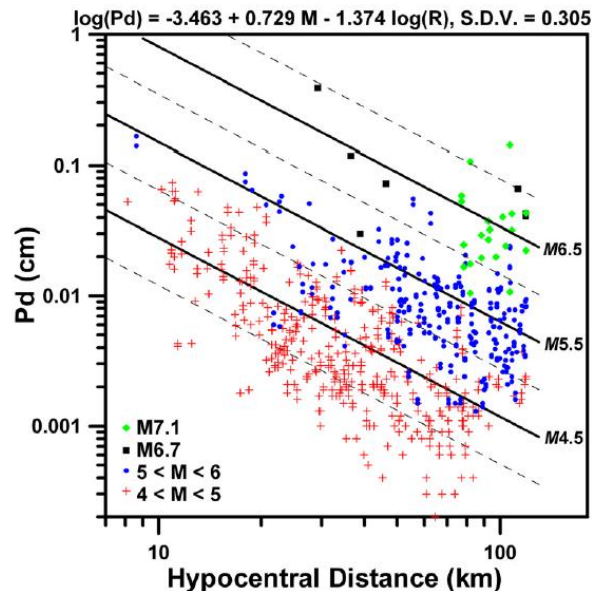


Figure 5 – Illustration of the relation between the P_d parameter and earthquake magnitude and hypocentral distance for California records (Wu and Zhao, 2006).

In practice, experience shows that the maximum amplitude of the first few seconds of the P wave (and of the S^1 wave) displays a relatively good correlation with the maximum amplitude of the signal as a whole:

¹ Although the EWS field generally considers an analysis of the P wave alone, some authors propose using, in the near field, an analysis of S waves. Although longer, this type of analysis may allow the uncertainties associated with magnitude significantly reduced. In the case of this study, and view of the

$$P_p \propto PGV$$

Equation 5

where p is the parameter being considered (displacement d or velocity v) and P_p the peak value of parameter during the first seconds of the P wave (typically 3 or 4 seconds).

In the context of onsite EWSs, there is theoretically no need to include in the warning process a magnitude calculation stage for the event, for the effects of the earthquake expected at the station (or in its immediate vicinity) are being considered. In this case, on the basis of a rapid assessment of PGV conducted using a relation similar to Equation 1, it is possible to determine threshold values that justify a warning, corresponding to different levels of intensity.

When a regional as opposed to an onsite EWS is being considered, however, it does become necessary to assign a magnitude to the event. The famous attenuation relations (Ground-Motion Prediction Equations – GMPE) that notably link PGD with the earthquake's magnitude M at a distance R between the observation point and the fault generally taking the form:

$$\log (PGV) = \log a + f_1(M) + \log [f_2(R)]$$

Equation 6

Thus Equation 5 and Equation 6 can be combined so as to estimate magnitude from P_p rather than from PGD:

$$\log (P_p) = \log b + g_1(M) + \log [g_2(R)]$$

Equation 7

Generally a linear formulation is retained for Equation 7, which then can be written:

$$\log (P_p) = A + B \times M + c \times \log (R)$$

Equation 8

In this case, the distance R is obtained from the real-time epicentral location procedure used by the EWS. It should be noted, however, that some authors have also proposed relations that are independent of distance for unusual contexts having very dense networks of stations distributed in a geographically homogeneous manner (notably in Taiwan – cf. Hsiao *et al.*, 2009).

To dispense with the dependency on distance R , some authors have scaled their data to reduce them to a reference distance, dr (Zollo *et al.*, 2006; Lancieri and Zollo, 2008):

$$\log (P_p^{dr}) = A' + B' \times M$$

Equation 9

where:

need to reduce as much as possible the time required for the warning to be issued in the context of the Pyrenees (cf. chapter 4), we will be concentrating on methods based on an analysis of P waves alone.

$$\log(P_p^{dr}) = \log(P_p) - C \cdot \log(R/dr)$$

Equation 10

i. The P_d Method

	Author	Instru- ment Type	D _{epi}	Region	M	Relation	Standard Deviation
Magnitude	Hsiao <i>et al.</i> (2009)	Acc.	<40 km	Taiwan	5.5 - 7.3	$\log(P_d)=1.62 \times M_l - 12.36$	0.80
	Hsiao <i>et al.</i> (2010)	Acc./BB	<20 km	Taiwan	4.5 - 7.3	$\log(P_d)=0.455 \times M_l - 1.28 \times \log(R) - 1.777$	0.36
	Wu and Zhao (2006)	Acc./BB	<120 km	California	4.0 - 6.7	$\log(P_d)=-3.463+0.729 \times M - 1.374 \times \log(R)$	0.31
	Wurman <i>et al.</i> (2007)	BB	-	California	3 - 7.1	$M=1.04 \times \log(P_d)+1.27 \times \log(R)+5.16$	-
	Zollo <i>et al.</i> (2006)	Acc.	<50 km	Europe	4.0 - 7.4	$\log(P_d)=-5.97+0.81 \times M_w - 1.05 \times \log(R)$	0.60
						$\log(P_d,10)=-6.31+0.7 \times M_w$	0.22
	Zollo <i>et al.</i> (2007)	Acc.	<60 km	Japan	4.0 - 7.1	$\log(P_d-2s,10)=0.7498 \times M_{JMA} - 6.929$	-
						$\log(P_d-4s,10)=0.7024 \times M_{JMA} - 6.646$	-
	Lancieri and Zollo (2008)	Acc.	<60 km	Japan	4.0 - 7.1	$\log(P_d-2s,10)=-6.93+0.75 \times M_{JMA}$	0.32
						$\log(P_d-4s,10)=-6.46+0.7 \times M_{JMA}$	0.40
PGV	Wu <i>et al.</i> (2007)	Acc. / BB	<30 km	California	4.0 - 7.3	$\log(PGV)=0.903 \times \log(P_d)+1.609$	0.31
	Wu and Kanamori (2005 b)	Acc.	<30 km	Taiwan	5.1 - 7.6	$\log(PGV)=1.260 \times \log(P_a)-1.288$	0.29
	Wu and Kanamori (2008 a)	Acc.	<30 km	World (California, Japan, Taiwan)	4.1 - 8.3	$\log(PGV)=0.920 \times \log(P_d)+1.642$	0.33
	Zollo <i>et al.</i> (2010)	Acc.	<60 km	World (Italy, Japan, Taiwan)	4.1 - 8.3	$\log(PGV)=0.73 \times \log(P_d)+1.30$	0.41

Table 4 – Main empirical relations linking P_d with magnitude or PGV reported in the literature.

The method most commonly called upon is based on the maximum value of displacement, P_d , observed over a 3-second interval following the detection of the P wave. This methodology is implemented on a large number of EWSs, often in conjunction with the frequency-based approaches, τ_c and τ_P^{max} . The main relations that have been established are given in Table 4, below.

The P_v method

Because the calculation of P_d from accelerograms entails a double numerical integration which gives rise to low-frequency drift, Wurman *et al.* (2007) have demonstrated for these signals a better correlation of magnitude with P_v .

	Author	Instrument Type	D _{epi}	Region	M	Relation	Standard Deviation
M	Wurman <i>et al.</i> (2007)	Acc.	-	California	3 - 7.1	$M=1.37 \times \text{Log}(P_v) + 1.57 \times \text{Log}(R) + 4.25$	-
						$M=1.63 \times \text{Log}(P_v) + 1.65 \times \text{Log}(R) + 4.4$	-
PGV	Wu and Kanamori (2005 b)	Acc.	< 30 km	Taiwan	5.1 - 7.6	$\text{Log}(\text{PGV}) = 1.066 \times \text{Log}(P_v) + 0.681$	0.18

Table 5 – Empirical relations linking P_v with magnitude or PGV reported in the literature.

2.3.3. Other methodologies for assessing magnitude in real time

There are other methods for estimating magnitude that are used by different warning systems. The chapter below briefly describes these approaches, which will not be subsequently tested insofar as they appear poorly suited to the Pyrenean context (processing time too long, array not dense enough, insufficient data to calibrate the models, etc.).

CAV (Cumulative Absolute Velocity)

CAV (Cumulative Absolute Velocity) was introduced for the purpose of being a pertinent ground motion parameter for predicting the destructive potential of an earthquake. To a certain extent, CAV is therefore a function of earthquake magnitude and accordingly can be used to assess it in a first analysis. This method is applied notably in the Turkish PreSeis system in the context of a “neuronal” approach (Böse *et al.*, 2008).

The signal envelope

The envelope of the signal in acceleration can be represented by an exponential function having the form $Bt \cdot \exp(-At)$, where A and B are constants (B representing the slope of the first three seconds of the P wave in acceleration on the vertical component).

In their analysis of Japanese earthquakes over a magnitude range of $3.9 < M < 7.3$ recorded by the KNet network between 1997 and 2001, Odaka *et al.* (2003) thus found a good correlation between the slope coefficient B and earthquake magnitude.

The simulated Wood-Anderson method

The *simulated Wood-Anderson method* (Wu and Teng, 2002) consists in simulating Wood-Anderson-type signals coherent with the first ten seconds of the signals available on the first stations so as to compute magnitude in the classical way from these synthetic signals.

2.4. Application to early warning

2.4.1. Spatial and temporal integration of the data

In practice, comparisons between magnitude and the various indicators of seismic motion calculated on the P wave generally display considerable scatter when these indicators are considered in each station individually, and the linear correlation only appears clearly once the indicators have been averaged for each event over several stations. Thus, Lockman and Allen (2007) suggested that magnitude estimated from τ_c becomes stable starting with a mean computed on four stations (Figure 6), whereas Böse *et al.* (2009) consider three stations as satisfactory for their method based on a combination of τ_c and P_d . This said, magnitude estimations can be performed from fewer stations, but with less reliability.

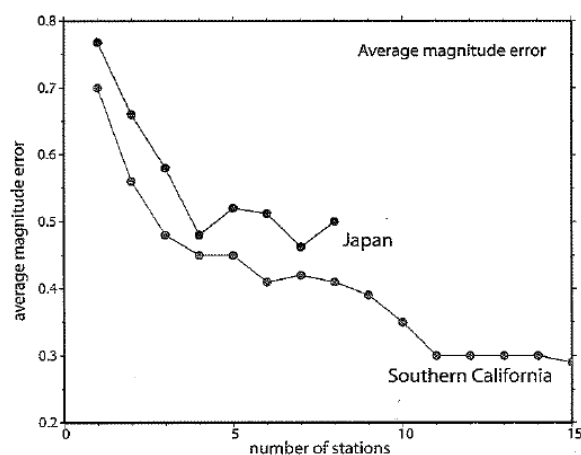


Figure 6 – Mean error observed on the real-time estimation of magnitude using τ_P^{max} for data from California and Japan (Allen, 2007).

There is furthermore the issue of the size of the time window to be taken into account in the data analysis. Generally speaking, the error on estimated magnitude does decrease as a greater portion of the signal is analyzed.

Sokolov *et al.* (2009)² have demonstrated the combined impact of the number of stations used and the length of the window taken into consideration on the relationship τ_c/M . It is notably seen from this study that the influence of long periods tends to decrease when the number of stations is increased and that far-field data are taken into account and/or the analysis window is increased (cf. Figure 7a). Moreover, it also appears that for deep-focus earthquakes, the number of stations considered has a greater impact on magnitude determination than the analysis length, proving that the spatial variability of the frequency content linked notably with site effects predominates over uncertainties associated with the fact that the calculation is not based on the entire signal. As a whole, this study confirms that the reliability of the magnitude estimated (from the characteristic period) increases when the time interval analyzed increases and a large number of records are considered (cf. Figure 7b).

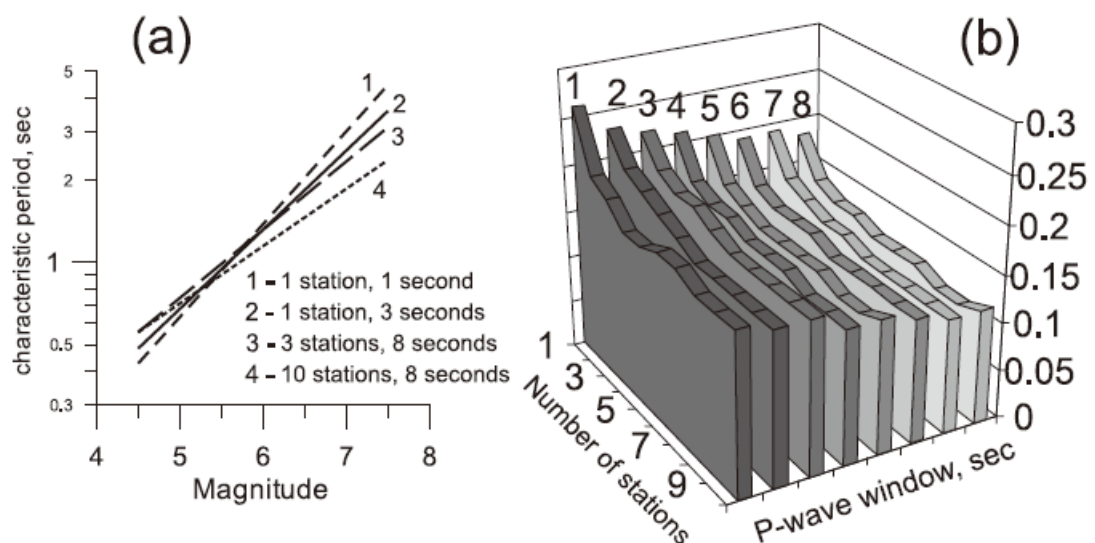


Figure 7 – a. Impact of the number of stations being used and the length of the window of analysis on correlations between moment magnitude and characteristic period τ_c . b. Mean error on magnitude determination versus the number of stations considered and the length of the P wave that was analyzed (Sokolov *et al.*, 2009).

² It should be noted that Sokolov *et al.* (2009) also present in their article an analysis of the inverse problem that aims to estimate magnitude from a random variable representing characteristic period.

2.4.2. Combined methods

Although the correlations observed between earthquake magnitude and the various seismic ground motion indicators computed from the P wave are generally clear-cut, they nevertheless do display scatter which may be a source of error for the estimated magnitude. Furthermore, these empirical correlations are primarily valid from a statistical standpoint, and accordingly their use for a specific event may result in an estimated magnitude that differs significantly from the reference magnitude. With a view to limiting this uncertainty, many authors prone the use of more than one independent indicator used in conjunction (usually two). The main bibliographical references concerning these combined methods are listed in Table 6.

In particular, certain authors consider that the parameters in terms of amplitude ($P_{d/v}$) and period (τ_c and τ_p^{max}) are complimentary, insofar as the former can be biased by signal saturation in the near field for large earthquakes (unlike τ_c and τ_p^{max}), while the latter are more susceptible to noise at small magnitudes.

	$P_{d/v}$	τ_p^{max}
$P_{d/v}$		Wurman <i>et al.</i> (2007) Wu et Kanamori (2005 a) Kamigaichi (2004)
τ_c	Böse <i>et al.</i> (2009 b) ^{os} Wu <i>et al.</i> (2007) Wu and Kanamori (2008 a, b) Zollo <i>et al.</i> (2010)	Hsiao <i>et al.</i> (2009) Shieh <i>et al.</i> (2008)

Table 6 – Main references to articles using a combination of indicators to assess the “os” earthquake’s destructive potential, this latter referring to an “onsite” EWS that does not require magnitude estimation.

2.4.3. Integration into a probabilistic approach

The early warning concept is intimately tied to the notion of system reliability, and accordingly to that of the acceptability of false alarms or of warnings that should have been issued but were not. It is therefore important to integrate into the early warning procedure an uncertainty associated with the values that have been estimated (magnitude, location, ground motion etc.).

To do so, a probabilistic integration of the empirical relationships presented earlier is frequently called on. This approach consists in assigning a probability density (pdf) to each parameter being sought by means of the Bayes’ theorem.

Such an approach (represented notably by the *Virtual-Seismologist* – Cua, 2005; Cua and Heaton, 2007 – and *RTMag* – Weber *et al.*, 2007 methodologies), which allows *a priori* information such as the *b*-value of the Gutenberg-Richter law to be taken into account, represents a powerful tool in the automatic decision process behind issuing the warning.

3. Preliminary analysis

3.1. *Adaptability of the SISPyR seismic network to early warning purposes*³

3.1.1. EWS description from a technical point of view

A EWS can technically be divided into 4 main parts: stations, communication system, data processing system and alert system; and we will see that all parts will share two basic requirements: high reliability and low delay time (latency).

In particular, as will be shown in this section, delay since the event occurs until the alert is generated at Data Centers will give us a “blind” zone around the epicenter. These “blind” zones around epicenters and their relation with possible targets will give us an idea about the viability of applying a EWS to the selected region using selected methodology.

i. **Stations**

Seismic stations will be the start point of any EWS. There is where the ground motion is measured and recorded.

A generic seismic station consists of 4 basic elements: seismic sensor, data acquisition systems (digitizer/datalogger), communication equipments and power supply system. Just as any alert system, all these elements and the relationship between them must be specially rugged and redounded.

So, to consider that a seismic station can be integrated into a EWS it should accomplish the following conditions:

✓ **Seismic sensor:**

- Should be adequate for the kind of seismic signal to register and measure in terms of bandwidth and dynamic range;
- It should be rugged and protected against ambient conditions;
- It must be properly installed to guarantee its data quality, reliability and availability.

³ From the GEOCAT short note : « *SISpyr Seismic Network applicability as a EWSS* »

✓ **Data acquisition system:**

- It should be adequate for the kind of seismic signal to acquire and register in terms of bandwidth, sample rate, dynamic range, resolution and local archiving.

✓ **Communication equipments:**

Communication system will be a key point of station usage for a EWS. Selected communication system will determine communication equipments to install at any station.

In any case, these equipments should be:

- Rugged to support remote site climatic conditions.
- Adequate for data transmission requirements in terms of latency, bandwidth, SLA and reliability.
- Some redundancy should be strongly recommended using a secondary communication system.

✓ **Power supply system:**

A good power supply system is basic for a correct station operation and data quality. Problems with station power supply will affect all station equipments and systems.

So, special care should be taken when planning, designing, installing and maintaining stations power supply systems. Also an adequate remote control and state-of-health monitoring added to preventive maintenance actions will avoid station failures and data quality degradation.

It is essential that stations power supply systems have some type of mains power failure backup system, like some UPS or similar. Maximum operating time of backup system should be dimensioned according with two parameters: needed time to improve mains power issue and stations redundancy (stations density).

As for any alert system, reliability, quality and service availability are critical parameters that should be considered. In case of stations, these parameters should be achieved thanks to the use of adequate equipments, building rugged installations and carrying out good preventive and corrective stations maintenance.

In spite of everything, unforeseen events require that stations have some redundant (backup) equipments (communication systems, power supply systems) and also an adequate network planning and stations distribution. Considering some station coverage “overlapping” will be helpful.

ii. Communication systems

Data communication between remote seismic stations and data processing centers will be properly designed and implemented to guarantee low data latency, high data reliability and high system availability.

Also, communication system’s bandwidth should be enough to transmit continuous streaming of seismic and state-of-health data from stations to Data Centers, in real time.

The use of a backup communication system also is recommended to avoid lost data in case of main system failure. Other redundancy mechanisms such as the existence of more than one Data Center receiving streaming data, subnetting structures implementation with redundant data paths, assuming that an intermediate node could be out of service by any reason (by unexpected failure or maintenance tasks), without QoS (Quality of Service) degradation. So, data communication systems will have three key points that will be considered:

- Data latency;
- Data reliability;
- System availability.

Also, the use of a satellite communication system as the main or secondary system is recommended to avoid the dependency with terrestrial communication infrastructures at regions where potentially damages can occur.

iii. Data processing systems

Once data arrive to Data Centers, data processing systems are in charge of analyzing continuous input data streams in real-time for event detection, location and compute different event related parameters.

For a EWS, at least three functional modules are needed: event detection module, event location module and earthquake’s “destructive power” estimation module (such as magnitude and/or peak ground motion, intensity, etc.).

These modules will be part of a complex system which can compute and analyze other event characteristics; but will be these four which will build the EWS processing chain. Different algorithms and programs can be used for EWS data processing chain implementation; but all of them must guarantee:

- High data quality;
- High reliability;
- Short processing time.

So, below each module of the processing chain will be described:

✓ **Event detection:**

Event detection will be the first module of the processing chain. This module will process any configured input data channel applying some algorithm in order to detect any occurred seismic event.

The selection of event detection module will be based on Data Center existing systems and it will be tuned to detect events according to desired parameters (region, magnitude, etc.).

In any case, a reliable selected module and the shortest processing time are desired.

✓ **Event location:**

Once the event is detected, in order to estimate the potential damages, “where and when it has occurred” will be needed to know. So, this second module will locate the event giving the coordinates of its hypocenter and origin time.

✓ **Event “destructive power” assessment:**

Also, it is necessary to know “how big is the event”, what generally means at least to compute the event magnitude.

In the case of a EWS, event’s magnitude is not computed classically because it would mean to wait until S waves arrive to measure seismic waveforms amplitudes and it would introduce a long delay for the alert. So, this module will apply, to input data channels, different kind of algorithms in order to estimate the event magnitude and the peak ground motion (cf. chapter 2.3).

iv. Alert system

The alert system will be the last module of the chain and it will be in charge of sending alert messages containing previously defined information to selected recipients. Even the complexity of alert system, it always will guarantee high reliability and short delay sending alert messages, as any other alert system.

3.1.2. SISPy network and systems description

At this section the seismic network defined inside the SISPy project as result of cooperation between partners will be described. The usefulness of these elements for a EWS implementation will be discussed in section 3.1.3.

i. Stations

Five different organizations (IGC, IGN, IEA, BRGM and OMP) are the owners of the seismic stations involved in SISPy project. These stations are listed at Table 7.

From this complete station list a group of them will be rejected because they cannot be used to implement a EWS on SISPy region. A deep evaluation of remaining stations will be performed at section 6 of this document. At this point we will consider 3 reasons to reject a station: out of SISPy area and far away from it, urban stations because they are too noisy, and non real time continuous streaming stations.

So, rejected stations are:

- CGAR, CMAS, COBS, ESAC, ETOS, EMOS, ERTA and Montauban: far away from SISPy area.
- CELS, GIRS, LLIS, VIES, GRAM, PAMP, OLOS, GIRR, VIER, PYAD, PYBB, PYLU, PYPD, PYPP and PYXX: urban stations.

Once rejected stations have been removed from Table 7, remaining stations have been represented on the following map (Figure 8) where is reported the SISPy's area of interest.

Station	Name	Owner	Latitude (deg)	Longitude (deg)	Elevation (m)	Sensor type	Municipality	Analog/Digital	Urban / Free Field	RT
CAVN	Les Avellanes	IGC	41.8816	0.7506	629	BB	Les Avellanes	Digital	Free Field	Yes
CBEU	Beuda	IGC	42.2556	2.6758	825	BB	Beuda	Digital	Free Field	Yes
CBRU	Bruguera	IGC	42.2844	2.1790	1328	BB	Bruguera	Digital	Free Field	Yes
CCAS	Cassà de la Selva	IGC	41.8828	2.9042	197	BB	Cassà de la Selva	Digital	Free Field	Yes
CEST	Esterri de Cardós	IGC	42.5987	1.2541	1325	BB	Esterri de Cardós	Digital	Free Field	Yes
CORG	Organyà	IGC	42.2291	1.3165	716	BB	Organyà	Digital	Free Field	Yes
CORI	Oristà	IGC	41.9724	2.0488	621	BB	Oristà	Digital	Free Field	Yes
CPAL	Palau Saverdera	IGC	42.3105	3.1624	223	BB	Palau Saverdera	Digital	Free Field	Yes
CTRE	Tremp	IGC	42.3223	0.7724	1318	BB	Tremp	Digital	Free Field	Yes
CFON	Fontmartina	IGC	41.7612	2.4346	973	BB	Fogars de Montclús	Digital	Free Field	Yes
CLLI	Llívia	IGC	42.4781	1.9730	1413	BB	Llívia	Digital	Free Field	Yes
CSOR	Soriguera	IGC	42.3744	1.1327	1227	BB	Soriguera	Digital	Free Field	Yes
CGAR	Garraf	IGC	41.2933	1.9137	584	BB	Begues	Digital	Free Field	Yes
CMAS	Mas de Barberans	IGC	40.7257	0.3139	530	BB	Mas de Barberans	Digital	Free Field	Yes
COBS	Casablanca	IGC	40.7131	1.3562	-160	BB	-	Digital	Free Field	Yes
CELS	St Celoni soil	IGC	41.6928	2.4992	150	ACC	St Celoni	Digital	Urban	Yes
GIRS	Girona soil	IGC	41.9808	2.8224	79	ACC	Girona	Digital	Urban	Yes
LLIS	Llívia soil	IGC	42.4647	1.9733	1190	ACC	Llívia	Digital	Urban	Yes
VIES	Vielha soil	IGC	42.7016	0.7969	986	ACC	Vielha	Digital	Urban	Yes
GRAM	Granollers	IGC	41.6000	2.2680	215	ACC	Granollers	Digital	Urban	Yes
AVIN*¹	Avinyó	IGC	41.8476	1.9651	331	ACC	Avinyó	Digital	Free Field	Yes
ARBS	La Rabassa	IEA	42.4345	1.5337	2166	BB	St Julià de Lòira	Digital	Free Field	Yes
EALK	Alkurruntz	IGN	43.2197	-1.5071	965	BB	Alkurruntz	Digital	Free Field	Yes

Station	Name	Owner	Latitude (deg)	Longitude (deg)	Elevation (m)	Sensor type	Municipality	Analog/Digital	Urban / Free Field	RT
EARA	Aranguren	IGN	42.7727	-1.5797	476	BB	Aranguren	Digital	Free Field	Yes
EBIE	Bielsa	IGN	42.6862	0.1428	2130	BB	Bielsa	Digital	Free Field	Yes
EJON	La Jonquera	IGN	42.4487	2.8886	570	BB	La Jonquera	Digital	Free Field	Yes
EORO	Oroz	IGN	42.8926	-1.3095	880	BB	Oroz Betelu	Digital	Free Field	Yes
YSOS	Yesa dam	IGN	42.4566	-1.1457	881	BB	Sos del Rey Católico	Digital	Free Field	Yes
ERTA	Horta de Sant Joan	IGN	40.9567	0.3335	547	BB	Horta de Sant Joan	Digital	Free Field	Yes
EMOS	Mosqueruela	IGN	40.3639	-0.4721	1694	BB	Mosqueruela	Digital	Free Field	Yes
ETOS	Mallorca	IGN	39.7678	2.8144	480	BB	Mallorca	Digital	Free Field	Yes
ESAC	San Caprasio	IGN	41.7219	-0.4693	815	BB	San Caprasio	Digital	Free Field	Yes
PAMP	Pamplona	IGN	42.8140	-1.6250	478	ACC	Pamplona	Digital	Urban	No
OLOS	Olot soil	IGN	42.1830	2.4900	436	ACC	Olot	Digital	Urban	Yes
GIRR	Girona rock	IGN	41.9860	2.8278	102	ACC	Girona	Digital	Urban	Yes
VIER	Vielha rock	IGN	42.7044	0.7922	994	ACC	Vielha	Digital	Urban	Yes
Urdes*	Lacq gas	OMP	43.5000	-0.6175	95	MB	Lacq	Digital	Free Field	Yes
ATE	Arette	OMP	43.0858	-0.7003	480	BB	Arette	Digital	Free Field	Yes
SJAF	St-Jean d'A	OMP	42.4845	2.8822	450	BB	St-Jean d'A	Digital	Free Field	Yes
Tercis*	Dax	OMP	43.7072	-1.0544	7	BB	Dax	Digital	Free Field	Yes
MLS	Moulis	OMP	42.9578	1.0947	529	BB	Moulis	Digital	Free Field	Yes
PYLO	Lourdes	OMP	43.0982	-0.0478	410	BB	Lourdes	Digital	Free Field	Yes
Montauban*	Montauban	OMP	44.0181	1.3558	208	BB	Montauban	Digital	Free Field	Yes
PYAD	Arudy	OMP	43.0975	-0.4258	450	ACC	Arudy	Digital	Urban	Yes
PYBB	Bagnères	OMP	43.0586	0.1489	567	ACC	Bagnères	Digital	Urban	Yes
PYLU	Luchon	OMP	42.7906	0.6014	630	ACC	Luchon	Digital	Urban	Yes

Station	Name	Owner	Latitude (deg)	Longitude (deg)	Elevation (m)	Sensor type	Municipality	Analog/Digital	Urban / Free Field	RT
PYPD	Prades	OMP	42.6142	2.4156	350	ACC	Prades	Digital	Urban	Yes
PYPP	St-Jean-PdeP	OMP	43.1557	-1.2407	270	ACC	St-Jean-PdeP	Digital	Urban	Yes
PYXX*	Hendaye	OMP	43.3467	-1.6200	75	ACC	Hendaye	Digital	Urban	Yes
FESP	Espira	BRGM	42.8187	2.8207	170	ACC	Espira de l'Agly	Digital	Free Field	Yes
FMON	Montoussé	BRGM	43.0624	0.4152	630	ACC	Montoussé	Digital	Free Field	Yes
FNEB	Nébias	BRGM	42.9031	2.1064	580	ACC	Nébias	Digital	Free Field	Yes

Table 7 – SISPyR stations list (based on existing information at report elaboration time) *Approximate coordinates because station is not yet installed. (1) Before named AVIS.

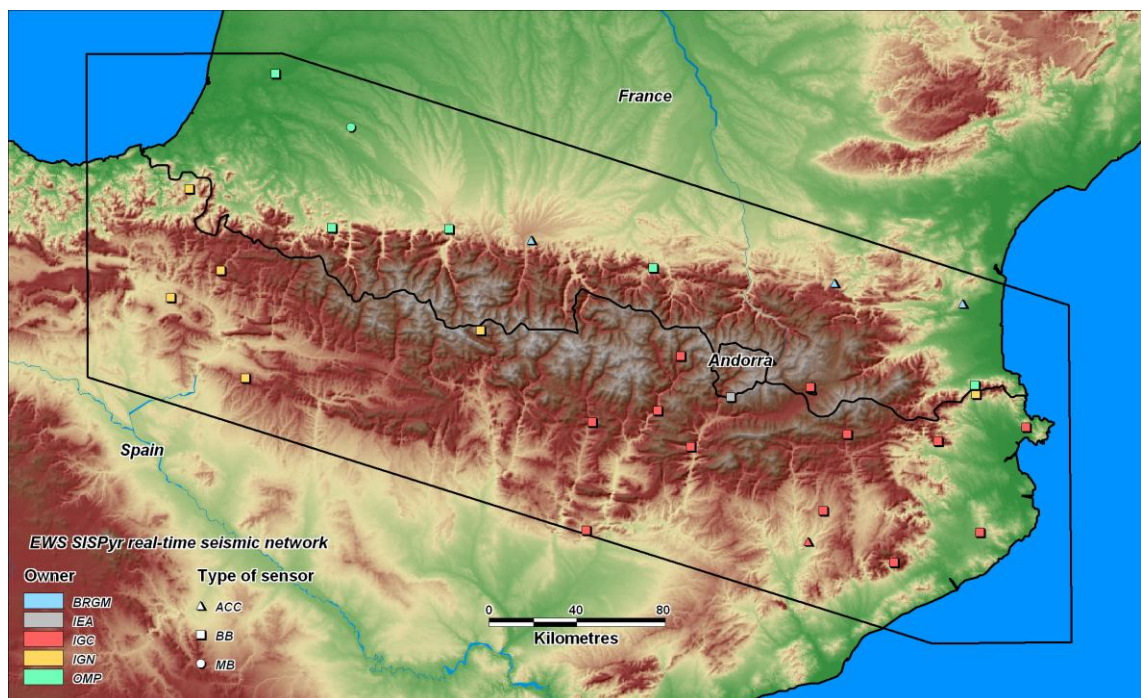


Figure 8 – Location of seismological stations considered for the EWS analysis according to owner organization and type. Also shown is the area covered by the SISPYR project.

ii. Network and subnetworks

Stations previously selected are grouped into sub-networks considering the primary Data Center from which continuous data is received. So, we can define 3 subnetworks:

- OMP subnetwork: group of stations that are directly received at OMP Data Center;
- IGN subnetwork: group of stations that are directly received at IGN Data Center;
- IGC subnetwork: group of stations that are directly received at IGC Data Center.

Stations belonging to each sub-network are summarized in Table 8.

At OMP Data Center listed stations are received in real time using Seedlink server. This server receives continuous data streams and stores them into hard drives according system configuration.

Both IGN and IGC sub-networks receive all listed stations, except AVIN, by satellite using Nanometrics VSAT system. This system receives real-time continuous data and stores them into hard drives using ringbuffers during a predefined window of time. AVIN station is received at IGC by Wimax using Scream! Software from Guralp Systems and, as others systems, it stores received data into hard drives during a defined window of time.

Each SISPyR sub-network shares real time data with others by public internet or dedicated lines. Also a Data Center (the BRGM), which does not receive any of the listed stations directly, is involved in SISPyR network schema. So, SISPyR network and sub-networks schema will be as follow (Figure 9).

Sub-network	Station	Owner
OMP	Urdes	OMP
	ATE	OMP
	SJAF	OMP
	Tercis	OMP
	MLS	OMP
	PYLO	OMP
IGN	EALK	IGN
	EARA	IGN
	EBIE	IGN
	EJON	IGN
	EORO	IGN
	YSOS	IGN
IGC	CAVN	IGC
	CBEU	IGC
	CBRU	IGC
	CCAS	IGC
	CEST	IGC
	CORG	IGC
	CORI	IGC
	CPAL	IGC
	CTRE	IGC
	CFON	IGC
	CLLI	IGC
	CSOR	IGC
	AVIN	IGC
	ARBS	IEA
	FMON	BRGM
	FNEB	BRGM
	FEST	BRGM

Table 8 – SISPyR subnetworks.

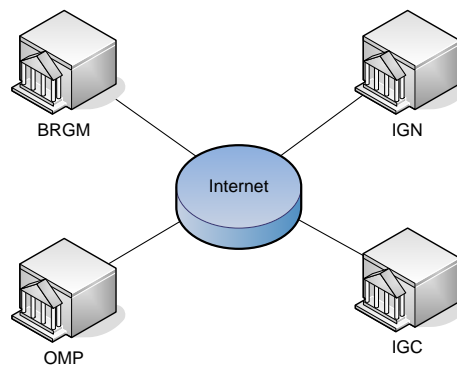


Figure 9 – SISPyR network and sub-networks

iii. Communication

SISPyR's network involves different described sub-networks. So, in order to consider all stations we must decide a unique data reception point from the existing primary ones.

Selection criteria will be “the Data Center that receives more stations as primary Data Center”, and it is the IGC Data Center.

According to this decision, complete network communication schema will be as follow (Figure 10).

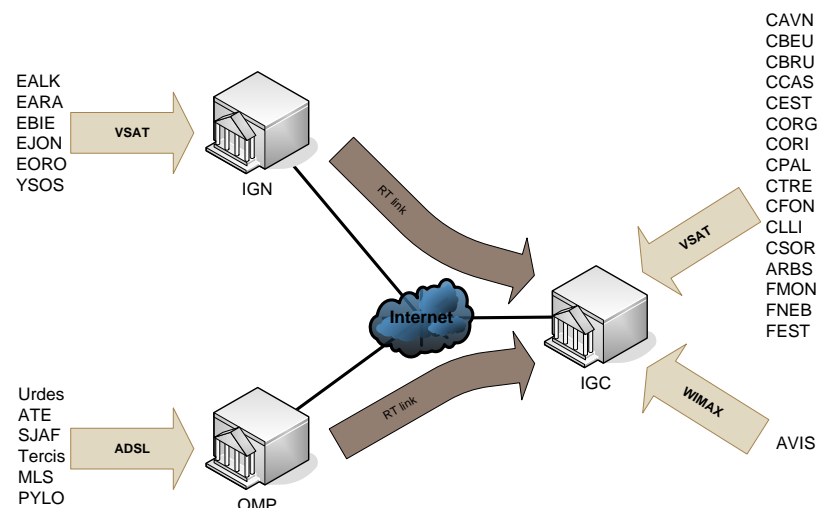


Figure 10 – SISPyR network communication schema for IGC

Once the schema is defined, some individual operational parameters for each station are measured at IGC Data Center during a period of 2 days and results

are shown on Table 9. Due to the fact that currently not all SISPyR's selected stations are being received in real-time at IGC, only measures for received stations have been done.

Station	Averaged latency (s)	Avg. latency standard deviation (s)	% of data received in RT
EBIE	8.4	2.63	80.06
EJON	7.05	2.85	99.70
ATE	6.59	1.94	100.00
SJAF	2.75	1.33	96.70
MLS	2.92	1.25	96.30
PYLO	0.47	0.84	100.00
CAVN	3.51	1.17	100.00
CBEU	3.15	0.94	100.00
CBRU	3.98	1.07	100.00
CCAS	2.71	0.93	100.00
CEST	3.44	1.01	100.00
CORG	3.53	0.96	100.00
CORI	3.23	0.93	100.00
CPAL	3.11	1.06	100.00
CTRE	2.92	0.96	100.00
CFON	3.84	1.05	100.00
CLLI	3.17	0.95	100.00
CSOR	3.22	0.99	100.00
ARBS	3.5	0.97	100.00
FMON	3.23	0.97	100.00
FESP	3.28	1.09	100.00
FNEB	3.25	1.02	100.00

Table 9 – Data latency for some of the EWS SISPyR stations

It is not the purpose of this document to describe existing data reception systems and related infrastructure, but the exposition of their main (in terms of EWS) operating parameters.

iv. Data processing

At Data Center, received seismic data should be processed by EWS processing chain. Taking into account existing IGC's Data Center infrastructure and data processing systems, it is proposed to base EWS processing chain in DAS2 system.

DAS2 system was developed inside ISARD project (see 2.3). Currently DAS2 is full operative for event detection, event location and seismic parameters computation in IGC and BRGM.

- **DAS2 core**

DAS2 has been built based on Earthworm modules. In 1993 the USGS (United States Geological Survey) starts the development of Earthworm project with the first objective of provide an automatic communication notification in case of earthquake.

In the course of time it has been necessary to cover new needs: to store real time received data, review of detected events or to incorporate accelerometric data, what made progress Earthworm to a modular architecture. So each functionality is encapsulated inside a standalone program that can be executed regardless the others.

- **DAS2 chain overview**

As it is said, DAS2 has been built based on Earthworm modules, due to ISARD's Seismic Network requirements⁴:

- Real-time processing of seismic data coming from Nanometrics, Seedlink and Scream! data acquisition systems;
- Phases picking;
- Event detection;
- Event location;
- Local magnitude computation;
- Data achieving.

DAS2's chain which covers listed requirements is shown on Figure 11.

⁴ Only requirements of interest for an EWS system are listed.

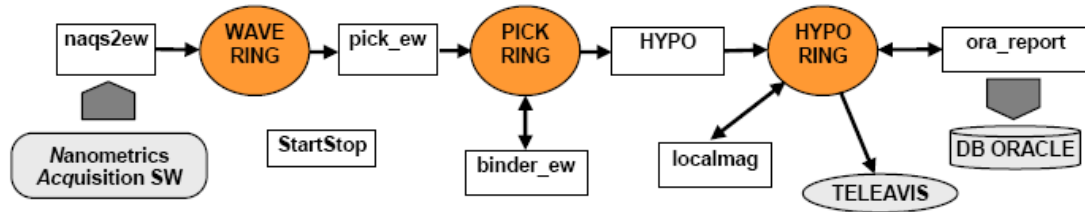


Figure 11 – DAS2 simplified chain schema

Each chain's module has been tuned according to operational network parameters and requirements given by network operators (IGC and BRGM).

• Pick_ew

Pick_ew is the phase's picking system based on Allen algorithm and it's applied to each configured input stream. The algorithm is divided into 3 stages: triggering, detriggering and quality check.

Triggering stages is based on classic STA/LTA algorithm, but instead to apply it over the input signal; it's computed over following characteristic expression (Equation 11):

$$E_i = R_{i-1}^2 + c_2 \cdot \Delta R_i^2 \quad \text{Equation 11}$$

been R the high-pass filtered input signal and c_i a parameter collection to be adjusted for each processed channel.

This expression empathizes the changes of input signals as at time domain as at frequency domain. So, a trigger will be declared each time that $STA_i > c_5 \cdot LTA_i$.

The trigger will finish (detriggering stage) when the number of zero crossings with a recovered STA (S_i) reach L_i , been S_i and L_i adjusted for each input channel.

Once the trigger is finished the system will check its quality considering duration and amplitude criteria. Specifically, a trigger will be considered not valid when the number of zero crossings since its declaration or some of three firsts signal maximum peaks does not reach a configured threshold.

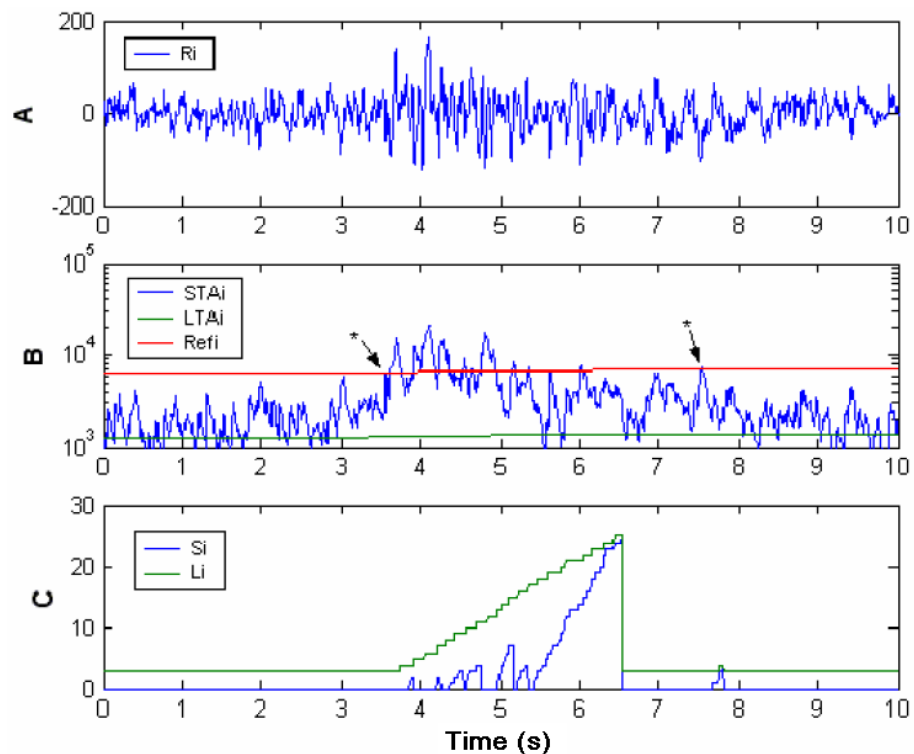


Figure 12 – Picking example

Described procedure can be followed on figure 5:

1. Filtered seismic trace R_i .
2. STA of the characteristic function and reference level. Points indicated as * refer to the moment when a trigger is declared (STA is higher than $c_5 \cdot LTA$).
3. Quantities of L and S related to the number of zero crossings of the seismic trace, which determine the point at which the trigger is declared over. The number of zero crossings while the trigger is alive is used to evaluate its quality.

• Binder_ew

Binder_ew (also called Binder) is the event declaration module used at DAS2's chain. It identifies events in a quick and coherent way from triggers detected by pick_ew, considering all of them as first arrivals (P-phases).

For each new P-phase, binder algorithm tries:

- To associated this new phase with an active event, and if it is not possible;

- To declare a new event from recent triggers still not associated, defining a probable hypocenter (*stacking phase*).

The stacking phase is activated after a new trigger is detected and it cannot be associated with any active event. The first step is to build a volume using cubic cells representing the region of study and where hypocenters can occur.

After that, for each new unassociated trigger the geometrical volume is represented according to seismic wave's velocity and observed arrival time differences. This volume will be a hyperboloid modified according to the defined crustal model. If triggers are coherent, they will intersect in a volume where the possible hypocenter will be located. In case of existing at least four coherent triggers a new event will be declared and its hypocenter will be the average of cells of the intersection volume which are at the same minimum distance from the initiating pick.

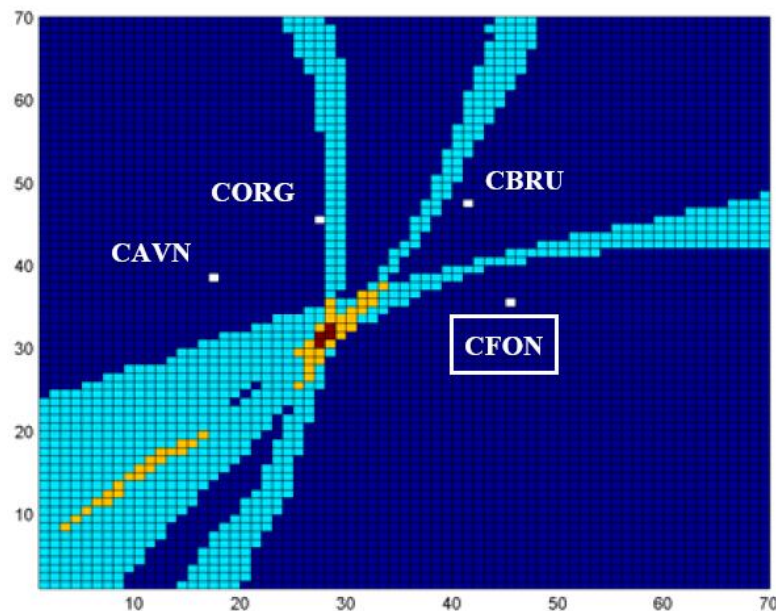


Figure 13 – Binder stacking stage example

Figure 13 shows a cross section at 2.5 km depth as an example this volume. The modified hyperbolas corresponding to the difference of arrival times between one station and the reference station (first stacked station), are drawn in light blue. The surface where the three hyperbolas overlap is drawn red and there will be the trial hypocenter for the new event.

Once the event is declared the *stacking stage* finishes and a second stage starts. This second stage will be called *Phase association stage*.

At this second stage, each time that a new trigger arrives, the system tries to associate it to a declared event computing related residual times (RMS). It considers the new arrival as P, P_g, P_n, S, S_g or S_n and checks if these results are inside a declared tolerance interval. If the new trigger is not associated to any declared event it will be past to *stacking stage*.

Each time that a new phase is associated to a declared event at *phase association stage* the system tries to relocate the event using a simple locator called L1. *Phase association stage* finishes after a timeout with any association success. Then we can use another more accurate localization program (hypoinverse, hypocenter, etc) to relocate the event.

• Localmag

Localmag is an Earthworm module which computes event's local magnitude considering its origin time and hypocenter coordinates. With this information it estimates P, S and S_g wave's arrival times in order to estimate required waveform lengths. On obtained traces, the algorithm removes DC and the instrument response and finally converts them into Wood-Anderson displacement traces.

Localmag module computes event's local magnitude using available horizontal seismic channels (waveforms).

3.1.3. Existing systems evaluation

i. **Stations, communication systems and networks**

At this point we will focus on SISPyR stations operation, their integration into networks and their communication systems. The complete system since data is recorded at stations until digital data arrives to Data Centers will be considered.

What is more, the possibility to use them for a EWS implementation in SISPyR region will be studied.

The analysis will be based in two clearly distinct categories of requirements:

- Basic requirements: will be minimum requirements that system must accomplish as seen at section 4. Systems that do not accomplish these requirements will not be integrated into a EWS. Also recommendations will be given to solve it.
- Recommended requirements: they will be all requirements and considerations that will improve the EWS operation, reliability and efficiency. Even these requirements will not be of a strict and mandatory

enforcement; but in fact they can be the difference of having a reliable and effective EWS or a poor one.

- **Stations and communication systems**

Stations to be evaluated are listed at Table 8. For these stations basic requirements described at section 3.1.1 will be checked. These requirements are:

- ✓ **Seismic sensor:**

- Should be adequate for the kind of seismic signal to register and measure in terms of bandwidth and dynamic range;
- It should be rugged and protected against ambient conditions;
- It must be properly installed to guarantee its data quality, reliability and availability.

- ✓ **Data acquisition system:**

- It should be adequate for the kind of seismic signal to acquire and register in terms of bandwidth, sample rate, dynamic range, resolution and local archiving.

- ✓ **Communication systems:**

- It must be “real-time”;
- Rugged to support remote site climatic conditions;
- Adequate for data transmission requirements in terms of bandwidth, SLA and reliability (latency will be analyzed at recommended requirements section).

- ✓ **Power supply system:**

- Rugged to support remote site climatic conditions;
- UPS or equivalent system installed.

Above listed requirements are considered basic for EWS stations. All of them are accomplished by most of these stations because they are also used at SISPYR partners Data Centers for “real-time” event detection and seismic alert. The reason why some are not actually used is owed to the fact that they are not yet completely installed and operative. These stations are: AVIN, Urdes and Tercis, and they will must to accomplish these requirements once they will go into service.

Once it will be checked that all basic requirements are accomplished by all EWS stations, recommended requirements will be also checked. These requirements, as explained at section 3.1.1 and will be:

- Redundancy: sensor, acquisition system, communication system and/or power supply;
- Data Latency;
- The use of non-terrestrial communication system.

Results of this check are shown on Table 10.

Station	Sensor redundancy	Acq. System redundancy	RT Com. System redundancy	Power supply redundancy	48h avg. latency (s)	Latency std. deviation (s)	Use non terrestrial comm. System
EBIE	No	No	No	No	8,40	2,63	Yes
EJON	No	No	No	No	7,05	2,85	Yes
EALK*	No	No	No	No	8,40	2,63	Yes
EARA*	No	No	No	No	8,40	2,63	Yes
EORO*	No	No	No	No	8,40	2,63	No
YSOS*	No	No	No	No	8,40	2,63	No
ATE	No	No	No	No	6,56	1,94	No
SJAF	No	No	No	No	2,75	1,33	No
MLS	No	No	No	No	2,92	1,25	No
PYLO	No	No	No	No	0,47	0,84	No
CAVN	No	No	No	No	3,51	1,17	Yes
CBEU	No	No	No	No	3,15	0,94	Yes
CBRU	No	No	No	No	3,98	1,07	Yes
CCAS	No	No	No	No	2,71	0,93	Yes
CEST	No	No	No	No	3,44	1,01	Yes
CORG	No	No	No	No	3,53	0,96	Yes
CORI	No	No	No	No	3,23	0,93	Yes
CPAL	No	No	No	No	3,11	1,06	Yes
CTRE	No	No	No	No	2,92	0,96	Yes
CFON	No	No	No	No	3,84	1,05	Yes
CLLI	No	No	No	No	3,17	0,95	Yes
CSOR	No	No	No	No	3,22	0,99	Yes
ARBS	No	No	No	No	3,50	0,97	Yes
FMON	No	No	No	No	3,23	0,97	Yes
FESP	No	No	No	No	3,28	1,09	Yes
FNEB	No	No	No	No	3,25	1,02	Yes
Urdes*	No	No	No	No	2,92	1,25	No
Tercis*	No	No	No	No	2,92	1,25	No
AVIN*	No	No	No	No	1,01	0,62	No

Table 10 – Recommended stations requirements check table. * Estimated latency values

Stations that are being installed at the same time that this report is being written have not been still checked. Nevertheless, to be able to continue with the study we will suppose the following premises:

- Any of them have redundant equipments (as planned);
- Any of them use satellite communication equipment.

Latency of these three stations is similar to any similar working station, and it will be: Urdes and Tercis will be equal to MLS, and AVIN will be equal to LLIR (non-SISPyR station).

Other stations are not currently received at IGC's Data Center so measures and latency values have been estimated considering similar operating stations received at IGC. These stations are EALK, EARA, EORO and YSOS.

✓ **Redundancy**

Looking above it is clear that equipments redundancy at all stations is absent. There is not any station with some duplicated or redundant data sensor, data acquisition system, communication system or power supply system.

To solve the problem, it is recommended to give redundancy to stations equipments, especially too communication systems because their vulnerability is higher than the other ones. This redundancy also can be reached increasing stations density to allow some faults tolerance reducing the effect of changes at the station map distribution.

Some simulations can be done in order to evaluate the shutting down effect of some different stations and then a weigh up if required economic effort is justified. If the system loses a station, the blind zones map changes and some targets could keep out of receiving the alert.

✓ **Use of non-terrestrial communication system**

In case of big event some terrestrial communication infrastructures could be damaged so if any station uses "only" terrestrial communication systems; it is in risk of losing communication link with Data Center.

So, for a real time alert system, it is recommended to use satellite communications system. If this is not possible, another option is to give redundancy to the communications network using different types of communication systems, including different base stations of services providers.

In the present case, there are nine stations which only use terrestrial communication systems: AVIN, EORO, YSOS, ATE, SJAF, MLS, PYLO, Urdes

and Tercis. SJAF and AVIN are redundant by others (EJON and CORI) using a satellite communication system.

✓ **Station data Latency**

Station data latency is defined as the delay between seismic signal is registered at any seismic station and the moment that this signal that has been digitized is received at Data Center to be processed. This latency corresponds to the time needed by each station to transmit data to Data Center: its value is different for any station and it can be very variable as we have seen in Table 10. Having a look on Figure 14 that shows graphically repartition of stations' communication latency underlines that while some stations exhibit quite important values around 9 seconds, most of them (75%) are associated to latency values lower than 5 seconds, what is quite reasonable for early warning applications.

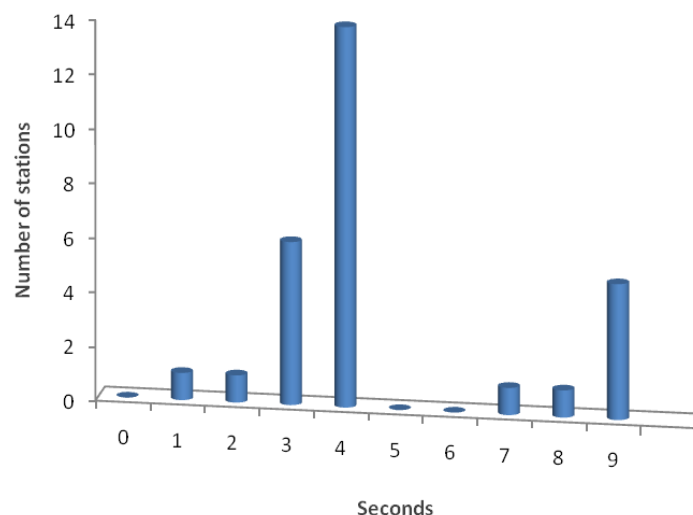


Figure 14 – Data communication latency

ii. Networks

As viewed at section 5.2, SISPyR EWS the seismic network consists of 3 subnetworks. Each sub-network is defined according the primary Data Center which receives data from its seismic stations. Figure 15 represents the three sub-networks of SISPyR EWS seismic network.

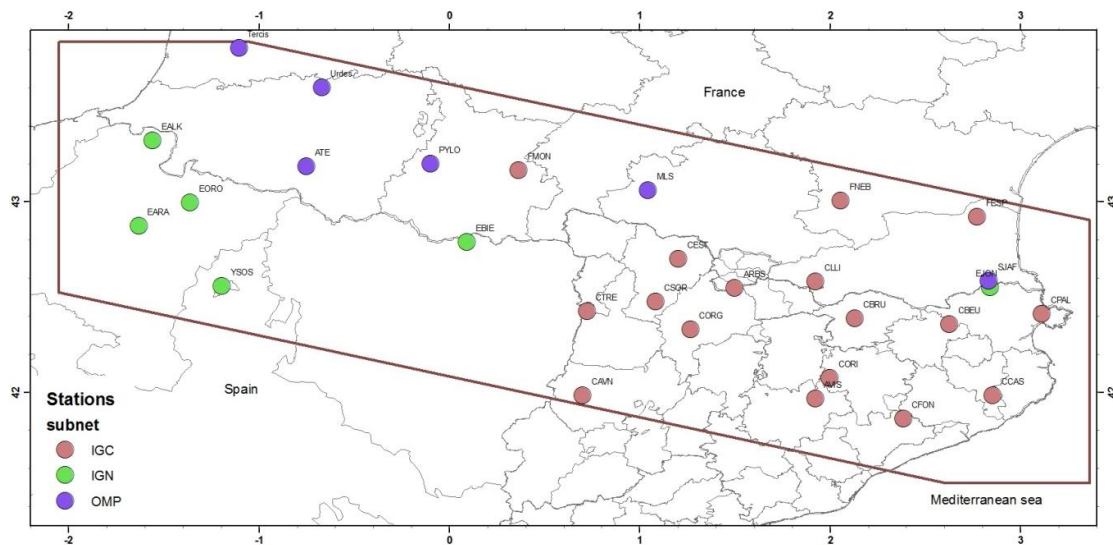


Figure 15 – SISPy sub-networks map

If we analyze Figure 15 we appreciate a clear relation between subnets and regions. This fact implies that a failure at any Data Center will affect so much the network topology because no redundancy exists in receiving seismic data from stations.

Important network topology changes will affect so much the system detectability and blind zones, depending on where the hypocenter is located.

So, network topology, clearly, could still be improved. An easy way to improve it could be receiving data from any station at, at least, two different Data Centers. On this way some failure at any Data Center will not change network topology, of course considering that data from all stations are shared between Data Centers and that alerts are computed and send from all Data Centers.

Also, all seismic data received directly from stations at one Data Center should be forwarded to other Data Centers. Following, a redundant path subnets communication schema is proposed to guarantee that the system will continue been fully operative after a complete Data Center failure (Figure 16).

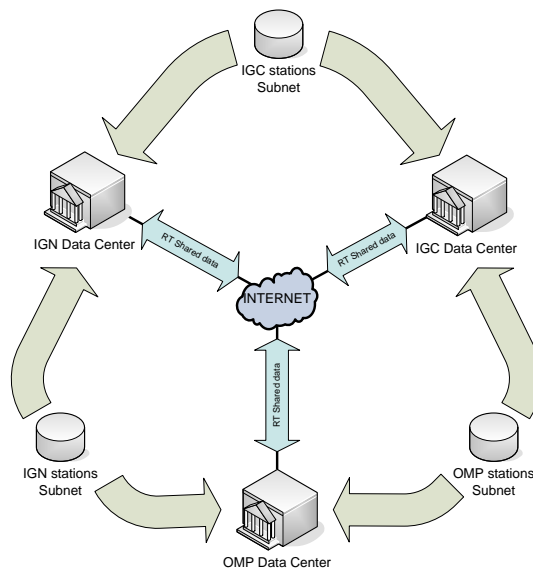


Figure 16 – Redundant path communication schema

In Figure 16, all SISPyR stations have been shared between Data Centers by Internet and each station is directly received at two Data Centers. This schema accepts any communication path failure or Data Center failure without operative penalty.

It also could be combined with different communication systems at the stations, also covering third party (communication services operators) failures.

iii. Data processing

As it is exposed in section 3.1.2.iv, the proposed data processing system will be based on DAS2 system installed and operative at IGC Data Center since June of 2007 and later on also in BRGM.

For this study, installation at IGC Data Center will be analyzed, and all results will be referred to this installation; but it should be equal for BRGM case.

At this section different aspects of data processing system will be analyzed:

- System operability: at this point the system reliability, stability and faults tolerance capabilities will be analyzed. Also expandability and interoperability will be taken in consideration;
- Event's detection: the experience in IGC about events detection will be analyzed. False detections and missing ones will be studied;

- Event location: DAS2 incorporates different event location modules that will be compared and considered;
- Event magnitude calculation;
- Alert system.

- **System operability**

As it is said before, DAS2 system is fully operative at IGC Data Center since June 2007. DAS2 is a system developed inside ISARD Interreg project and it is based on Earthworm (USGS) modules.

DAS2 architecture is a set of connected Earthworm (EW) modules using shared memory or network connections and creating a spider's web. Because of the nature of the system, it allows a complete customization depending on user needs.

The main objectives of DAS2 system at IGC, related with the present study, are event detection and location. To answer these two needs the following system schema is configured (Figure 17):

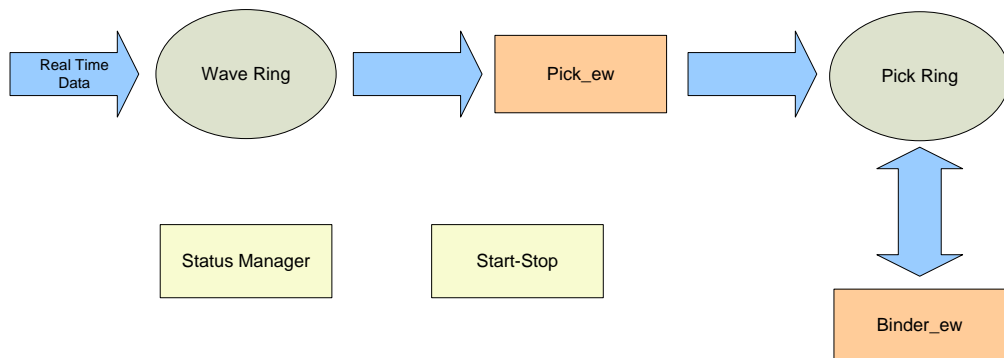


Figure 17 – DAS2 simplified first phase schema

Because the description of each module is given at section 3.1.2.iv, it will not be discussed again here, and basically we will point their main functions:

- Pick_ew: reads waveform data from “Wave Ring” and process them in order to declare picks according configured parameters and writes the results into a “Pick Ring”;
- Binder_ew: reads picks from the “Pick Ring” and tries to associate them to declare an event and obtain a first location. Event declaration and first location computation consists in several steps that are described at section 3.1.2.iv. Results are written into a “Pick Ring”;

- Status Manager: collects and monitors status messages from EW modules;
- Start-Stop: starts, stops and restarts, if needed, EW modules.

Since 2007 this system has been continuously upgraded until now. Most of the improvements solve initial stability problems and other ones add new functionalities.

Currently, DAS2 implementation has raised a very high stability and reliability (from an operational point of view) since it has been running without a break (without considering external factors) during the last three years.

System modularity and its open source roots make it easily connectable to other systems (high interoperability) and expandable to allow new functionalities.

Although the present system at IGC doesn't implement a complete redundant data processing system given system's characteristics, it could be achieved and it should be considered for a EWS.

• **Event detection**

At this section, event detection reliability of the system will be analyzed from January 2008 to September 2010. Last months of 2007 haven't been considered in order to remove change effects done over the system during its initial operative stage which could produce incorrect results interpretation.

Event detection reliability will be analyzed from two different points of view, each one answering to the following questions:

- How many false events have been detected by the system and how significant they are?
- How many events have not been detected by the system and why?

False events

False events are defined as events declared by DAS2 system, which do not correspond to earthquakes, explosions or, in general, to any identified source. False events can be generated by many reasons such as wind. So, in our analysis, false events will be referred as noises.

False events are one of the most important points for any alert system because they can produce "false alerts". Although false alerts are inherent of any alert system, its weight can determine the credibility of the system.

Figure 18 represents, per month, the number of noises detected by DAS2 system, the percentage respect the total amount of detected events, and the number of real time processed stations used for events detection.

Analyzing Figure 18 we can extract some conclusions:

- The number of detected noises has a stationary behavior, been higher during summer and almost zero during winter;
- There isn't a clear dependency between the number of operating stations and the number of detected noises;
- During June 2010 a major update of picking and detection algorithms has been performed obtaining a clear improvement of the system. We can observe that since this date, even during summer months, the number of detected noises falls to almost zero.

Even the number of noises has been reduced so much, it is not possible to fix them to zero, and it means that some "false detections" must be assumed, but we can predict their effects for a EWS taking a look to local magnitude computed by DAS2 (as an approximation to magnitude that will be estimated by EWS). So, considering all detected noises since January 2010, it's observed that their computed local magnitude (MI) is always lower than 2.4.

Event detection capability

DAS2 event detection capability will be analyzed according to specific purposes for which it is operative at IGC, because configuration parameters have been set on that scope. Each system implementation requires customized settings according to specific needs and requirements; but it should be assumed that its performance will be similar.

So, following results will be exposed considering that the scope of IGC's system is to detect events in Catalonia region and neighbors. In fact, the seismic network topology and DAS2 settings are defined for this purpose. That means that detected or not detected events out of Catalonia will not be considered.

On Figure 19, the total number of events, automatic detected events and its percentage are represented as function of manual local magnitude computed by seismologists.

On this figure it is observed that automatic detections increase when MI increases. What is more, from $MI \geq 1.9$ it almost keeps a 100% of detection, except for 2 events which will be listed.

% Noises, Number of Noises and Number of Stations

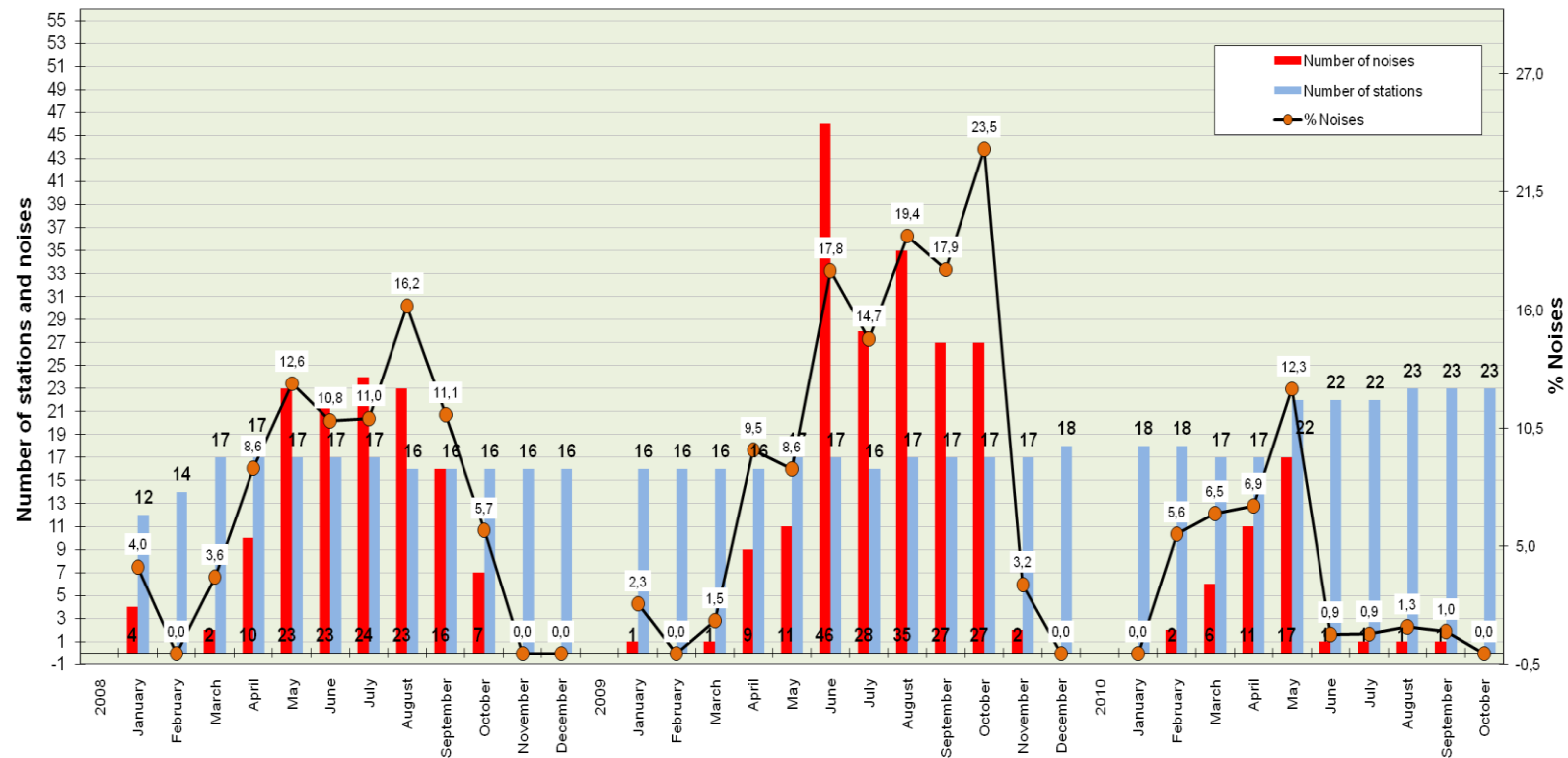


Figure 18 – Percentage of « noises » and number of stations

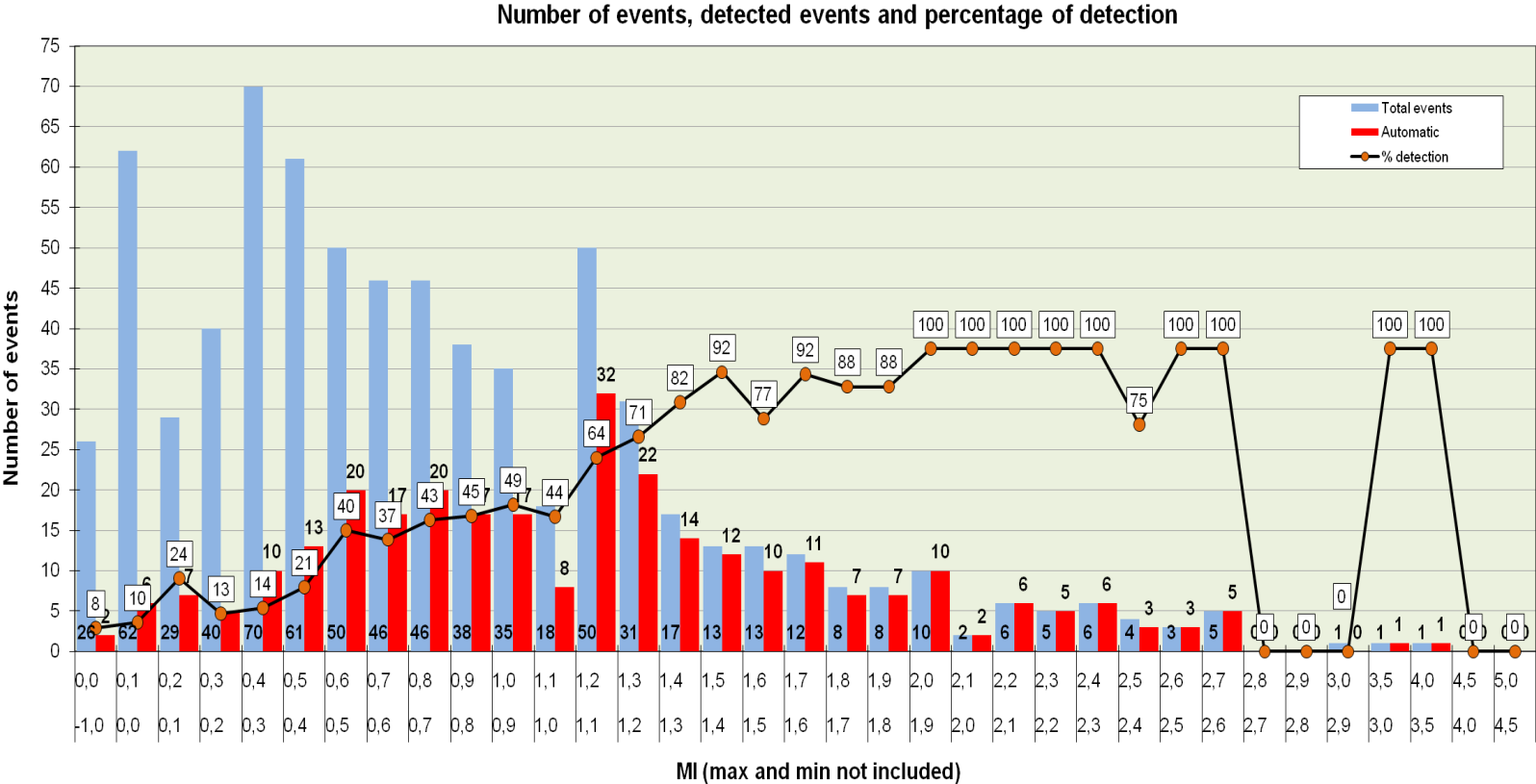


Figure 19 – Number of events, detected events and percentage of detection

The 2 events which make drop the detection percentage of 100% for $M_I \geq 1.9$ have not been detected by the system for the same reason. In both cases, there are two events which occur in a short period of time and event detection module fails identifying them. So, some improvements are needed to increase event detection module's capabilities in order to be able to discriminate, and correctly identify, events in case of occurrence in a short delay.

Event detection delay

Event detection delay will be the period of time since all waveforms needed for event detection are written at the first data processing shared memory region of DAS2 and the moment when the event is declared.

After analyzing several events processed by DAS2 system, we can affirm that event detection latency is in the order of few milliseconds. That depends on the load of the computer where DAS2 system is installed, normally less than 0.1 second. This delay should be added as an offset to others previously mentioned.

- **Event location**

Event location chain at DAS2 system consists of three stages: stacking, L1 and hypoinverse/hypocenter; been the first of them what declares the event and calculates a first event hypocenter and origin time. So, at this section each stage performance will be discussed in terms of errors (difference between DAS2 event locations and locations done with the assistance of seismologist) and delays.

In order to make a discussion, all events detected by DAS2 system in Catalonia with $M_I \geq 2.4$ from January 1st 2008 to the end of September 2010 have been taken into account, been $M_I = 2.4$ the threshold level configured at the IGC's alert system. So, applying this criterion a list of 13 events is obtained, as shown on Table 11.

Code	Date	Manual results					Automatic results				
		OT	Lat. (°)	Long. (°)	Depth (km)	MI	OT	Lat. (°)	Long. (°)	Depth (km)	MI
I0802301	22/02/2008	03:27:32	41,88	2,91	7	2,5	03:27:32	41,88	2,91	6	2,7
I0803200	16/03/2008	19:30:07	42,66	0,83	1	2,4	19:30:09	42,66	0,86	0	2,5
I0806300	22/06/2008	18:48:31	41,86	2,59	4	3,1	18:48:32	41,87	2,59	1	3,1
I0807200	21/07/2008	18:59:33	41,87	2,59	3	2,6	18:59:33	41,87	2,59	0	2,8
I0807300	22/07/2008	22:36:32	41,86	2,59	4	3,8	22:36:32	41,87	2,58	0	3,8
I0807370	23/07/2008	00:27:06	41,86	2,59	4	2,4	00:27:07	41,87	2,59	0	2,5
I0807430	23/07/2008	03:39:52	41,87	2,59	4	2,4	03:39:52	41,87	2,59	0	2,4
I0901050	04/01/2009	38:08.0	42,35	1,45	0	2,6	07:38:08	42,34	1,45	0	2,6
I0901200	15/01/2009	52:30.3	41,27	1,57	0	2,5	15:52:30	41,24	1,58	7	2,6
I0902310	28/02/2009	02:53.4	42,56	1,35	10	2,6	08:02:53	42,58	1,34	0	2,6
I0909190	16/09/2009	15:44:10	41,77	1,88	12	2,6	15:44:10	41,78	1,87	4	2,5
I0911240	17/11/2009	15:10:01	42,69	1,05	4	2,5	15:10:01	42,67	1,05	1	2,5
I1002110	24/02/2010	21:21:15	42,26	2,32	6	2,6	21:21:15	42,26	2,32	4	2,4

Table 11 – Events selected for analysis showing differences between manual and automatic results.

For the analysis the four hypocenter variables will be considered: latitude, longitude, depth and origin time; as shown at charts below. Represented values are, in all cases, calculated with the following expression:

$$\text{Represented Value} = \text{Automatic Value} - \text{Value obtained by seismologists (manual)}$$

About processing time, we will consider the reference ($t=0s$) as the moment when the event is declared by Binder and, as said before, the moment when the first event location result is obtained. In fact, when Binder declares the event, it produces 2 different locations: a first one produced by the stacking stage and a second one produced by L1 module, both at the same time.

The analysis of these four parameters, assuming the low number of population of the sample, allows concluding that at the instant when the event is detected a hypocenter exists with a 92% of probability of:

- Lat error ≤ 10 km;
- Long error ≤ 10 km;
- Depth error ≤ 10 km;
- OT error ≤ 1.6 seconds.

And, after 10 seconds, with a probability of 100%, results will be:

- Lat error ≤ 10 km;
- Depth error ≤ 12 km;
- Long error ≤ 10 km;
- OT error ≤ 1.6 seconds.

Many of these lists could be produced depending on the processing times and the desired confidence interval considered; but taking into account the disadvantage of waiting 10 seconds sending EWS alert probably would not be compensated by the increase of the 8% of the confidence interval. So, for this preliminary analysis, the initial location produced by L1 will be selected as a valid location, understanding that a deeper analysis will be required giving an event location delay since an event is detected with less than one second, because the event declaration and this first L1 location appear together at the corresponding shared memory region of DAS2 system.

- **Event magnitude and peak ground calculation**

Since DAS2 computes event magnitude and peak ground using complete event's waveforms, it isn't useful for a EWS implementation. So, it will be necessary to develop a specific module based on different existent algorithms which should be previously analyzed.

In any case, DAS2 modularity will allow the integration of a new module that will read event messages from "pick_ring" and, after requesting seismic waveforms to "WaveServer_V", it will produce event magnitude estimation. Magnitude and peak ground estimation should be written into the "hypo_ring" as an EW message, as currently is done by "localmag" module. All other modules of data processing chain can keep as they are. Some other possibilities exist and can be discussed.

- **Alert system**

The current alert system at IGC is "Teleavis 5" which is in charge of receiving events' messages from DAS2 and sending alerts to different receipts, depending on configured settings. These alert messages could be sent by fax, SMS or e-mail, and their content can be customized. Depending on desired alert formats and contents, the existing system could be used as it is implemented or some changes can be taken into account, especially aspects related with intrinsic redundancy, currently not implemented.

3.1.4. Discussion

The main conclusion of the previous analysis is that the existing network and system could be the base of a EWS implementation for SISpyr region. Its reliability will depend on selected sources and targets because of the heterogeneous coverage of SISPyR network. Despite the results of the simulations to identify blind zones exposed later with some selected sources and targets (cf. paragraph 3.3.1), we conclude with some considerations concerning network and data processing system.

✓ **Network**

- Some additional redundancy is recommended as for the stations as for communication systems. It is desired that all stations are equipped with 2 different communication systems, one of them using satellite transmission, and a backup power supply system.
- It is recommended to implement a redundancy path between Data Centers in order to support the failure of one of them without losing operability and functionality, as shown on Figure 16. Furthermore, waveforms from each station should be directly received by at least 2 different Data Centers.

✓ **Data processing system**

DAS2 system could be the base of a EWS data processing system, but the following improvements and upgrades are necessary:

- Improvement of event detection capability of the system to increase its efficiency discriminating and properly detecting different events when they occur in a very short time.
- Specific settings must be decided and configured adapting event detection and location modules to SISPyR region.
- A module development, resulting of selected algorithms, to estimate events' magnitude and peak ground values.
- Improvement of alert sender system ("Teleavís") incorporating some intrinsic redundancy, allowing to run more than one DAS2 system at the same time and implementing some mechanism (master/slave) to accept having more than one instance of "Teleavís" running at the same time. Depending on requirements, different changes will be necessary to carry out on "Teleavís" module.

3.2. *Spatial analysis of the network*

3.2.1. Consequences of real-time network coverage on early warning

Classically, the analysis of signals triggering an earthquake early warning is conducted from the n first stations to have detected the event. Accordingly, the greater the density of stations in the epicentral zone, the more promptly the imposed number of stations to be activated will be reached, which in turn will reduce as much as possible the time required for data analysis.

Conversely, the occurrence of an earthquake in a zone having poor coverage by a real-time seismic network will not produce a prompt warning due to the greater amount of time needed for the signal to be recorded on n stations.

Mapping the parameter Dn (defined as the distance separating each station from the n^{th} nearest real-time station) thus makes it possible to visualize rapidly those zones where the network's coverage seems sufficient to consider using a EWS based on the analysis of records in n stations, as well as those where coverage is not as satisfactory. Classically the minimum number of stations used in early warning varies, in an array-based regional approach, between two and four stations: we therefore calculate $D2$, $D3$ and $D4$.

An examination of these maps (Figure 20) clearly reveals the configuration of the SISPyR real-time network, which affords better coverage east of the Pyrenees, thanks in particular to the many real-time Catalan stations. However, even with its good coverage, the East Pyrenees area is characterized by a $D4$ value ranging between 30 and 50 km, while the West Pyrenees is characterized by values between 50 and 80 km. Although from a qualitative standpoint this result changes little when a smaller number of stations is considered, the Dn parameter does drop sharply.

The Dn parameter, however, is not fully representative of the real-time seismic network coverage in the sense of early warning since this coverage has to take into account latency of each station: in other words, in our case "coverage" is no longer defined by the question "what is the density of seismic records in a given area?", but "what is the density of seismic records in a given area and at a given instant?".

In the next maps network has been modified, no reception of EJON and new installation of CVIE, in order to have a more reliable approximation.

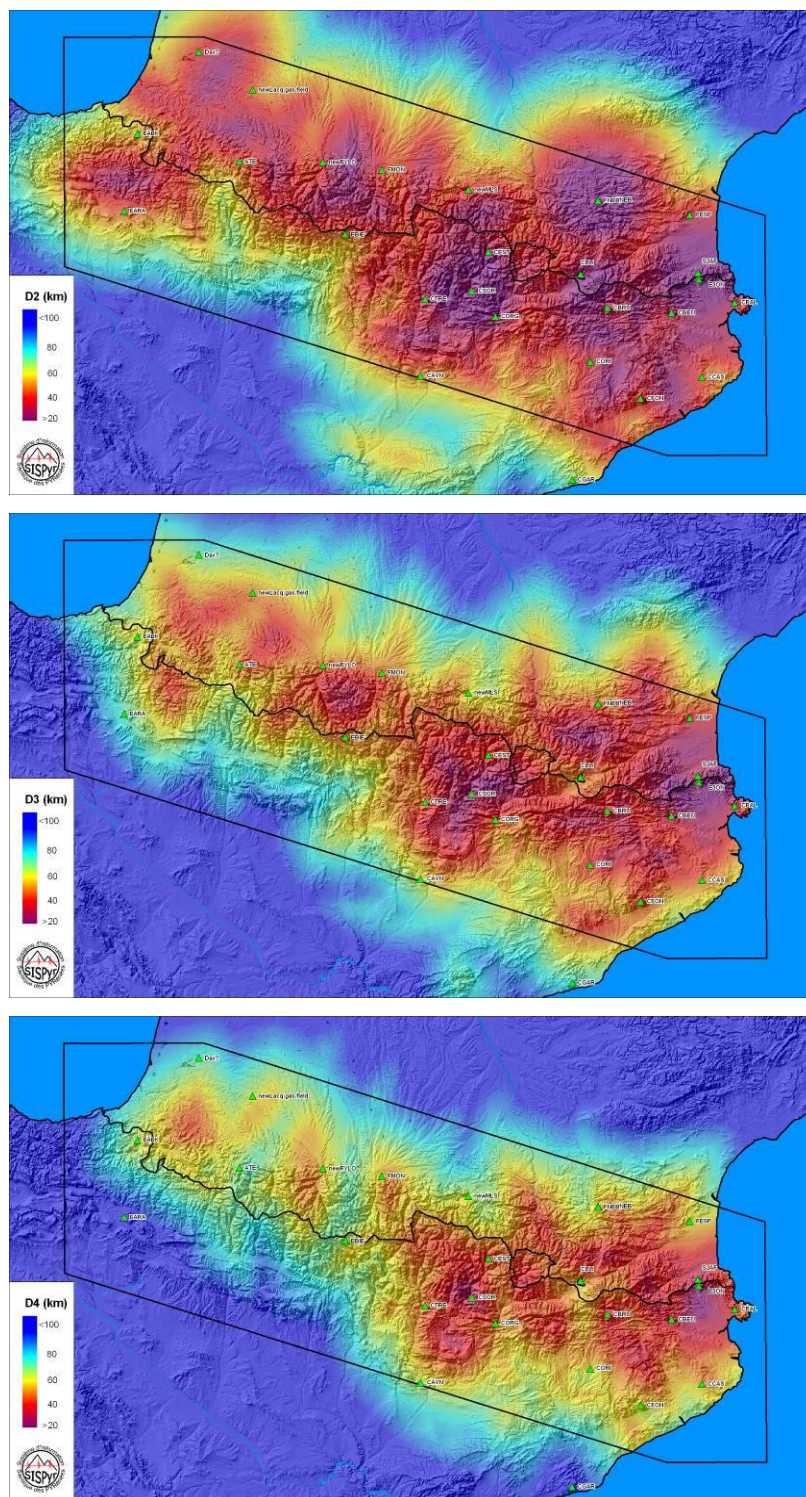


Figure 20 – Mapping D_n (distance to the n^{th} closest real-time station) for two, three and four stations, and locations of the real-time stations affiliated with SISPYR.

3.2.2. System latency and effective network coverage

Hypotheses

It appears necessary to define a common and single terminology for different components involved in the warning time delay. Thus, following terminology is defined:

- Time related to data acquisition: the “**available time**” T_a^n is then defined as being the time at which the n (n refers to the minimum number of records required for the analysis – cf. paragraph 3.2) first records are available at the data center. T_a^n is composed of:
 - t_r^n : “**registering time**” defined as the time necessary for the trigger of the n first stations and the record of the P wave ;
 - t_l : “**latency time**” defined at each station as the typical time separating the recording itself to its reception at the data centre.

T_a^n is then equal to the longer value of the sum between t_r and t_l at each n stations.

- Time related to data analysis: the “**analysis time**” T_{an} is then composed of:
 - t_e : “**event time**” defined as the time delay necessary to declare the seismic event and to locate it;
 - t_p : “**processing time**” defined as the time necessary to analyse the data in terms of early warning purpose (assessment of magnitude, opportunity of alerts, etc.).

The “**warning time**” T_w is finally defined as being the time at which the system is able to produce an alert. ($=t_a^n + t_{an}$). The “**lead time**” T_l is then defined for a given location as the time interval between the arrival of the warning and the arrival time of the S waves⁵. This terminology is summarized on Figure 21.

⁵ That definition of T_l does not consider time necessary to transmit and disseminate the early-warning which depends on the way of transmission: fax, mobile, etc.

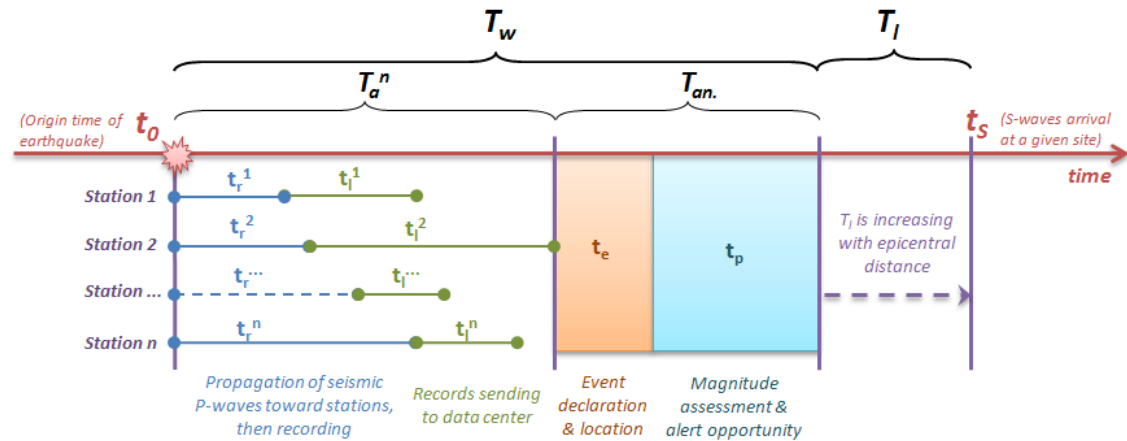


Figure 21 – Different components of warning time.

Regional assessment of effective network coverage

As mentioned above on paragraph 3.1.3.i, latency of the real-time seismic network associated to data transmission from each stations to a common data centre strongly conditions efficiency of a EWS. Then, the complete system latency time represented by the so called “warning time” T_w (cf. Figure 21) will be for a specific hypocenter the result of adding seismic P-waves travel times to the n nearest stations plus recording time-length (t_r^n), stations latency (t_l^n) and data processing time (T_{an}).

Thus, this complete system latency may be regionally assessed:

1. modifying the net because of future changes, no reception of EJON and the new installation of CVIE;
2. modifying distance-maps of paragraph 3.2.1 removing - during assessment of D_n - close-field stations that exhibit a time interval between P and S waves arrival smaller than the time-length of the P wave necessary to assess Pyrenean earthquakes' magnitude in real-time: in our analysis, we will consider that this time-length is equal to 2 seconds (see chapter 6).
3. converting these new maps into time-maps considering a typical P-wave velocity of 6 km/s⁶;
4. taking stations' latency times into account: so as to do that, we will considered average values indicated in Table 10 majored by one sigma ;

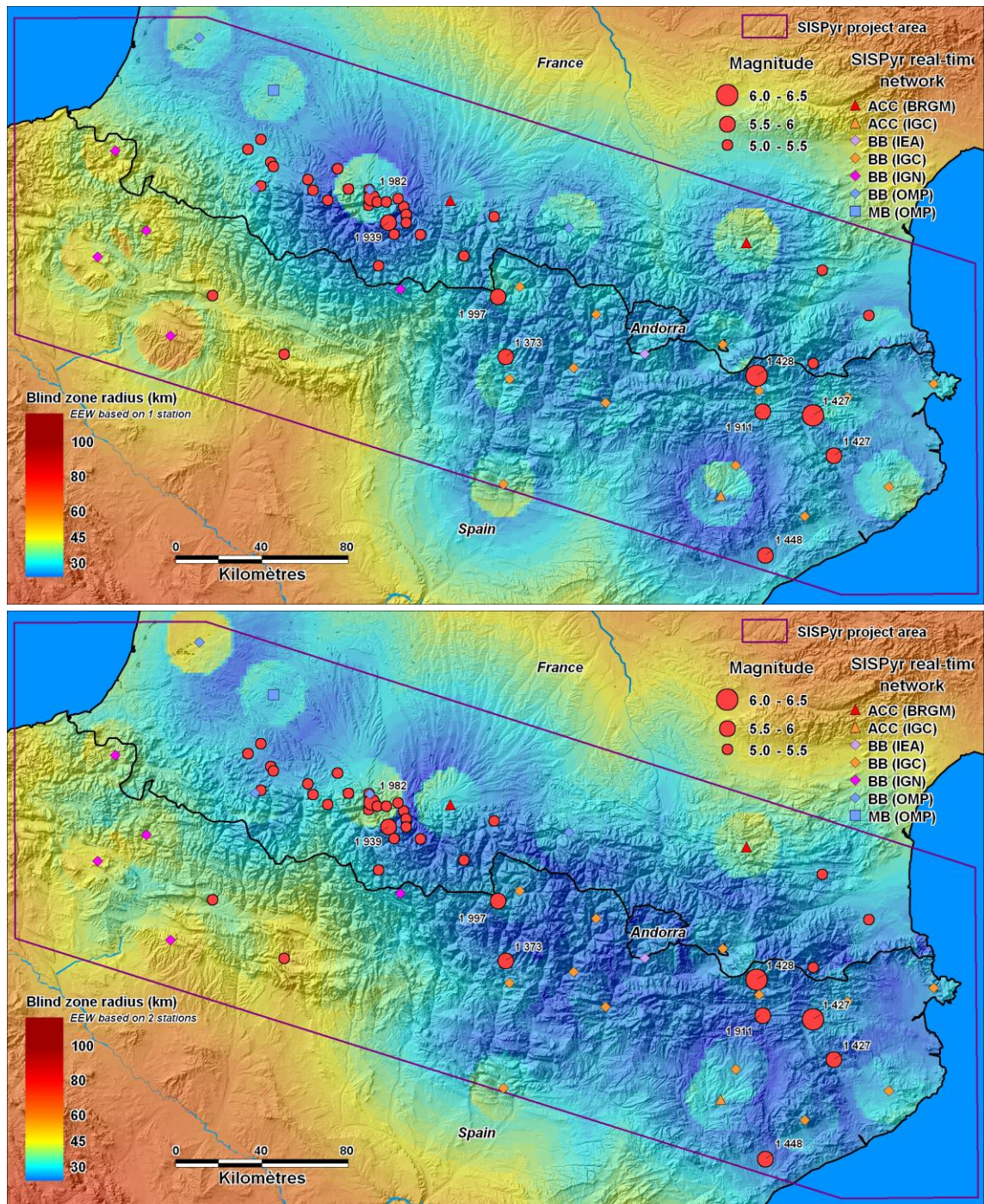
⁶ From Souriau and Pauchet, 1998.

5. applying to these new maps a 2 seconds offset corresponding to the minimum recording time and to the analysis time T_{an} .

Nevertheless, time necessary to send out an alert (T_w) is not a very pertinent information in itself. Indeed, to make it pertinent, it is necessary to confront it with information about arrival time of destructive waveforms (i.e. S-waves and following surface waves). As a consequence, we convert these maps into maps showing the extension of blind-zone knowing that its radius is given by the formula: $D_{bz} = (V_S^2 * T_w^2 - z^2)^{0.5}$, with z the earthquake's focal depth and V_S velocity of S-waves ($V_S = V_P/1.75^7$). Neglecting z this formula becomes: $d_b \sim V_S * T_w$.

These maps are shown on Figure 22. On map corresponding to the "1 station" map, radius of blind zone is organized in concentric circles surrounding stations with an increase of radius with distance. Nevertheless, for all cases, one can see an increase of its radius very close to stations. This paradox is due to the fact that exists a minimum distance, about 15.6 km, for which a given station is useless because of an insufficient time difference between P and S waves' arrivals for the magnitude assessment (based on a minimum 2s P-wave length in the current analysis). Another noticeable thing that can be seen on this first map is the difference of close-field values between stations: that is due to differences existing between station's communication latency (for instance, radius of blind-zone is smaller near AVIN & PYLO stations than near EALK, EARA or YSOS stations that are associated to greater communication latency). As more stations are required for issuing the early-warning, one can observe on following maps a progressive extension of blind zone, as well as a confirmation of inhomogeneity of results in whole Pyrenees due to differences on seismic monitoring effective coverage. As a consequence and as previously said, such a system would be much more efficient for earthquakes occurring eastward of the Pyrenean massif.

⁷ From Souriau and Pauchet, 1998.



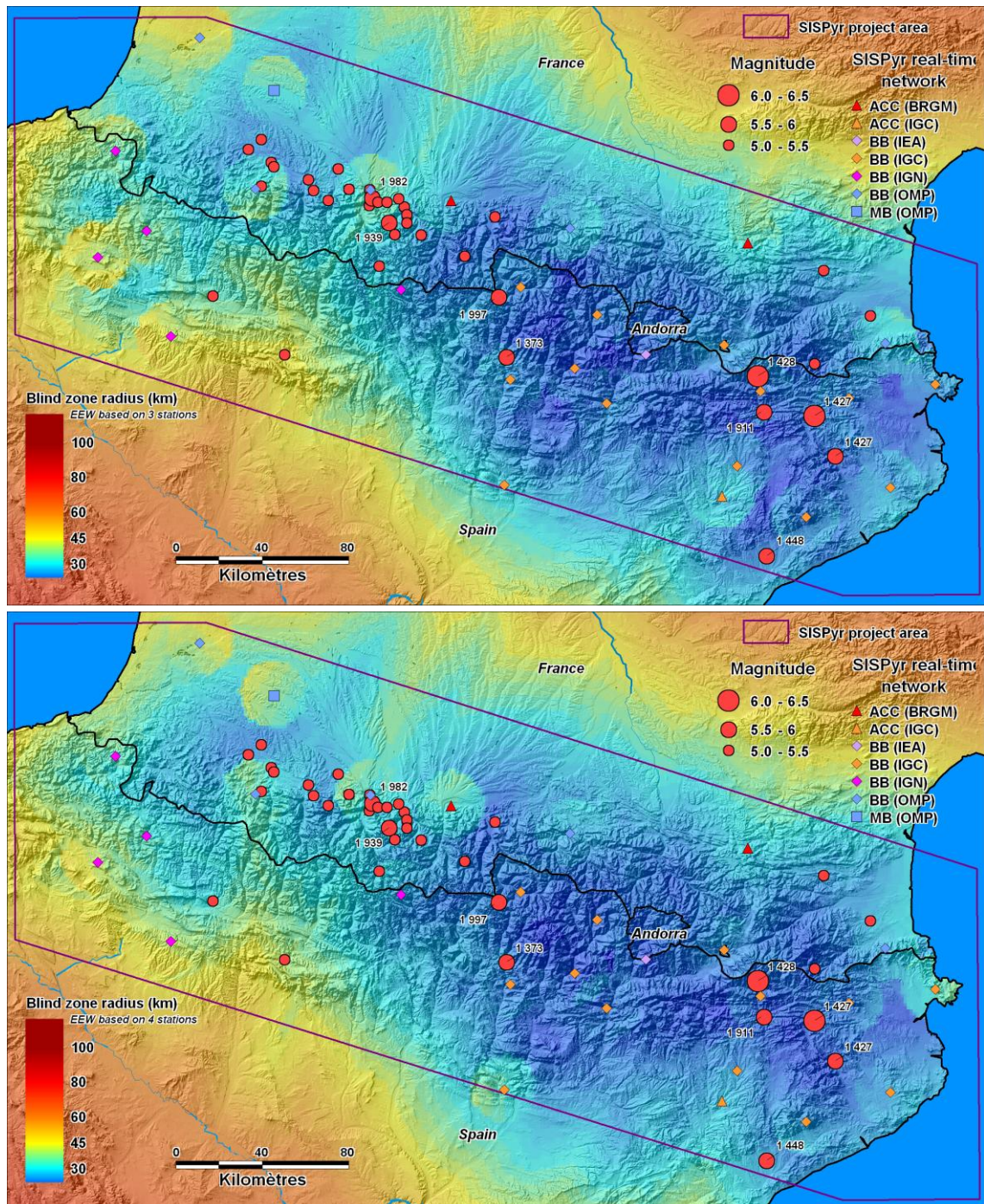
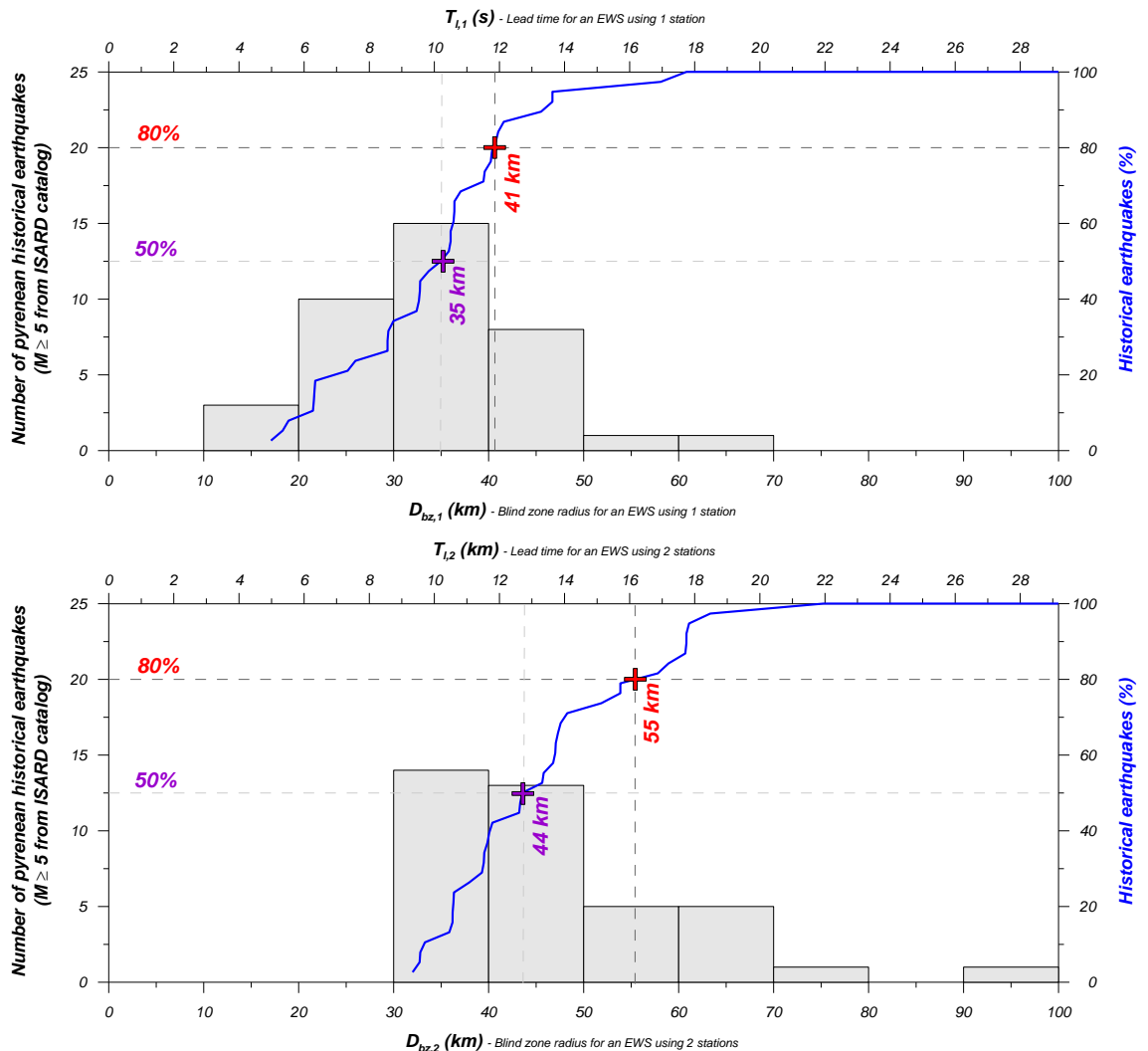


Figure 22 – Mapping extension of the blind zone in function of the epicentre location with an EWS using a minimum of 1, 2, 3 or 4 stations (from up to down) for magnitude assessment. Are also represented the SISPYR seismic real-time network as well as epicentral locations of the main Pyrenean earthquakes ($M \geq 5$ for the period 580 – 2003 / Source: ISARD catalogue).

What is important in the framework of a EWS is actually to achieve a good coverage by the real-time network with respect to potential seismic sources and not to the entire land area that one intends to protect. Radius of blind zone must accordingly be confronted with Pyrenean seismicity in order to ascertain whether the seismogenic zones most liable to generate destructive earthquakes are appropriately covered by the SISPyR real-time network. To do so, we have compared the mapping of blind-zone extension with the epicentral locations of the main historical earthquakes that have occurred in the Pyrenees (magnitude greater or equal to 5 – ISARD catalogue) – cf. Figure 22. A preliminary examination of these maps shows that most of these historical epicenters lies in zones that are fairly well covered the SISPyR real-time network. More precisely, and considering only those epicenters that lie within the project's area, it turns out that 80 % of these events are associated to radius of blind-zone smaller than or equal to 41, 55, 63 and 68 kilometers respectively for EWS based on analysis performed thanks to 1, 2, 3 or 4 stations (Figure 23).



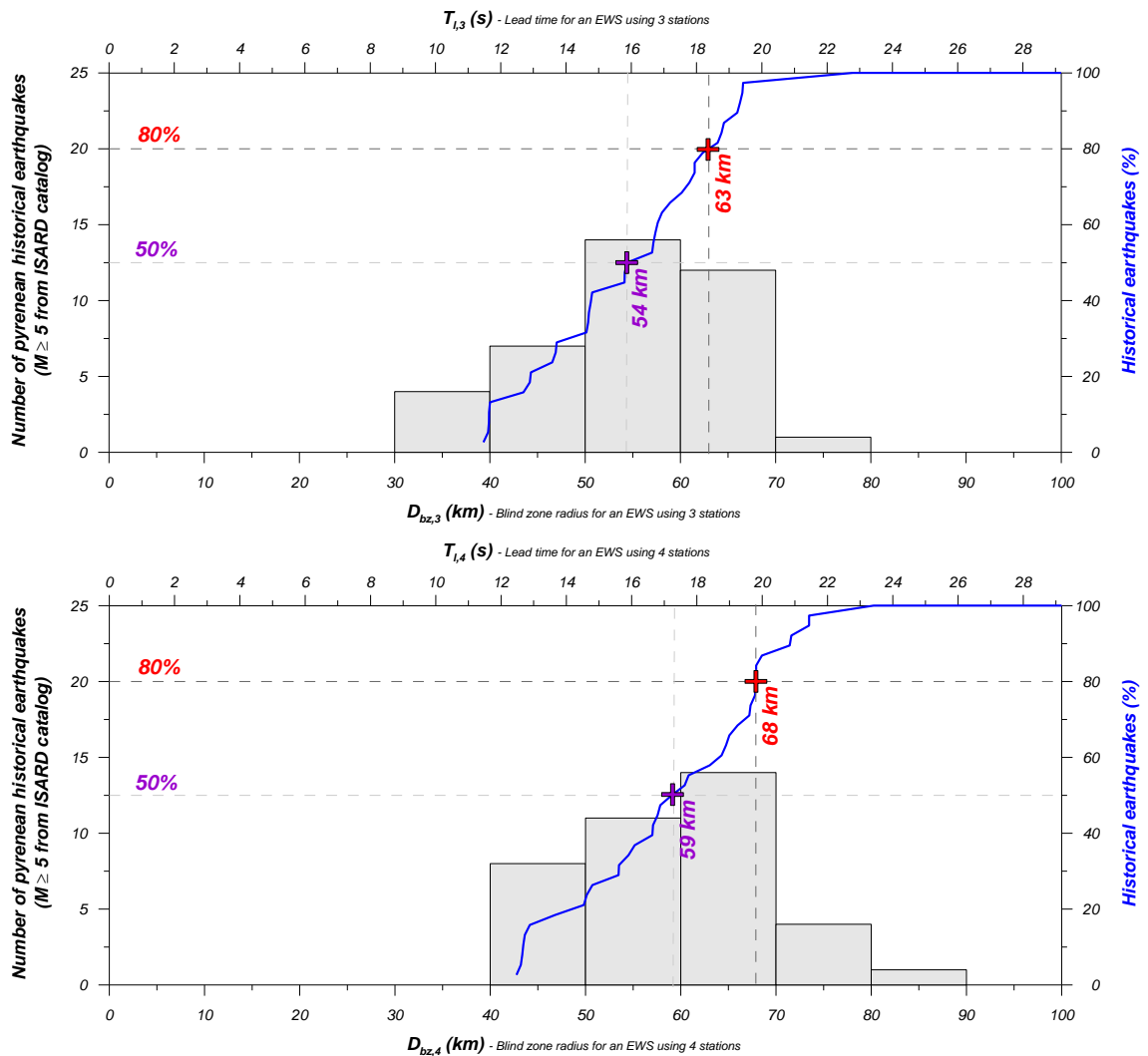


Figure 23 – Distribution of the epicentres of the main Pyrenean earthquakes ($M \geq 5$ for the period 580 – 2003 / Source: ISARD catalogue) versus extension of the blind zone (D_{bz}) and lead time (T_l).

3.3. Theoretical performance analysis

The next step is to assess if, in case of destructive Pyrenean earthquake, damaged area (at least its outer part) could benefit of early warning, or conversely if blind-zone is likely to cover entirely sinister area. Indeed, a feasibility study for a EWS presupposes that one is able to assess the delay times to be expected within the zone of concern. This delay, actually, conditions the system's effectiveness. With this in mind, we have proceeded to perform simulations of lead times.

3.3.1. Earthquake early warning scenarios

In a first time, we have chosen to illustrate the potential usefulness of Pyrenean EWS through scenarios corresponding to 4 real historical events that occurred in Pyrenees (cf. Figure 24):

1. 02/02/1428 Ripollès earthquake: $M_I \sim 6.2$;
2. 21/06/1660 Bigorre earthquake: $M_I \sim 5.8$;
3. 19/11/1923 Viella earthquake: $M_I \sim 5.5$;
4. 13/08/1967 Arette earthquake: $M_I \sim 5.3$.

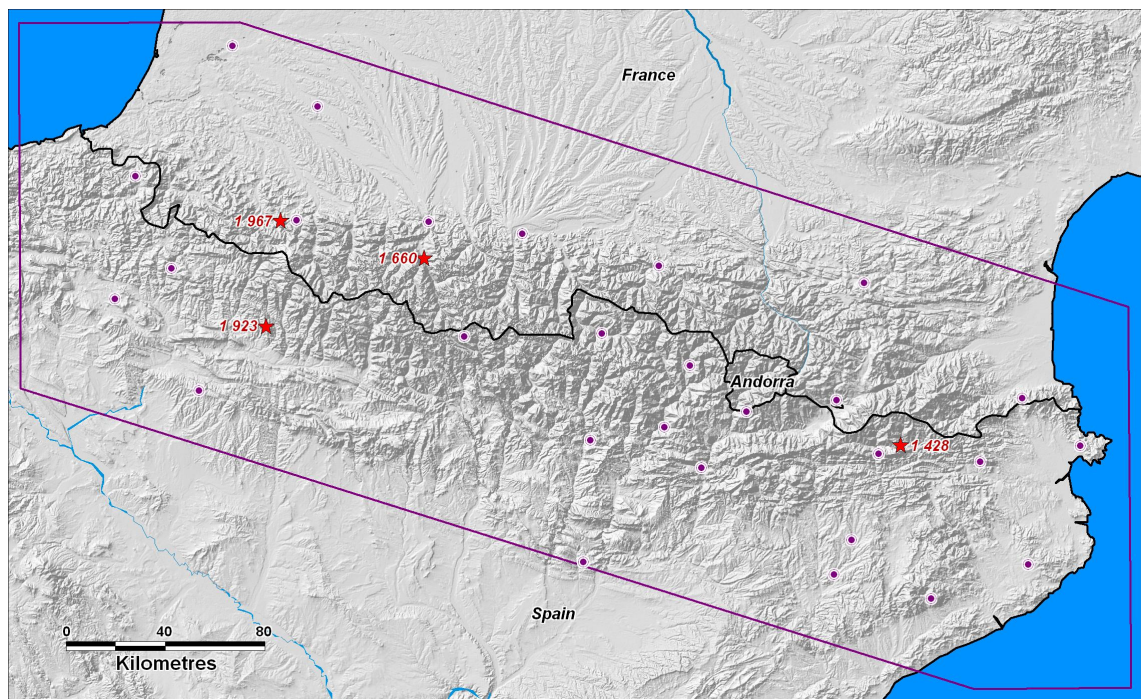


Figure 24 – Location of epicentres of historical earthquakes considered in early warning scenarios. Are also represented the real-time SISPYR network as well as the area covered by the SISPYR project.

1428 Ripollès earthquake

The first seismic scenario considered corresponds to an earthquake similar to the Maximum Observed earthquake of the Eastern Pyrenees, occurred the 2nd of February of 1428, in the Ripollès area, near the French-Spanish border. The study of this earthquake has been published by Olivera et al (2006),

determining the following focal parameters: epicentral intensity (I_0) of IX, $M_w=6.5$ ($M_l=6.2$), and focal depth (z) of 9 km.

Corresponding intensities observed in Spain and France, with a zoom of the epicentral area, are shown on Figure 25.

In order to simulate the intensities probably felt in the region the attenuation relation from Sponheuer (1960, without site effects) has been used:

$$I = I_0 - 3 \cdot \log_{10} \left(\frac{\sqrt{d_{epicentral}^2 + z^2}}{z} \right) - 3 \cdot 0.001 \cdot \log_{10}(e^1) \cdot \left(\sqrt{d_{epicentral}^2 + z^2} - z \right)$$

The best fit with observed intensities of Figure 25 is got with an epicentral intensity of IX and a focal depth of 10km. The resulting intensity map is compared on Figure 26 and Table 12 with blind zone extension corresponding to Pyrenean EWS based on a 1, 2, 3 or 4 stations analysis.

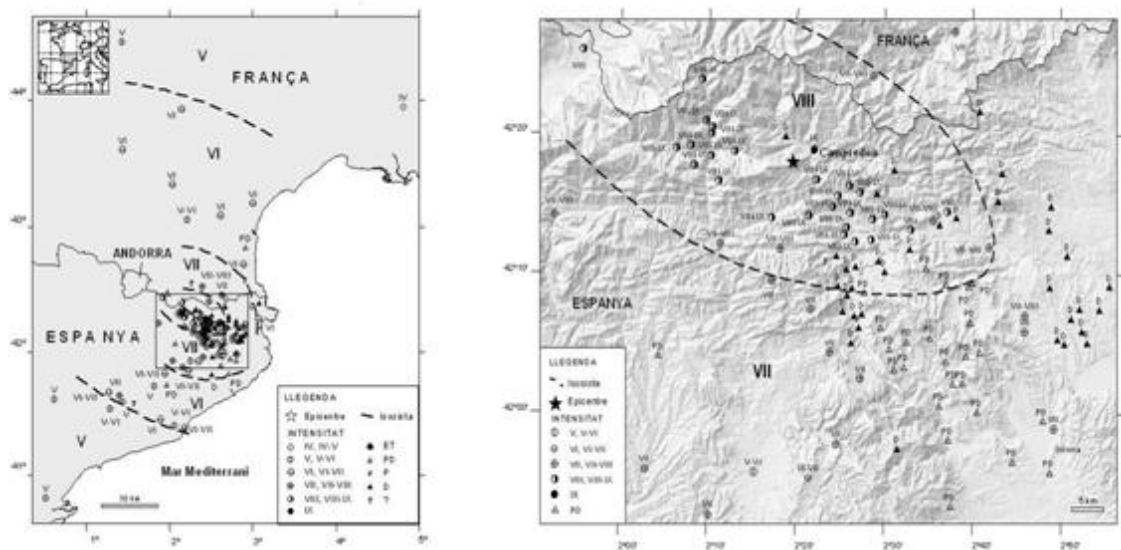


Figure 25 – Observed intensities and epicentre of the 2nd of February of 1428 earthquake (from Olivera et al, 2006).

The first interesting thing that has to be notice from this scenario, is that all the EWS configurations considered (i.e. with a minimum of 1, 2, 3 or 4 stations used) lead to blind-zone less extended that isoseist corresponding to intensity VI, which can be considered representative of the damaged area: **this criterion (i.e. blind-zone less extended that isoseist VI) will be considered afterwards as the minimum performance guarantying efficiency of a EWS.** In the case of the 1428 event, blind zone is even always smaller than isoseist VII. Then one cans conclude that an operational declination of the current real-

time network into a EWS could be suitable for major earthquakes such as the one of 1428, at least on the eastern part of the Pyrenean Massif.

Regarding more in details Table 12, we can see that among closest big cities, Girona would be the more severely stricken city with intensity VII that could be alerted thanks to a EWS, while Perpignan and Andorra la Vella would have intensity slightly smaller.

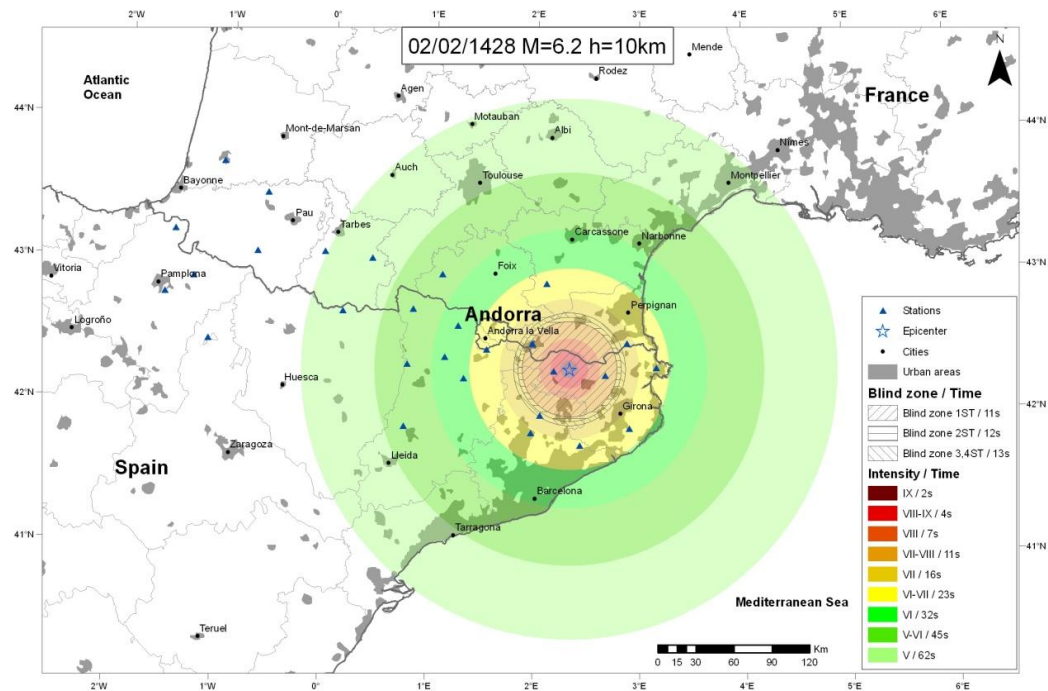


Figure 26 – Comparison between isoseist curves corresponding to the 02/02/1428 earthquake and blind-zone extensions of a virtual Pyrenean EWS based on the current real-time SISPy network.

INTENSITY	IX	VIII-IX	VIII	VII-VIII	VII	VI-VII	VI	V-VI	V		
Epicentral dist. (km)	7	15	24	38	55	79	109	154	212		
Affected cities	<div><div></div></div>				<div><div></div></div>	<div><div></div></div>	Girona (16s)	Perpignan (19s) And. Vella (21s)	Carcassone (30s) Foix (28s) Barcelona (30s)	Narbonne (33s)	Albi (53s) Toulouse (48s) Montauban (61s) Auch (62s) Tarbes (64s) Lleida (48s) Tarragona (47s) Montpellier (57s)
Blind-zone extend											
S-waves arrival time											

Table 12 – Comparison between extension of each isoseist curve with extension of blind-zone corresponding to a EWS based on 1, 2, 3 or 4 stations (dash parts): scenario corresponding to the 1428 earthquake.

Knowing that the alert would be really early in the case of the 1428 event is not enough and estimation of lead times T_l – corresponding to the delay available at a given point to take protection actions before S-waves arrival – is also needed. Making the estimation at the outer part of isoseist VI, it appears that for this scenario the lead times vary from roughly 17 seconds in the case of a EWS using 4 stations, to around 19 seconds for an onsite system (cf. Figure 27).

The 4-station configuration corresponds to the current SISPyR automatic system which needs a minimum of 4 stations to declare an earthquake. It would lead to following lead times T_l : 3 seconds at Girona (I=VII), 6 seconds at Perpignan and 8 seconds at Andorra la Vella (I=VI-VII), 15 seconds at Foix and 17 seconds at Barcelona and Carcassone (I=VI).

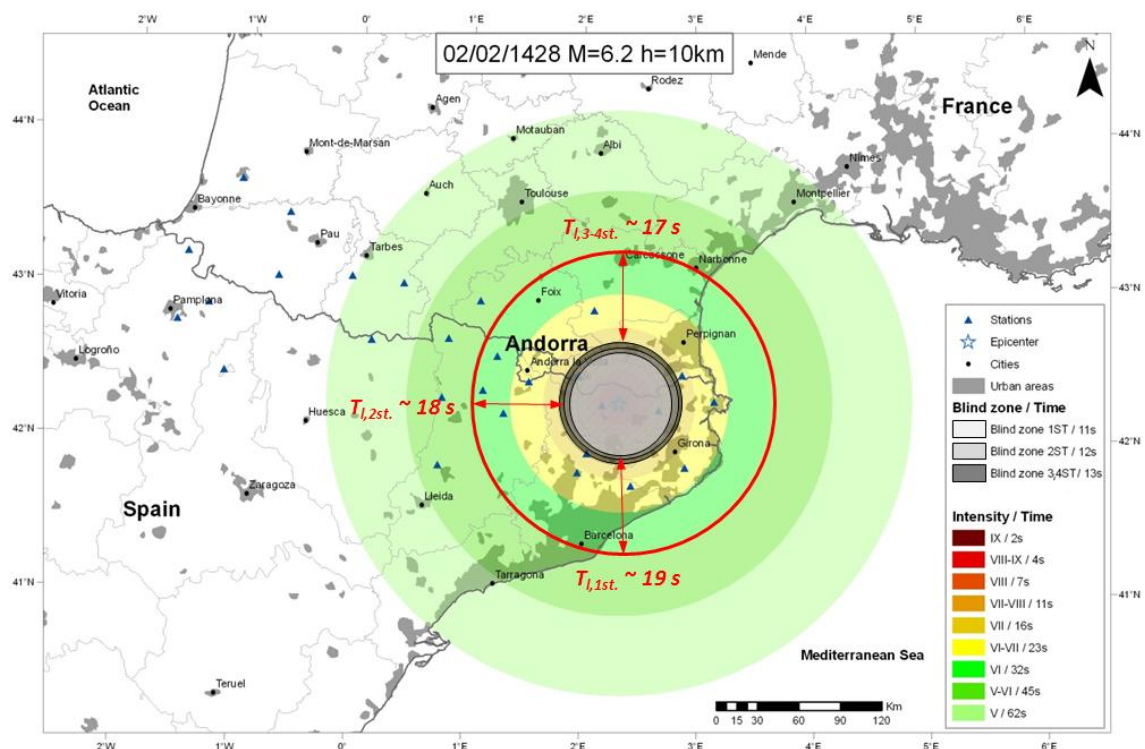


Figure 27 – Assessment of the lead times T_l at the outer limit of isoseist VI corresponding to the 02/02/1428 earthquake.

1660 Bigorre earthquake

The second seismic scenario corresponds to an earthquake that occurred the 21st of June of 1660 in the Bigorre area near the French-Spanish border. Historical sources suggesting an epicentral intensity of VIII-IX and considering the regional typical focal-depth value of 10 km, we get the intensity map shown on Figure 28 and described on Table 13. Regarding intensity levels in biggest

cities, we can see that Tarbes would be the one with the highest intensity (VII) while Pau would have a lower but also damaging intensity (VI-VII).

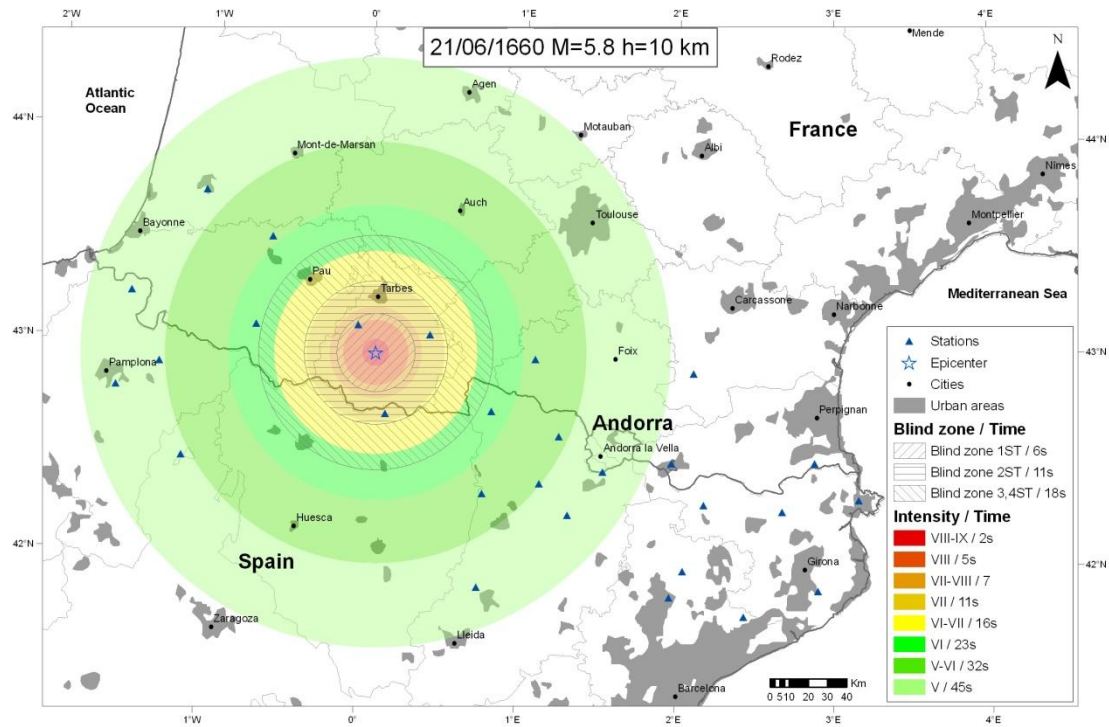


Figure 28 – Comparison between isoseist curves corresponding to the 21/06/1660 earthquake and blind-zone extensions of a virtual Pyrenean EWS based on the current real-time SISPYR network.

INTENSITY	VIII-IX	VIII	VII-VIII	VII	VI-VII	VI	V-VI	V
Epicentral dist. (km)	7	17	24	36	53	77	110	154
Affected cities	<div>6s</div>			<div>Tarbes (9s)</div> <div>11 s</div>		<div>Pau (15s)</div> <div>18 s</div>		<div>Auch (26s)</div> <div>Huesca (30s)</div>
Blind-zone extend								
S-waves arrival time								
								<div>Mont-de-Marsan (33s)</div> <div>Bayonne (42s)</div> <div>Pamplona (39s)</div> <div>Lleida (46s)</div> <div>And. Vella (39s)</div> <div>Toulouse (40s)</div> <div>Agen (43s)</div>

Table 13 – Comparison between extension of each isoseist curve with extension of blind-zone corresponding to a EWS based on 1, 2 or 3-4 stations (dash parts): scenario corresponding to the 1660 earthquake.

As for the 1428 event, all the EWS configurations considered lead to blind-zone less extended than isoseist VI in case of 1660 earthquake. Nevertheless, the lesser magnitude of this second earthquake conducts to performances not quite

as the previous ones. Those results in the fact that no more than the half of isoseist VI could be alerted thanks to EWS based on 3 or 4 stations (that 2 configurations lead to same results in this specific case): in particular, Tarbes and Pau could not be alerted. Regarding 1 and 2 station(s) system's configurations, early warning could respectively be used for isoseists VII and smaller and VI-VII and smaller.

In respect of lead times, it appears that for the 1660 scenario T_l varies from roughly 4 seconds in the case of a EWS using 4 (or 3) stations, to around 15 seconds for an onsite system. The 4-station configuration would lead to following lead times T_d : Auch, Huesca, Pamplona, Toulouse, Mont-de-Marsan and Bayonne could be alerted with response times of 8, 12, 21, 22, 15 and 24 seconds respectively. Concerning the single station configuration, it would leads to lead times of 3 and 9 seconds for Tarbes ($I=VI-VII$) and Pau ($I=VII$) respectively.

1923 Viella earthquake

The third seismic scenario considered corresponds to the earthquake that occurred the 19th of November of 1923, in the Viella area, close to the French-Spanish border. The best fit with observed intensities (Susagna et al., 1994) is got with an epicentral intensity of VIII and a focal depth of 5 km. The resulting intensity map is compared on Figure 29 and Table 14 with blind zone extension corresponding to Pyrenean EWS based on a 1, 2, 3 or 4 stations analysis.

Contrary to previous scenarios corresponding to 1428 and 1660 events, EWS does not seem to be useful in the case of the Viella earthquake: in other words, in any cases the whole isoseist VI is located into the blind-zone. This comes from the combination between the lesser magnitude and focal depth of this earthquake which are traduced by narrower isoseists, and the lower density of the network in Central Pyrenees that in Cataluña which implies longer warning times. Additionally, it may be noticed that 3 and 4 stations configurations are again equivalent (as for the 1428 and 1660 events), apart from 2 stations configuration.

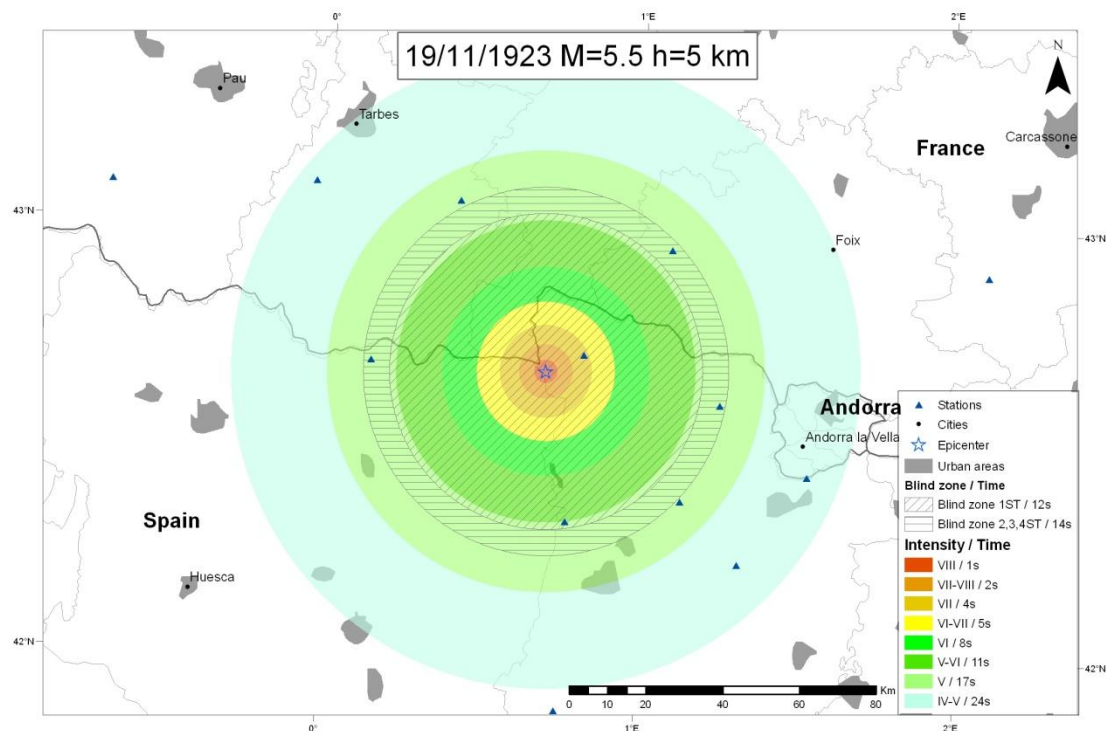


Figure 29 – Comparison between isoseist curves corresponding to the 19/11/1923 earthquake and blind-zone extensions of a virtual Pyrenean EWS based on the current real-time SISPyR network.

INTENSITY	VIII	VII-VIII	VII	VI-VII	VI	V-VI	V	IV-V
Epicentral dist. (km)	3	7	12	18	27	39	57	82
Affected cities								And. Vella (21s) Foix (24s) Tarbes (24s)
Blind-zone extend							12s 14s	
S-waves arrival time								

Table 14 – Comparison between extension of each isoseist curve with extension of blind-zone corresponding to a EWS based on 1, 2 or 3-4 stations (dash parts): scenario corresponding to the 1923 earthquake.

1967 Arette earthquake

The fourth seismic scenario considered corresponds to the earthquake that occurred the 13th of August of 1967, in the Arette area, near the French-Spanish

border. With an epicentral intensity of VIII and a focal depth of 5km, we obtain the resulting intensity map shown on Figure 30 and detailed in Table 15.

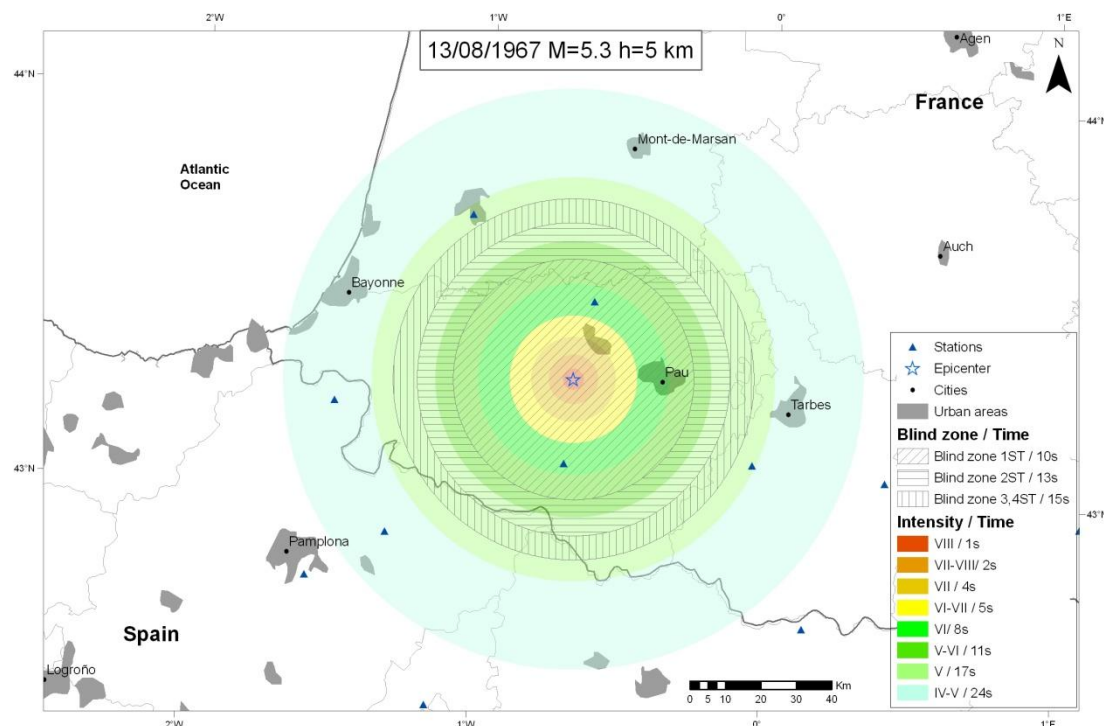


Figure 30 – Comparison between isoseist curves corresponding to the 13/08/1967 earthquake and blind-zone extensions of a virtual Pyrenean EWS based on the current real-time SISPYR network.

INTENSITY	VIII	VII-VIII	VII	VI-VII	VI	V-VI	V	IV-V
Epicentral dist. (km)	3	7	12	18	27	39	57	82
Affected cities	Pau (8s)						Bayonne (21s) Mont-de-Marsan (20s) Tarbes (19s)	
Blind-zone extend								
S-waves arrival time								

Table 15 – Comparison between extension of each isoseist curve with extension of blind-zone corresponding to a EWS based on 1, 2 or 3-4 stations (dash parts): scenario corresponding to the 1967 earthquake.

As for the Viella earthquake scenario, it appears that a EWS based on the current SISPyR real-time network would be ineffective in case of seismic events similar to the 1967 Arette earthquake.

3.3.2. Exploration of theoretical performance at regional scale

Specific analysis performed on previous paragraph 3.3.1 may be extended to regional scale considering that locations of historical events presented on paragraph 3.2 are representative of regional seismicity. Indeed, placing at each of these epicentres virtual earthquakes with magnitudes ranging from 5.0 to 6.5, it is then possible to assess correspondent theoretical isoseists as done on paragraph 3.3.1, and to compare them with warning times in order to deduce associated lead times.

In order to interpret this new analysis in an easier way, we represent on Figure 31 only results corresponding to percentiles 50 and 80% as done on paragraph 3.2 (cf. Figure 23).

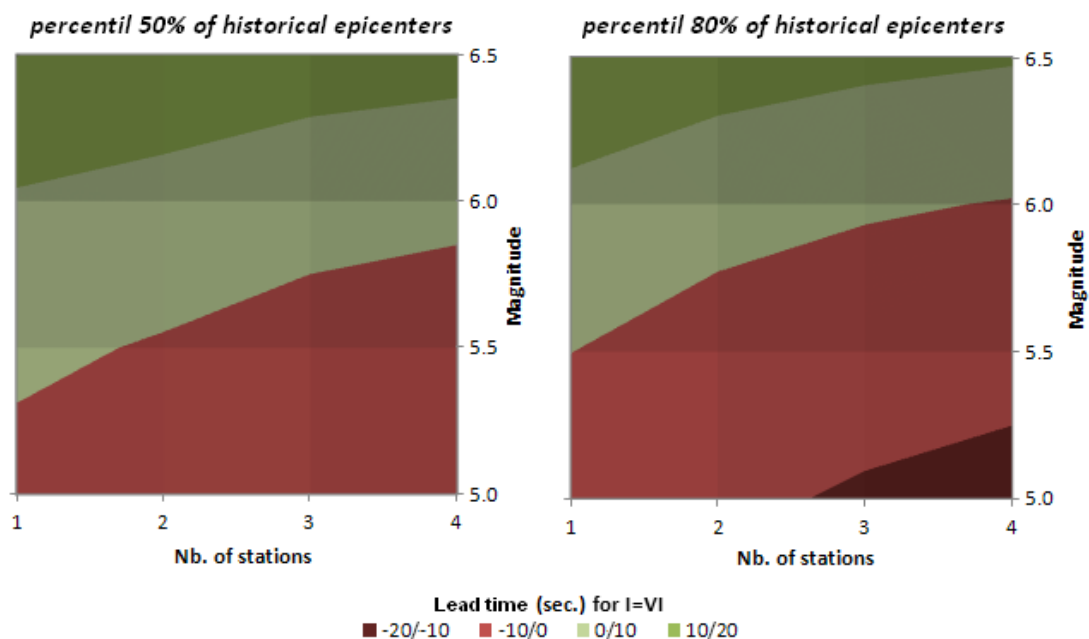


Figure 31 – Theoretical performance at regional scale of a Pyrenean EWS confronting past seismicity to theoretical blind zones extension. Configurations for which 50% (left) and 80% (right) of historical epicentres lead to positive lead times (i.e. blind zones smaller than isoseist I=VI) are indicated thanks to green colour gradation, while negative values are indicated thanks to red colour gradation.

Figure 31 clearly underlines that, unless to face major earthquake characterized by a broad sinister area like the ones of 1428 or 1660 illustrated on chapter 3.3.1, performances of a EWS based on the current SISPyR network should – in

order to be fully efficient on the whole Massif of Pyrenees – be able to emit alerts from an analysis on a very limited number stations (1 or 2). Otherwise zones incurring damage (intensities greater than or equal to VI) risk lying within the blind-zone and accordingly could not benefit from early warning. In that cases, lead times of ten or so seconds are expected far from the epicenter, and it is highly probable that, in view of the relatively moderate Pyrenean seismicity, the associated intensities would be fairly weak (IV to VI) and do not justify the implementation of a EWS.

It should be borne in mind, however, that besides that fact that these are only preliminary simulations based on robust hypotheses, the used intensity prediction equation does not take into account potential lithological site effects, which could cause damage at greater epicentral distances, in zones that could benefit from longer early lead times. Furthermore, in zones with better coverage by the real-time network, the lead times will be longer, thereby enabling the extent of blind-zone to be reduced.

3.4. *Discussion*

Even though regional EWS usually rely on dedicated seismic networks, a look on the SISPyR real-time network shows that the existing stations may be used for early warning purposes. Indeed, current SISPyR real-time network still satisfies an important part of EWS requirements such as real-time centralization of data. Moreover, even though it has still a limited coverage, the real-time network is composed of numerous seismic stations.

Then, having a look on both intensity predictions related to earthquake scenarios and theoretical blind-zone extension shows that in some cases the current network could be used efficiently to provide early warnings of seconds up to around twenty seconds in areas where intensity greater or equal to VI are expected. Nevertheless, illustrations such as Figure 22 also indicate that performances of a EWS based on the SISPyR network would not be homogeneous in whole Pyrenees due to differences on seismic monitoring coverage. As a consequence, such a system would be much more efficient for earthquakes occurring eastward of the Pyrenean massif.

In spite of encouraging results, it is then important to point out that operational setting up of this type of innovative tool in Pyrenees technically faces to important barriers due to 1) the moderate seismicity context of Pyrenees implicating strong attenuation of destruction effects with distance that implies that the EWS should be effective at short epicentral distances, and to 2) the current limited coverage of the real-time network as well as to the time-latency of the existing system.

Unlike other countries equipped with denser seismic monitoring networks and characterized by high levels of seismicity, we are not in a position to take into consideration a longer data analysis in order to warn and thereby optimize system reliability, for the consequence would be blind-zones that were too extensive and would totally cover the zones of potential damage. Conversely, this would suggest that we should concentrate on the fastest analysis methods by reducing to a minimum the time required for data acquisition (a first analysis on a very small number of stations with a very short time window after the detection of the P wave). Thus it is plausible to consider a “hybrid” system that would initially conduct an “onsite” analysis (from a single station) and then make the warning gradually more substantive by means of a regional approach (using several stations).

Another way making a Pyrenean EWS more efficient would be obviously to make the network denser favouring low latency data-transfer solutions. Then, considering an ideal network with a regular topology triangular mesh with a mesh-size (S_M) of 30 km and a worse-case epicentre location below a station (inducing a difference of arrival time between P and S wave at this station smaller than the required 2 seconds: ~1.25 s.) as shown on Figure 32, one can expect a 44 km blind-zone radius associated with:

- No early warning for areas with intensities greater or equal to VI in case of earthquakes with magnitude of 5.0 or 5.5;
- An early warning with lead times reaching a maximum of around 6 and 18 seconds for the area with $I \geq VI$, respectively for earthquakes with magnitude of 6.0 or 6.5 and a focal depth of 10 km.

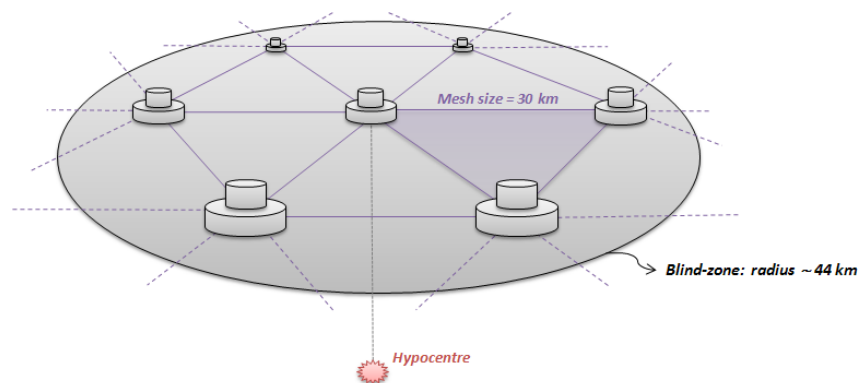


Figure 32 – Hypothesis of an earthquake occurring below a station belonging to a triangular-mesh network.

Conversely, in case of “well-located” epicentres (cf. Figure 33), this ideal network topology could theoretically provide slightly better results as shown on Figure 34. This “ideal network” approach allows us to say that in any cases

principle of early-warning do not seem adapted for earthquakes associated to magnitude lower than around 5.7 (depending on focal depth, local attenuation properties, site effects, etc.).

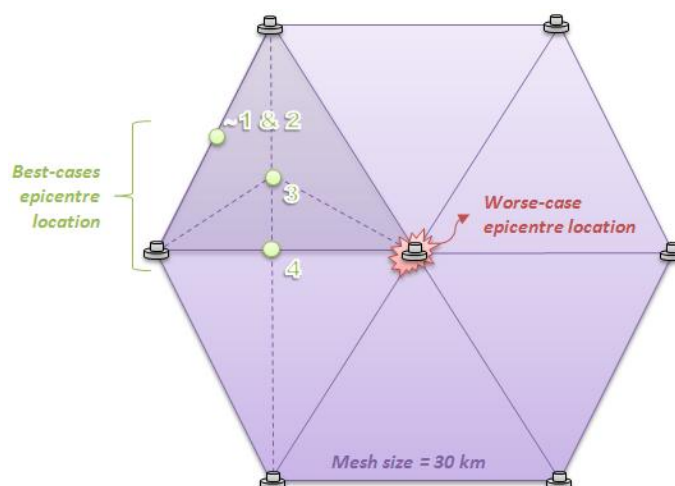


Figure 33 – Hypothesis of an earthquake occurring at different positions inside a triangular-mesh network. Numbers indicated close to each “best-cases” epicentres’ locations are related to the minimum number of stations used by the EWS.

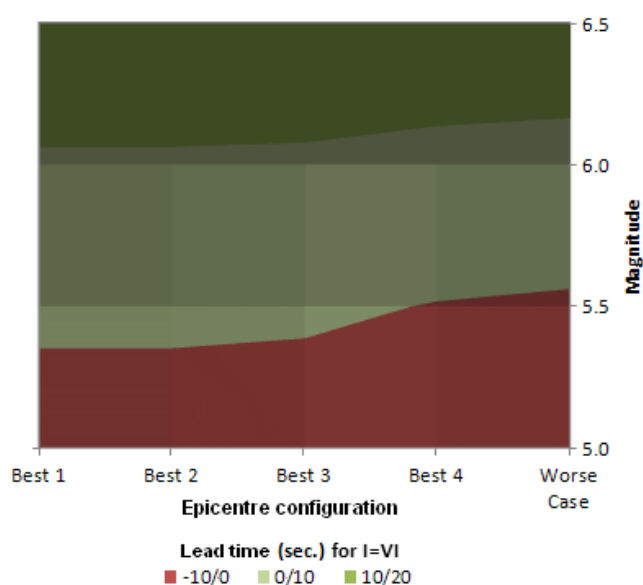


Figure 34 – Theoretical performance at regional scale of a Pyrenean EWS lying on a 30 km triangular-mesh network, for different epicentre configurations corresponding to Figure 33.

In any cases, even on configurations that theoretically lead to early-warnings, it is necessary to assess in what extend these warnings could allow to minimize impact of earthquakes occurring in Pyrenees (cf. chapter 9).

4. Catalogue of Pyrenean waveforms

To be able to test on the Pyrenees the different methodologies for estimating magnitude in real time that were identified in chapter 3.3, a catalogue of seismic signals representative of Pyrenean seismicity must first be compiled.

4.1. *Data selection*

An attempt is made to build a catalogue of waveforms, not statistically representative of seismicity all along the Pyrenees chain, but containing as many records as possible corresponding to all the magnitude ranges to be considered so as best to constrain our regression analyses. While particular attention must be paid to large-magnitude events (the highest probable value being on the order of 6.5), which are liable to produce the most damage, recordings of more moderate earthquakes should also be included so as to be certain we can distinguish them in the framework of a real-time analysis.

Considering the moderate seismicity that prevails in the Pyrenees and the progressive installation of seismological instruments in the range, we have in a first time integrated into the catalogue all available data, regardless of the type of instrument or mode of transmission that was used, so as to have access to a maximum number of seismic traces. Nevertheless, due to the absence of real-time transmission on short-period SISPyR seismic stations and to the lower frequency band of these stations, they have been disregarded in our catalogue. In addition, since the methodologies for estimating magnitude in real time to be tested were based on an analysis of vertical recordings, only this component was considered.

In practice, the waveform catalogue for Action 5 is an outgrowth of the one compiled in the framework of Action 3, which is composed of accelerometric and velocimetric records provided by the various organizations that operate stations in the region (IGN, IGC, OMP, BRGM). In order to supplement this original catalogue, the RAP-Pyrenees (OMP/BRGM) accelerometric data covering the period 2001-2009 were added, together with additional accelerometric signals contributed by IGC.

At the end of the day, the Pyrenees catalogue used in Action 5 is made up of recordings corresponding to 193 events with LDG local magnitudes ranging between 2.5 and 5.6 (see next paragraph). These records were obtained on both accelerometric stations and broad-band velocimetric ones (cf. Table 16).

	ACC	BB	TOTAL
Number of signals	1058	1371	2429
Distribution	44%	56%	100%

Table 16 – Distribution of traces included in the Action 5 catalogue with respect to instrument type.

4.2. Reference magnitude

In order to be able to assess the validity of the magnitude estimates obtained from the analysis of the first seconds of the seismic signal, we needed to succeed in comparing them with reference values. It is thus absolutely necessary to associate a reference magnitude which is expressed according to a common and uniform scale with each earthquake in the catalogue.

Since each organization responsible for a seismic monitoring network ensures its own magnitude calculation, the seismicity catalogues dealing with events in the Pyrenees list several magnitude values. Thus, according to the event being considered, there may be one or more magnitudes given among those determined by IGN, LDG, OMP and IGC. Although all these organizations compute “local” magnitudes (noted M_l), because the data and the methodologies used to compute them differ, these do not correspond exactly with each other. Therefore a single reference scale must be defined.

Among the aforementioned magnitudes, those provided by LDG and IGN (written respectively M_{LDG} and M_{IGN}) are the most representative in our case insofar as they have been calculated in the same way for a long time. Because, among the events compiled in our catalogue, the M_{LDG} magnitude is the one that is the most often supplied, this will be taken as the reference magnitude scale in the remainder of the study.

However, for some earthquakes listed in the catalogue, no local LDG magnitude is available. To solve this problem, we have compared the two magnitude types noted M_{LDG} and M_{IGN} for all events for which both are supplied so as to be able to propose an empirical way to convert a M_{IGN} value into M_{LDG} . This comparison displays a very good correlation between these two types of magnitude, with a half-unit increment to the LDG magnitude as compared with that of IGN (cf. Figure 35). Thus for the four earthquakes in the catalogue for which M_{IGN} is available but not M_{LDG} , we will be using the following relation to compute the reference magnitude:

$$M_{LDG} = M_{IGN} + 0.6$$

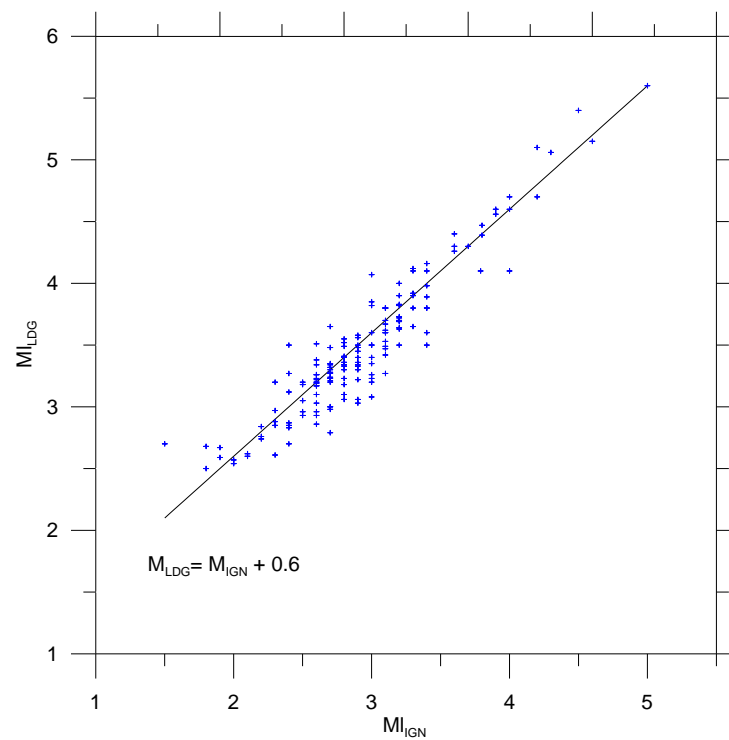


Figure 35 – The linear relation observed between M_{LDG} and M_{IGN} .

4.3. *Catalogue*

The some 2400 time histories included in the waveform catalogue for Pyrenean earthquakes are depicted on Figure 15 versus epicentral distance and on Figure 16 versus reference magnitude.

The characteristics of the events listed in this catalogue appear in Table 25 in Appendix A of this report.

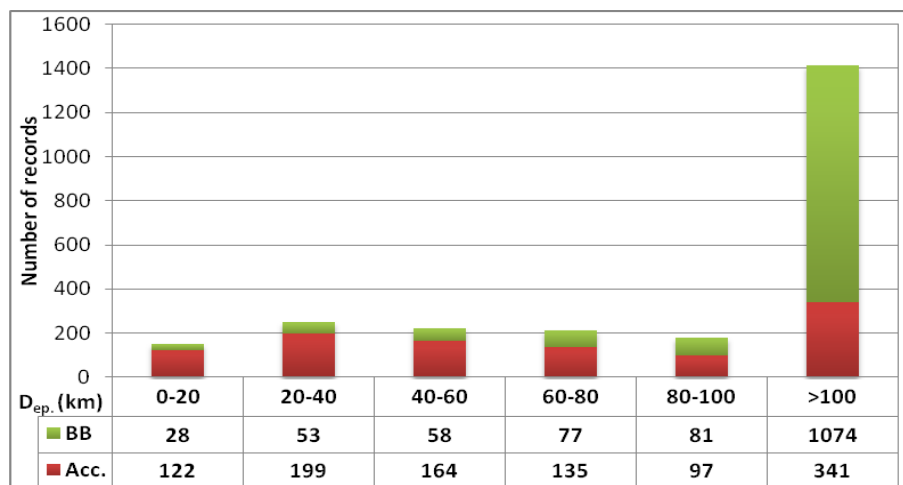


Figure 36 – Distribution of the catalogue data versus epicentral distance and recording type.

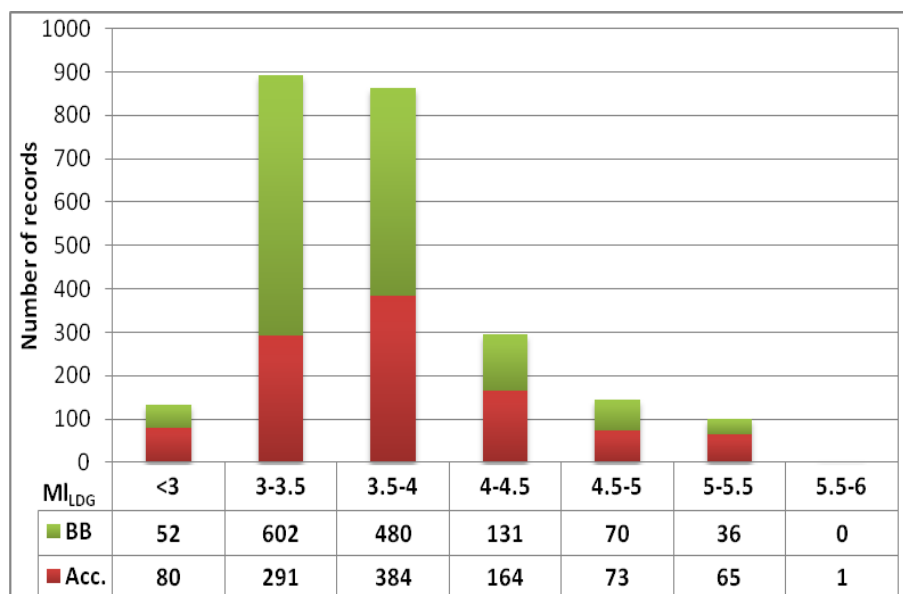


Figure 37 – Distribution of the catalogue data versus reference magnitude and recording type.

4.4. Data pre-processing

4.4.1. Correction for instrument response

The waveform catalogue thus compiled was first corrected for instrument response (only data recorded on broad-band seismometers had not been corrected) using the transfer functions of each instrument.

4.4.2. Picking P-wave arrival times

Because the methodologies for estimating magnitude in real time chosen in the context of this study are based on an analysis of the first few seconds of the P wave, their arrival time must be read.

To do so, we initially tried an automatic-picking algorithm (a tool available under SAC), that we subsequently compared with results obtained by manual reading on a selection of traces. Besides the fact that the automatic-picking algorithm does not work when the traces are too noisy, we were able to show that the time difference between the two picks was about 0.3 s on average, i.e., around 10 % of the analysis interval used by EWS (cf. Table 17). This discrepancy, greatest for recordings obtained on broad-band sensors, with an average of 0.45 s, may be a serious drawback because an erroneous pick may lead to an analysis of noise or of S (instead of P) waves according to whether the time pick is too early or too late. In the context of the present study, which aims to establish reference relations usable for the real-time determination of magnitudes for Pyrenean earthquakes, we accordingly decided to favor a manual reading of the P wave, and this was generalized to the entire catalogue.

<i>MI</i> _{LDG}	Data Type					
	ACC			BB		
	No. Traces	No. Auto Readings.	Av. Diff. of Readings (s)	No. Traces	No. Auto Readings	Av. Diff. of Readings (s)
3	-	-	-	18	2	0.23
3.2	3	3	0.08	6	0	-
3.5	10	6	0.11	11	9	1.63
3.7	5	4	0.13	8	4	0.35
4	12	6	0.11	5	4	0.09
4.2	9	5	0.14	12	10	0.07
4.5	14	10	0.13	20	8	0.18
5.4	19	13	1.17	18	14	0.29
5	12	8	0.14	8	7	0.72
Total	84	55	0.25	106	58	0.45

Table 17 – A comparison between automatic and manual picks for the earthquake time histories contained in the Pyrenean catalogue.

4.4.3. Spectral analysis: a common frequency domain

Because the signals in the Pyrenees catalogue were of different types (accelerometric and broad-band velocimetric data) and recorded using various

instruments, the spectral content characterizing each acquisition instrument must be studied in order to derive the common frequency band to be integrated into our analysis of all the types of data.

The bandwidths indicated by the manufacturers for the main sensors involved are given below in Table 18.

	ACC		BB
<i>Instrument</i>	Guralp & Kinometrics	CMG3T	STS2
<i>Characteristic instrumental response</i>	[0,05 – 50] Hz	[0,01 – 50] Hz	[0,01 – 100] Hz

Table 18 – The characteristics of the main acquisition instruments in the Pyrenean seismic monitoring network (instrumental response provided by the manufacturers).

However, a visual examination of the Fourier spectra of the traces recorded on the different instruments displays a strong heterogeneity in the areas of validity of the signals for stations of the same type, areas that are furthermore limited as compared with what the manufacturers indicate. Thus when one wants to study simultaneously data obtained by different types of station, sensors impose a **limitation on the area studied to a band between 0.1 and about 50 Hz.**

5. Methodology for calculating parameters τ_c , τ_P^{max} , P_d and P_v

5.1. Computing proxy parameters

In order to return to the context of real-time acquisition, we have chosen to apply an iterative integration algorithm enabling data to be processed continuously as they are being acquired.

5.1.1. Iterative integration

We built upon the method proposed by Shieh *et al.* (2008) for determining the parameter τ_c . The author also provides a specific integration algorithm for computing τ_c that uses parameters such as the gain G and the filtering constant Q . As these parameters were hard to assess on each station, this method was not retained.

According to the origin of the data (accelerometric or velocimetric), the signal must be integrated once or twice to obtain displacement. Because the integration process produces a low-frequency drift in the signal, it is customary to apply a high-pass filter with a 0.075 Hz cut-off frequency (the procedure chosen for filtering the data is described later in detail in paragraph 6.3).

Given the raw acceleration A_i , the raw velocity V_i is then calculated as follows:

$$V_{raw,i} = V_{raw,i-1} + \frac{(A_i + A_{i-1})\Delta T}{2} \quad \text{Equation 12}$$

$$V_i = Butter(V_{raw,i}, 0.075\text{Hz}) \quad \text{Equation 13}$$

The velocity signals (integrated accelerograms or velocimetric data) are then converted to displacement U_i :

$$U_i = U_{i-1} + \frac{(V_i + V_{i-1})\Delta T}{2} \quad \text{Equation 14}$$

These two relations are used with V_0 and U_0 set to zero.

5.1.2. Calculating parameter τ_c

Parameter τ_c is calculated from the velocity and displacement values derived from the vertical component of the P wave time history (cf. paragraph 3.3.1.i). It is conditioned by a specific calculation of velocity. This latter is determined not by integrating the acceleration signal or on the raw velocity signals, but from variations in the displacement that has first been filtered (cf. paragraph 3.3.1.i). The velocity V_i thus obtained is then written:

$$V'_i = \frac{(u_i - u_{i-1})}{\Delta T} \quad \text{Equation 15}$$

5.1.3. Calculating parameter τ_p

The parameter τ_p is calculated using a recursive relation following the procedure described in paragraph 3.3.1.ii from the vertical component of the P-wave velocity. The difficulty in applying this method arises from the initialization of the parameters X_0 and D_0 . The issue of the initialization of these parameters is in fact not brought up in the articles dealing with this method. Consequently, several alternatives have been envisaged.

On advice from Prof. Richard Allen, joint instigator of the τ_p method with Hiroo Kanamori (cf. Allen et Kanamori, 2003), we started out by setting X_0 and D_0 to 1, launching the initialization stage on the noise to ensure τ_p was stabilized at the onset of the P wave. Paradoxically, the circumstance of having records with low levels of noise distorts the meaningfulness of the τ_p indicator thus computed, which has a value that initially tends towards 2π (≈ 6.28) and which only progressively decreases to become unusable after 1 or 2 seconds (cf. Figure 38).

If X_0 and D_0 are set at zero instead of one, the parameter τ_p seems to stabilize faster and displays a clear change in behavior with the onset of the P wave (cf. Figure 38).

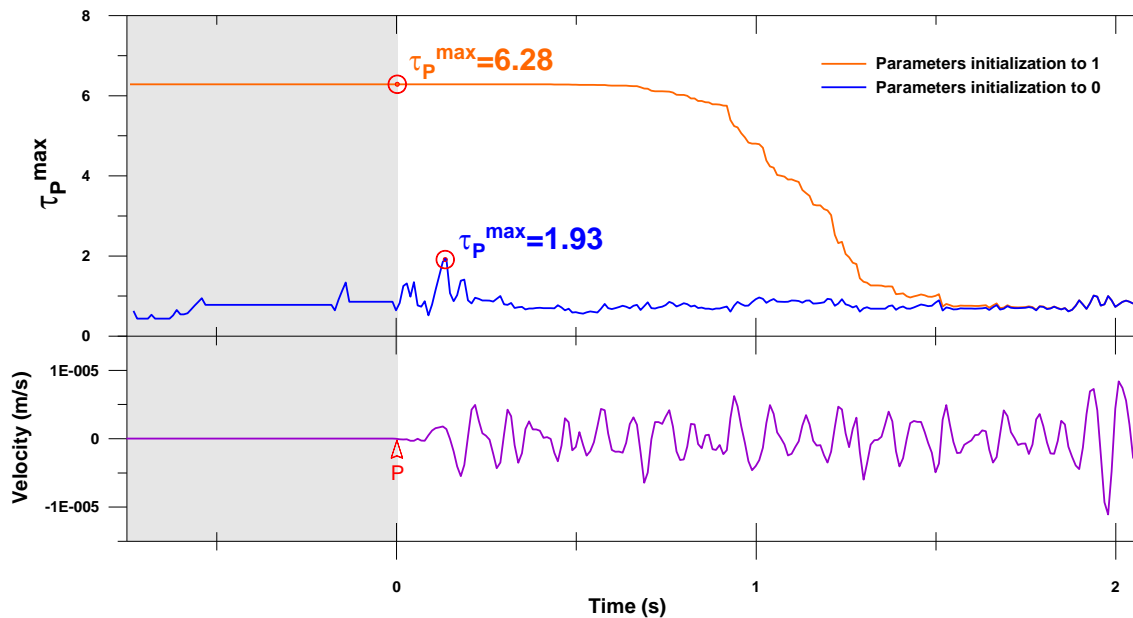


Figure 38 – Calculation of the parameter τ_p according to whether X_0 and D_0 are set at zero or at one.

Subsequently, the issue arises of the length of the time window for the background noise analysis required to set the parameter τ_p . To address this, we first computed τ_p^{max} using different durations of initialization for all the traces in the catalogue that satisfy the selection criteria presented in chapter 6.1. Then, we compared the values thus obtained by taking as a reference the values obtained from an initialization over three seconds of noise (an interval considered sufficient for obtaining stabilized values of τ_p). The results of this comparison, depicted on Figure 39, indicate that an initialization over only two seconds of noise is satisfactory. To a lesser extent, a one-second interval also yields good results. Encouraged by this, and in order to avoid having to perform a continuous “a priori” calculation before the onset of the P wave, we also

tested the effect of doing away with the initialization stage, beginning to calculate τ_p only with the onset of the P wave. Although for a certain number of traces the value of τ_p^{max} thus obtained is valid (i.e., equal to what is obtained after a 3-second initialization), this approach does present a considerable degree of scatter which mainly leads to overestimating τ_p^{max} (cf. Figure 39).

This test phase underscores the need to set the parameter τ_p on the basis of the noise preceding the P-wave onset over a time window of at least one second. Because all the records in our catalogue do not have the same “pre-event time”, we are retaining for the remainder of our study an initialization over at least one second (and a maximum set at 3 seconds).

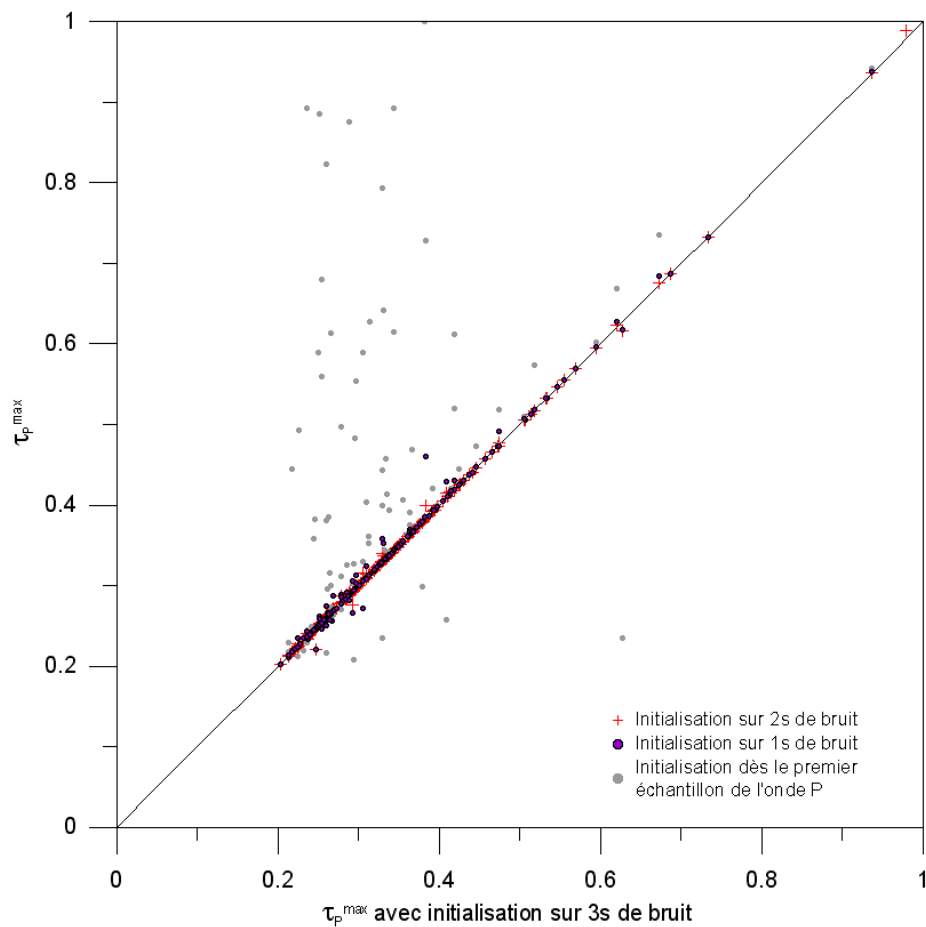


Figure 39 – Variation of the parameter τ_p^{max} versus the chosen initialization interval. Calculations performed on the traces in the catalogue that satisfy the selection criteria.

5.1.4. Calculating parameters P_d and P_v

P_d and P_v correspond respectively to the maximum amplitude in displacement and in velocity over a given portion of the vertical component of the P wave.

The displacement and velocity used result from either an iterative integration or velocity signals that have been filtered.

5.2. ***Selection of the traces to be used***

When the waveform catalogue was compiled as described in chapter 5, no control was imposed on the quality of the data or the recording conditions. In the framework of an analysis that intends to establish relations that can be used to estimate magnitudes in real time in the Pyrenees, it is accordingly necessary to define several selection rules for the data notably to ensure the quality and representativeness of the results.

5.2.1. Discriminating between P and S waves

The methods described above are based solely on an analysis of the first few seconds of the P wave. At short epicentral distances, however, the time interval separating the onsets of the P and S waves may be shorter than the analysis duration for the P wave (typically approximately 3 s), and this may result in a hybrid analysis of the P and S body waves for which the correlations are no longer valid. One therefore must be able to discriminate between the S and the P waves both while defining empirical correlations and during real-time processing.

Consequently we are considering in our test catalogue only those recordings where P and S arrivals are far enough apart so as to proceed to compute the various selected parameters. This precaution is particularly important because both the frequency content and the amplitude differ markedly according to whether P or S waves are being considered (S-wave amplitudes are larger than P-wave ones, borne by lower frequencies).

Rather than systematically picking the S-wave onset, we have considered the procedure proposed by Wurman *et al.* (2007) consisting in merely computing the theoretical arrival time for the S waves and retaining only those recordings in which the interval between P- and S-wave arrivals (noted $\Delta t_{P,S}$) is greater than or equal to the duration of the analysis ($T_{analysis}$). This test is written:

$$\Delta t_{P,S} = D_{focal} * (V_P - V_S) / (V_P * V_S) \geq T_{analysis}$$

Another option is to associate a minimum epicentral distance corresponding to a given time difference $\Delta t_{P,S}$. Supposing a hypocentral depth of 5 km, we thus calculated, for indicative purposes, a set of minimum epicentral distances associated with P-S time differences ranging between one and four seconds (cf. Table 19).

$\Delta t_{P,S}$ (s)	Minimum epicentral distance (km)
1	6.2
2	15.2
3	23.5
4	31.6

Table 19 – Minimum epicentral distance versus the time interval between P- and S-wave onsets. Calculation carried out with the hypotheses given in Table 7.

As an example, Figure 40 depicts the S-wave pick obtained from the P-wave pick and the station's focal distance. This example shows plainly that the approach used to discriminate between P and S waves in this study is relatively robust.

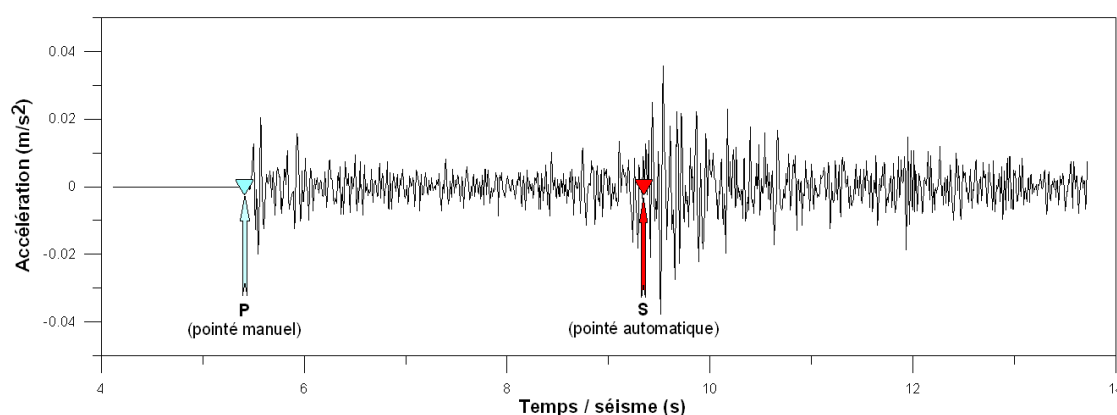


Figure 40 – An example of an “automatic” pick of the S wave based on a calculation of the theoretical time difference between P- and S-wave arrivals.

5.2.2. Selection based on epicentral distance

Because the principle behind the early warning system relies on an analysis of signals recorded in the stations closest to the epicenter, it is preferable to exclude far-field records from our analysis by imposing a maximum epicentral distance as a selection criterion. However, as with the previous selection filter, this filter must not overly reduce the number of records to be processed. Indeed, because of the relatively diffuse seismicity in the Pyrenees, far-field recordings are generally far more plentiful than ones closer to the source. We accordingly tested the influence of a threshold value for maximum epicentral distance on the number of remaining traces. When the threshold is lowered to 100 km - thus reproducing conditions similar to what a EWS might be like - and an SNR filter is applied (see next paragraph), the total number of remaining traces decreases only by around 20 %. Henceforth in the study we will therefore

be adopting the criterion whereby only traces recorded nearer than 100 km from the epicenter will be retained.

5.2.3. Selection based on signal noise

To ensure the validity and the pertinence of the computations, it is important to work with a large number of seismic signals while eliminating traces that are too noisy. The noise-based selection filter thus seeks to remedy the presence of such traces. However, applying too restrictive a filter would overly reduce the number of signals to be processed. A compromise thus needs to be found to satisfy both these conditions.

The influence of using various minimum values of signal-noise ratio (SNR - calculated on unfiltered records as being the ratio between the mean amplitude of the first few seconds of the P wave and that of the noise preceding the P-wave onset) on the calculation of magnitude proxies is illustrated below on Figure 41 through Figure 44 (only relations in terms of M_{LDG} are shown). It is seen from these figures that a lowering of the SHR threshold mainly results in increasing the number of traces retained, notably for small magnitudes ($M_{LDG} \leq 3.5$). However, these additional points tend to increase data scatter when frequency-related parameters are considered (cf. Figure 41 and Figure 42), they do align well with the points calculated from signals presenting a large SNR when amplitude-related parameters are considered (cf. Figure 43 and Figure 44).

Consequently, it seems necessary to retain a high value of SNR when computing parameters τ_c and τ_p^{max} , whereas lowering the threshold value for SNR imposed when computing parameters P_d and P_v allows a useful enhancement of the data set to be achieved and hence a better constraint of the empirical relations we are seeking to determine. The choice of SNR threshold values will be discussed on paragraph 5.3.2.

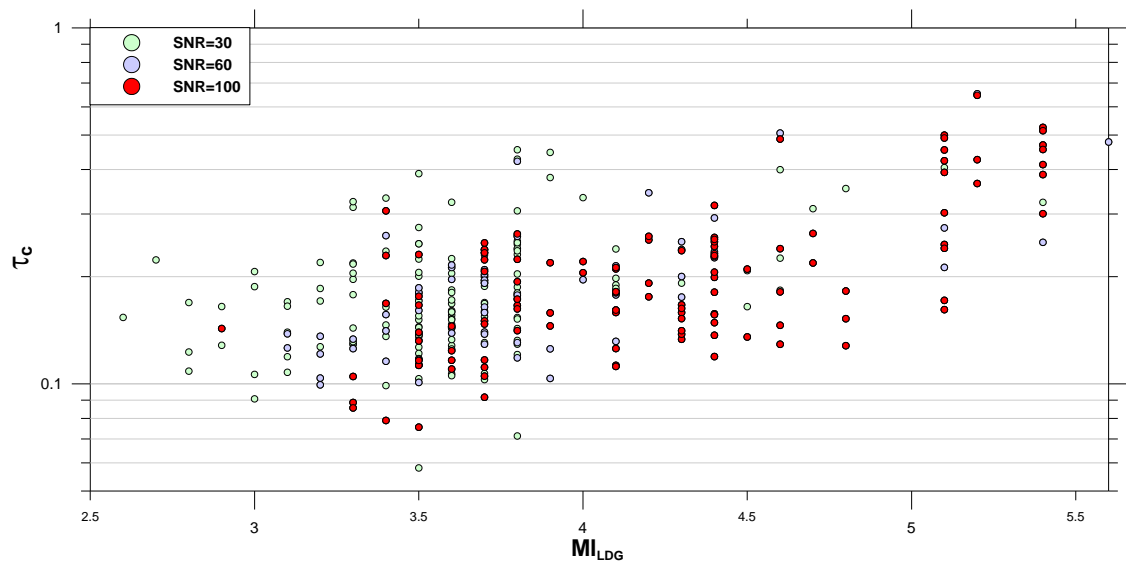


Figure 41 – Distribution of τ_c with magnitude versus the minimum signal-noise ratio (SNR) minimal retained. Calculations carried out with $T_{analysis} = 3$ s and a maximum epicentral distance of 100 km.

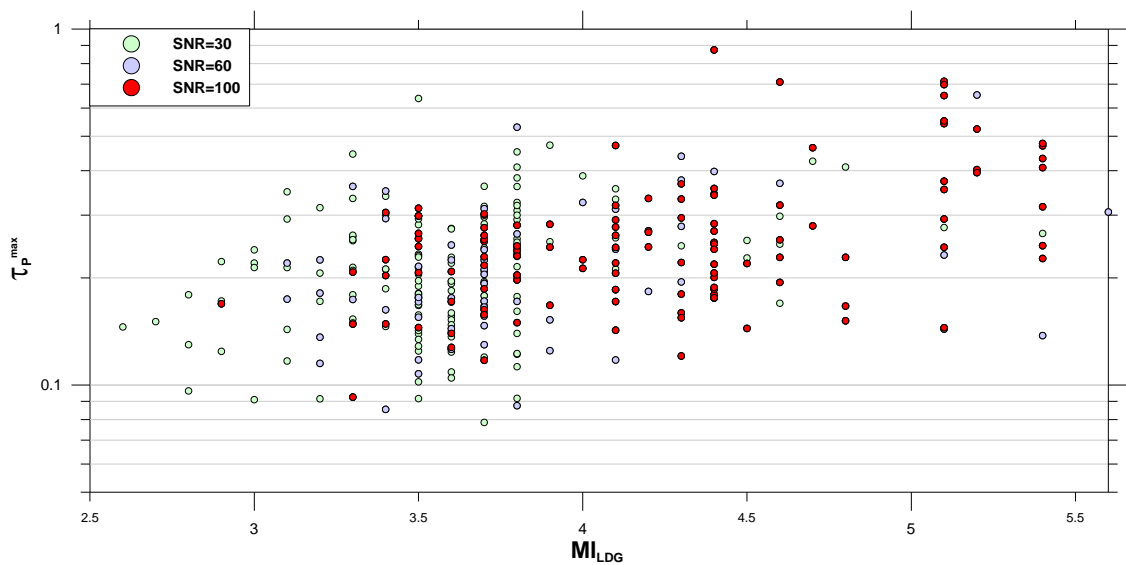


Figure 42 – Distribution of τ_p^{max} with magnitude versus the minimum signal-noise ratio (SNR) minimal retained. Calculations carried out with $T_{analysis} = 3$ s and a maximum epicentral distance of 100 km.

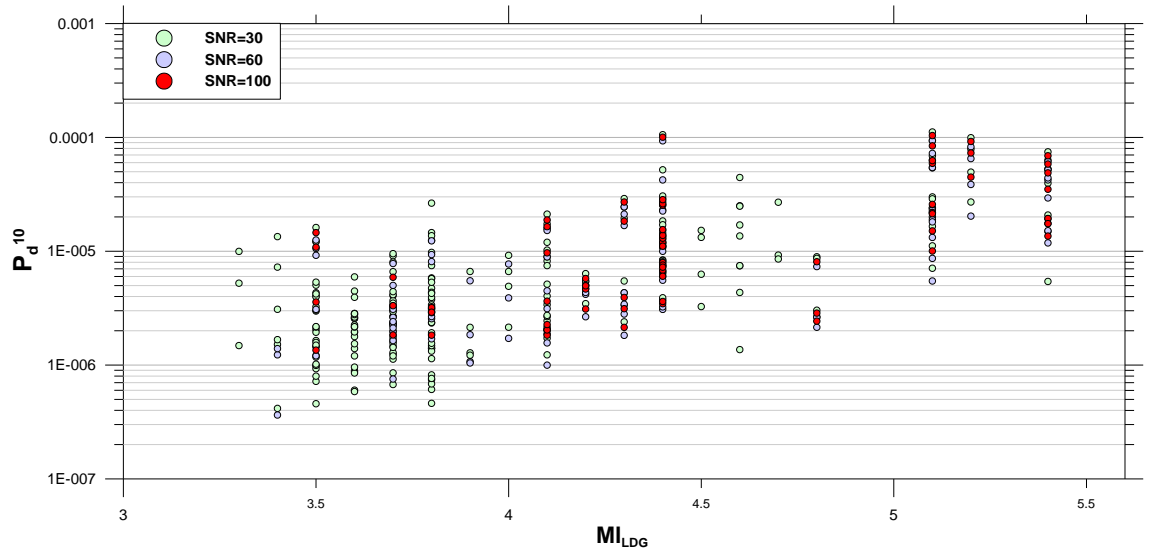


Figure 43 – Distribution of $P_d^{10,LDG}$ with magnitude versus the minimum signal-noise ratio (SNR) minimal retained. Calculations carried out with $T_{analysis} = 3$ s and a maximum epicentral distance of 100 km.

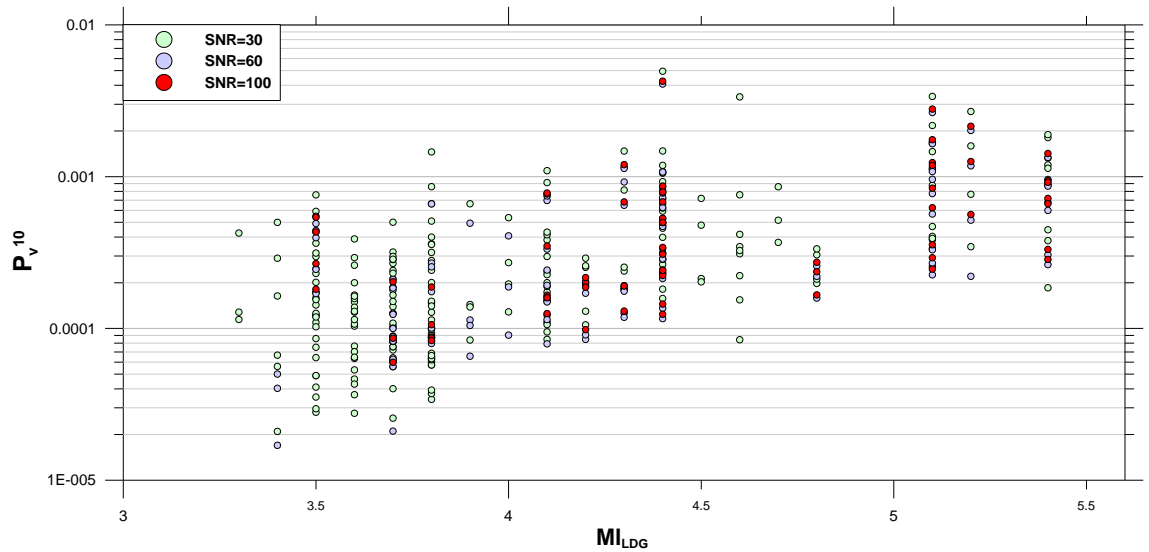


Figure 44 – Distribution de $P_v^{10,LDG}$ with magnitude versus the minimum signal-noise ratio (SNR) minimal retained. Calculations carried out with $T_{analysis} = 3$ s and a maximum epicentral distance of 100 km.

5.3. Data filtering

Because the available data were acquired on different instruments (accelerometers and broad-band velocimeters), it is mandatory to filter them in order to be able to work on a uniform frequency range.

As emphasized earlier, we realized it was necessary to restrict our analysis at least to the frequency band between 1 and 50 Hz, this being so we could include seismic recordings in our study obtained on different types of instruments (cf. paragraph 4.4.3). However, this frequency domain could be shrunk if required for calculation of proxies.

In addition of this “uniformization” filter, it is also necessary to be able to correct the low-frequency drift mentioned earlier that results from the numerical integration process by applying a high-pass filter (cut-off frequency greater than or equal to 0.075 Hz).

For all filtering operations, we will be using a Butterworth-type filter. Such filters are least inclined to distort the signal with respect to its bandwidth, for its response in phase is virtually linear and its gain relatively constant over the bandwidth. Another advantage to this filter is that it is causal and creates no precursor, which is an asset when filtering first arrivals (Glangeaud et Coppens, 1997).

The first issue that arises consists in choosing between:

- Applying two successive filtering passes:
 - a “uniformization” filter: a Butterworth band-pass filter $[1 - f_{\max}^8]$ Hz applied at the beginning of signal processing;
 - a “correction of integration drift” filter: a Butterworth high-pass filter with a 0.075 Hz cut-off frequency applied at the end of the integration process.
- Applying a single filtering pass that combines the two aforementioned filters: a Butterworth band-pass filter $[1 - f_{\max}]$ Hz applied at the end of the integration process.

To avoid multiplying the number of filters, which is liable to produce parasites in the data, we have opted for using just one filter at the end of the various integration stages.

5.3.1. The number of poles

A decision must then be made on the number of poles to choose for the Butterworth filter. Increasing the number of poles, which comes down to increasing attenuation and accentuating the transition between the conserved bandwidth and the reject band (cf. Figure 45), tends to minimize data scatter, as

⁸ f_{\max} being lower or equal to 50 Hz

emphasized as an example in Figure 46 with the parameter τ_c . This said, it is important to stress that while scatter generally decreases with the filter order, this regrouping of the data is also accompanied by a decrease in the slope value (cf. Figure 46).

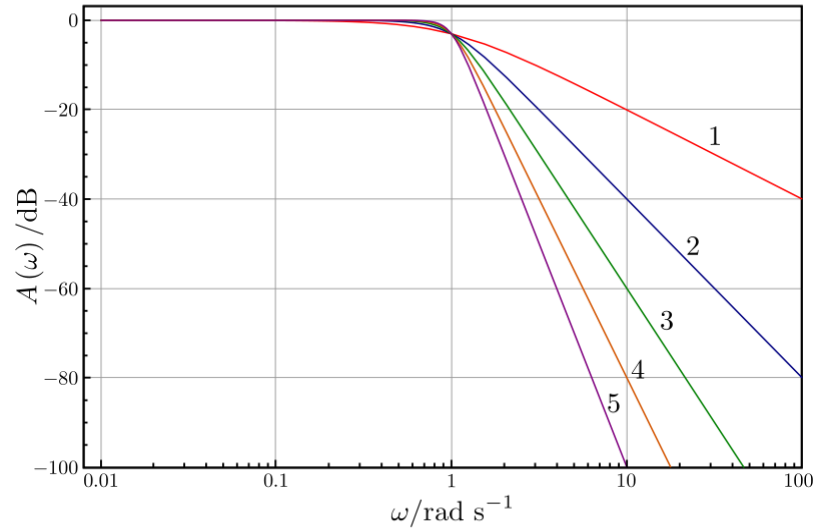


Figure 45 – The frequency response of a Butterworth filter of order n varying from 1 to 4 (source: Wikipedia).

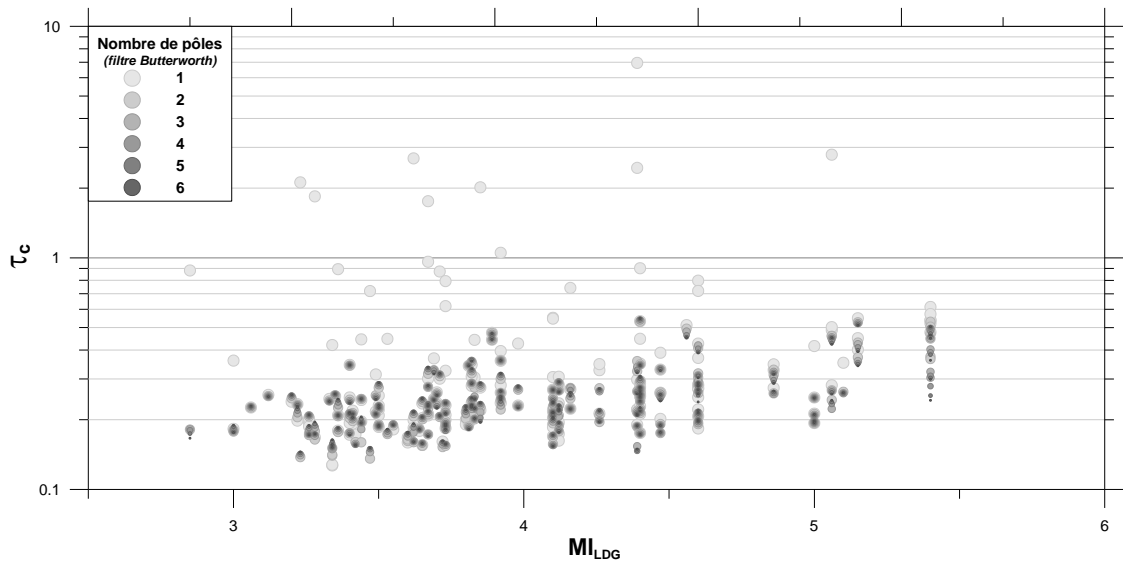


Figure 46 – Distribution of τ_c with magnitude versus the order chosen for Butterworth filter. Calculations performed on traces from the catalogue that satisfy the selection criteria.

We thus have compared the correlation coefficients for the linear relations obtained between the decimal logarithm of the various indicators and magnitude for different values of the number of poles selected for the filtering stage. To do so, we have considered at this point a direct dependence between magnitude and each of the two amplitude parameters, P_d and P_v , without taking into account dependency on distance, which does not affect the results qualitatively.

It appears from this comparison that the parameter τ_c presents a maximum correlation coefficient for a pole number equal to two, while for the three other parameters, the correlation improves with an increasing number of poles.

As to parameters τ_c and τ_p^{max} , our results are quite similar to those in Shieh *et al.* (2008), which displayed a better correlation of τ_c and τ_p^{max} with magnitude for filters of the 2nd and the 5th orders respectively.

In view of these results and because, generally speaking, it is not recommended to work with too high an order of Butterworth filtering, liable to distort the signal, we are retaining the following numbers of poles:

- τ_c : 2nd order filtering;
- **P_d and P_v** : 2nd order filtering, as the correlation of parameters P_d and P_v with magnitude improve very little beyond this;
- τ_p^{max} : 5th order filtering in line with the results in Shieh *et al.* (2008).

5.3.2. Bandwidth & SNR threshold for calculating proxy parameters

Lastly, the issue of the width of the frequency band chosen for the band-pass filter used to calculate proxy parameters has also been dealt with, as well as the choice of SNR thresholds. To that end, a parametric analysis had been performed on correlation coefficient got from raw linear regressions between magnitude and each proxy parameter (cf. Figure 47).

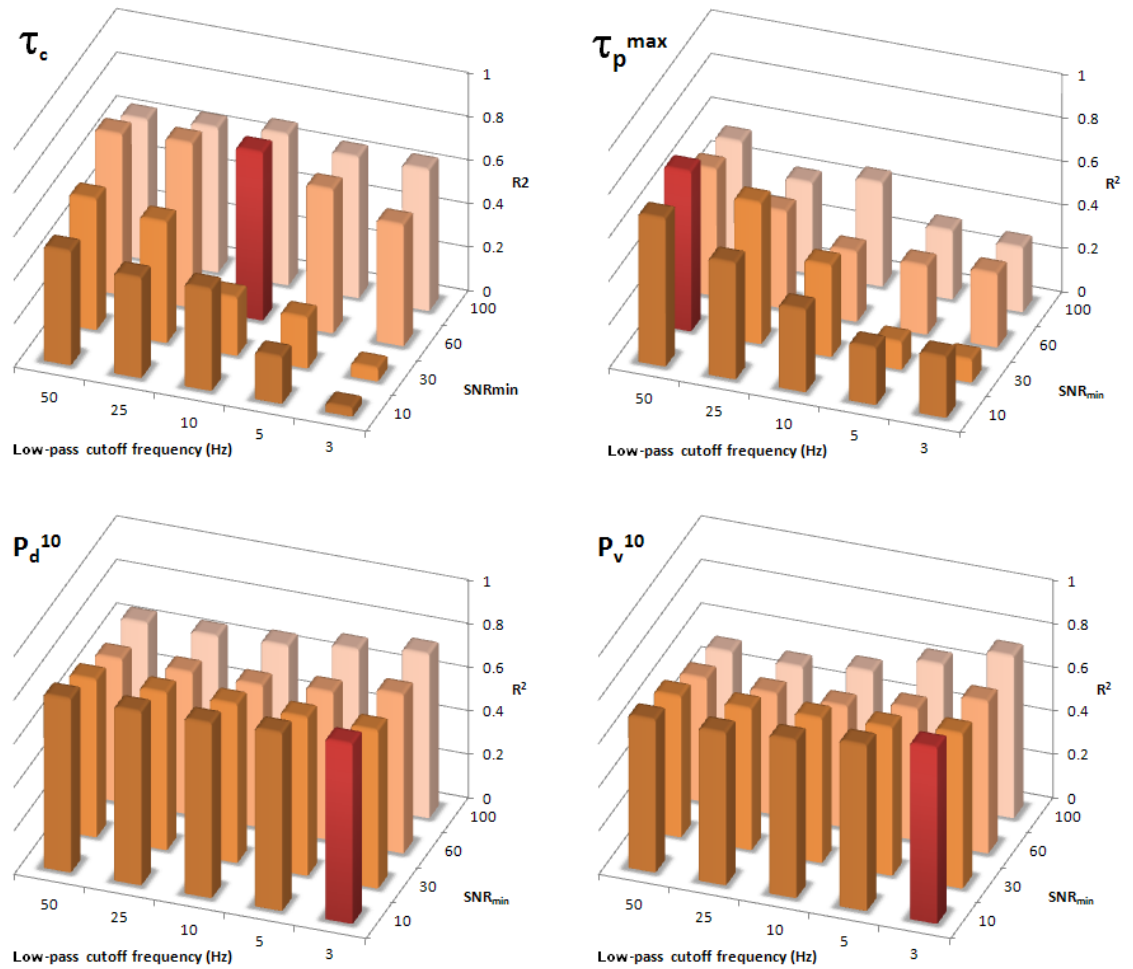


Figure 47 – Parametric analysis of low-pass cut-off frequency and SNR threshold impacts on correlation quality between ML_{LDg} magnitude and proxy parameters. In each illustration, SNR/frequency couple giving best results is shown in red.

This analysis shows that:

- τ_c parameter exhibits best correlation with magnitude for a 10 Hz low-pass cut-off frequency and a 60 SNR threshold value. Nevertheless, the extension of the cut-off frequency up to 50 Hz only slightly degrades the correlation coefficient.
- P_d and P_v parameters exhibit best results considering a narrow frequency domain between 1 to 3 Hz coupled with a low SNR threshold value equal to 10 Hz. As for the τ_c parameter, the extension of the cut-off frequency up to 50 Hz only slightly degrades the correlation coefficient.

- Calculation of τ_p^{max} parameter is supposed to concentrate on frequencies lower than 3 Hz. Nevertheless our analysis shows that in our case it is pertinent to conserve the high-frequency information contained beyond 3 Hz. This observation is compatible with the conclusions in Olivieri and Schweitzer (2007), which use a high-pass filter at 1 Hz to compute τ_p in the case of moderate-magnitude earthquakes (≤ 4.0). Moreover, best results are got with a 30 SNR threshold value.

Early warning supposing an analysis of close-field data characterized by high-frequency content and empirical correlations being on the whole stable up to cut-off frequency of 50 Hz, we will retain this filter value in order to keep maximum of the information carried by records.

5.3.3. On the effectiveness of filtering

In order to make sure that the chosen filtering offers a satisfying response to the issues pinpointed in the introduction to this paragraph, we engaged in an effort to verify the results, consisting initially in a visual examination of the appearance of the filtered traces. This examination allowed us to confirm that the chosen filtering procedure did effectively eliminate the low-frequency drift phenomenon of the signal due to its single or double integration in the time domain.

Subsequently, we examined the distribution of the results obtained for each parameter in terms of the type of sensor that recorded the signal (ACC or BB). This comparison reveals that the clusters of points for each sensor type are comparable and indistinguishable from one another (cf. the example of results obtained

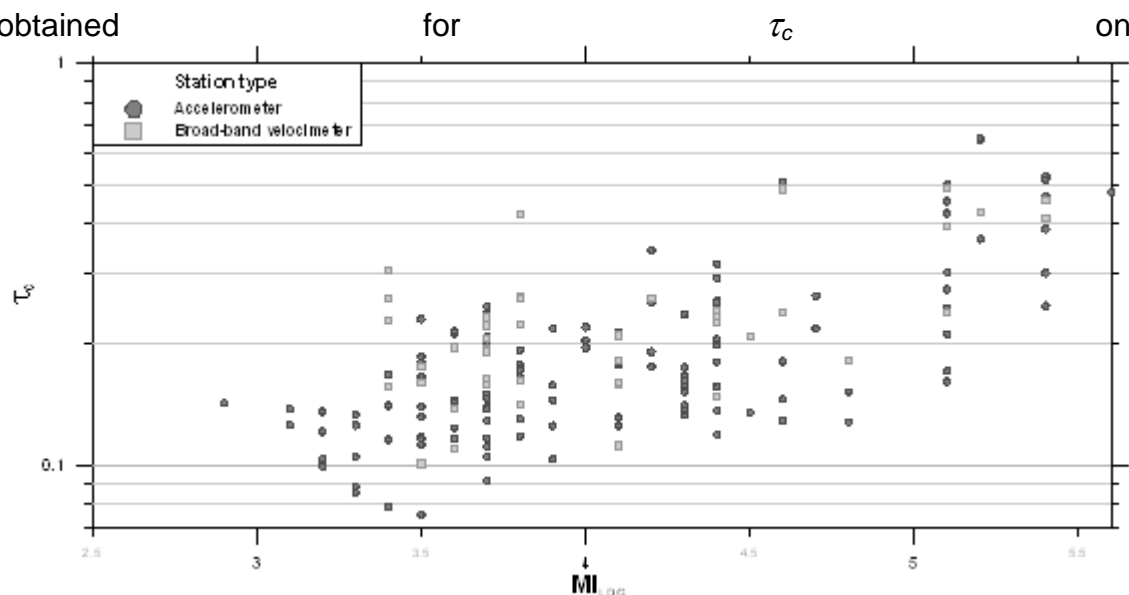


Figure 48). This circumstance confirms that “uniformization” band-pass filter applied to the data is entirely suitable to a collective use on accelerometric and broad-band velocimetric data.

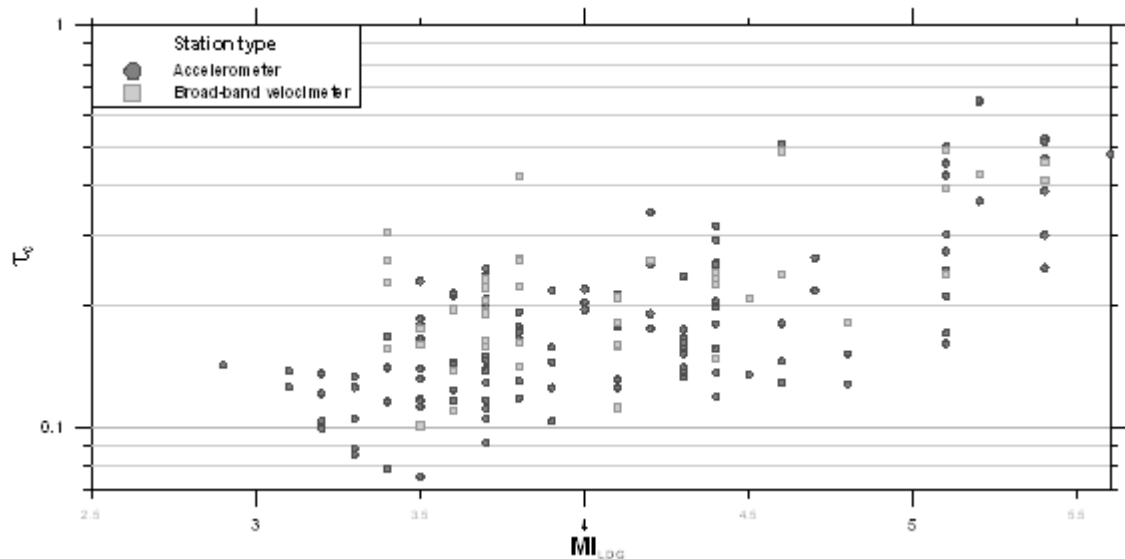


Figure 48 – The distribution of τ_c with magnitude versus instrument type. Calculations performed on traces from the catalogue that satisfy the selection criteria.

5.4. A review of the parameters used to calculate proxies

In this paragraph we are reviewing the calculation parameters chosen to determine real-time proxies for magnitude, which are τ_c , τ_p^{max} , P_d and P_v (cf. Table 20 below):

	τ_c	τ_p^{max}	P_d	P_v
$T_{analysis}$	1 to 3 s			
$D_{epicentral, max}$	100 km			
SNR_{min}	60	30	10	10
Filter bandwidth	[1-50] Hz			
Filter order	2	5	2	2

Table 20 – Table summarizing the different types of processing applied to the signals so as to calculate the different parameters.

Furthermore, the definitive catalogue used subsequently in the study to define the reference relations that would allow the magnitudes of Pyrenean

earthquakes to be assessed in real time, composed of the traces of the general catalogue that satisfied the selection criteria summarized in Table 20, is likewise presented on Figure 49 and Figure 50. It should be noted that the longer the analysis interval, the more data is contained in the catalogue.

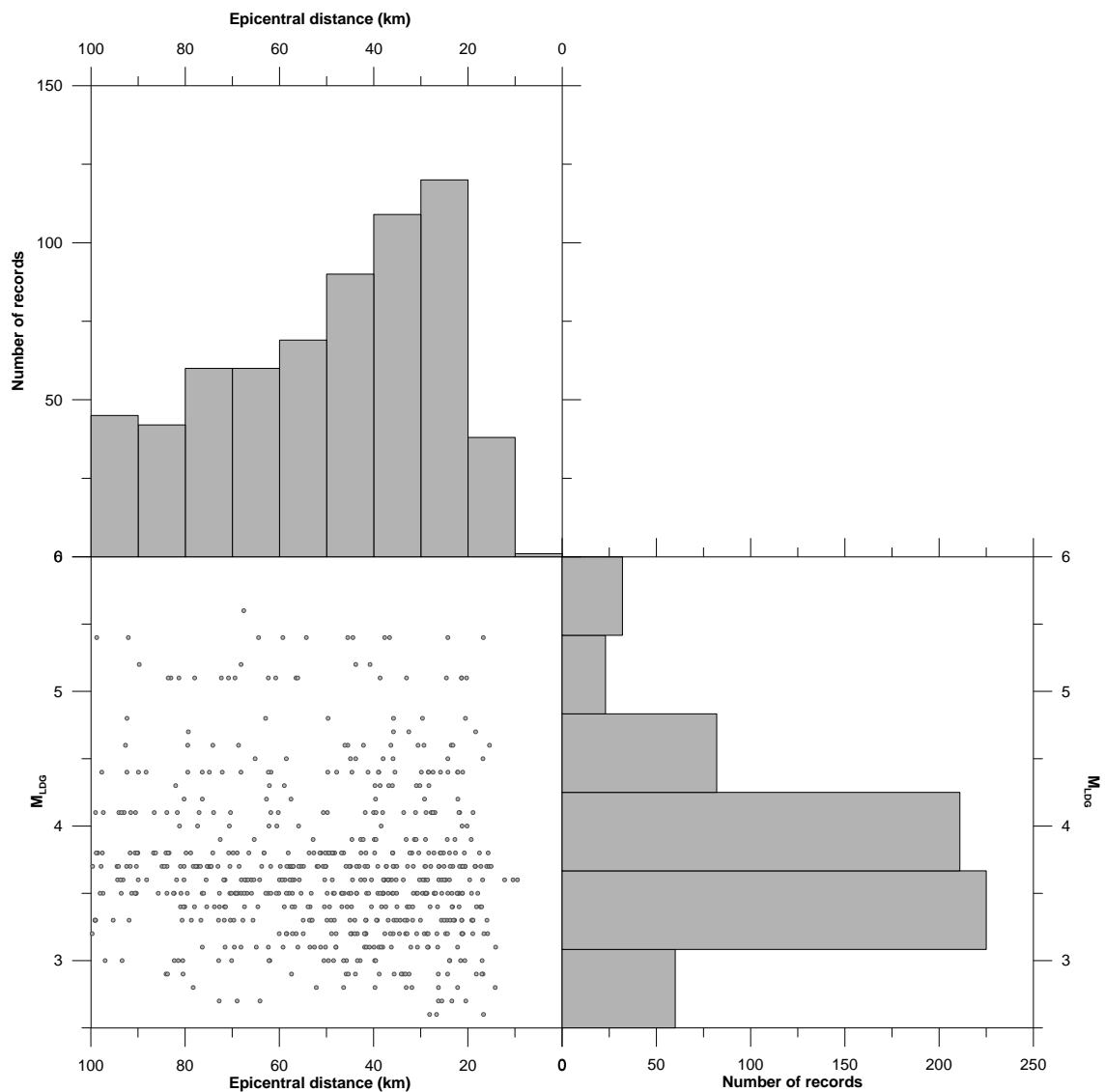


Figure 49 – Distribution of the seismic signals that satisfied the selection filters versus magnitude and epicentral distance corresponding to calculation of parameters P_d/P_v with a 2s P-wave analysis time length.

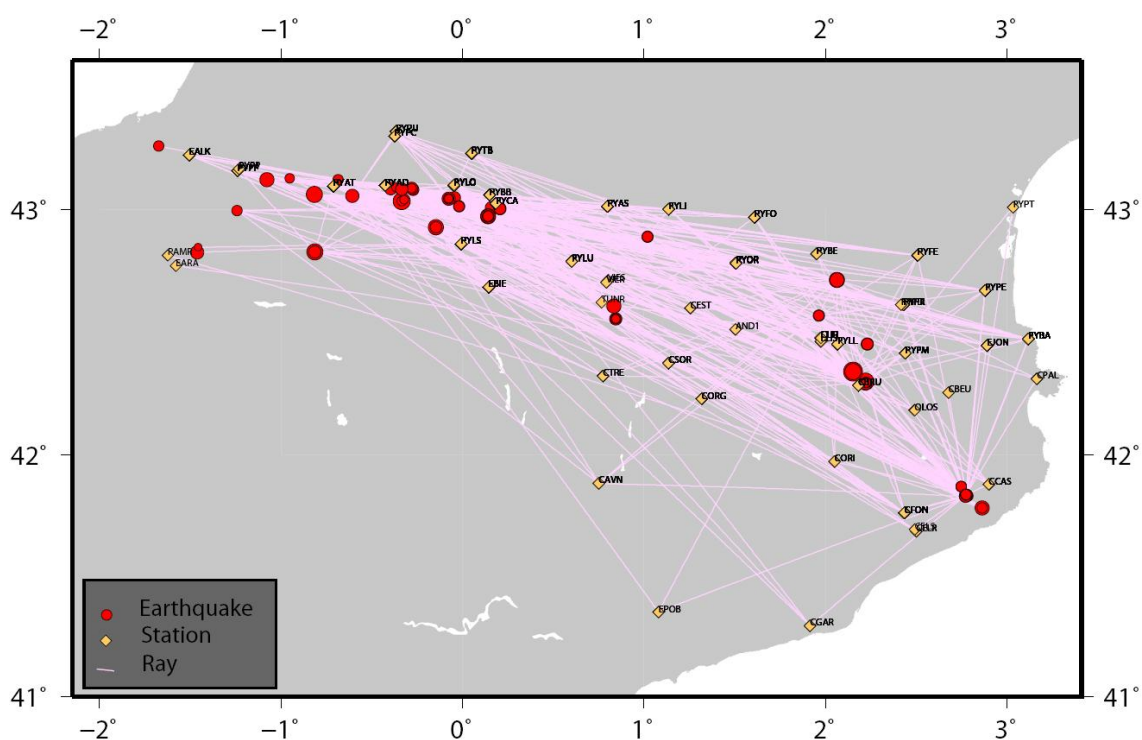


Figure 50 – Map of earthquakes included in the catalogue and of corresponding recording seismological stations.

6. Reference relations

Once the “proxy” parameters of magnitude have been computed on the Pyrenean earthquake waveform catalogue according to the methodology described in chapter 5, it is possible to compare these parameters with the reference magnitudes in order to try to establish empirical relations enabling magnitude to be estimated in real time from an analysis of the first few seconds of the P wave.

To reduce scatter as much as possible, it is better to study the values of the parameters under consideration averaged for each event rather than the results obtained station by station (Wu and Kanamori, 2005/2007). To do so, we are not considering a mean of the indicators τ_c , τ_p^{max} , P_d and P_v , but rather a mean of their decimal logarithms, which are supposed to be linearly correlated with magnitude. Thus, and to avoid assigning too much weight to certain seismic traces, only those earthquakes for which we have at least two traces satisfying the selection criteria presented in chapter 6.1 (cf. Table 12) will be retained for analysis, thereby providing one mean per event.

6.1. *Establishing reference relations*

6.1.1. The τ_c method

The values calculated for the parameter τ_c on the traces satisfying the selection criteria presented in chapter 6.2 (cf. Table 12) are depicted on Figure 51 versus magnitude (M_{LDG} and M_{IGN}). The mean value per event is indicated by heavy black dots.

An examination of the means for each event reveals a clear correlation between the parameter τ_c and magnitude for magnitudes ranging between 2.9 to 5.6 M_{LDG} - or 2.4-5.0 M_{IGN} - (cf. Figure 52).

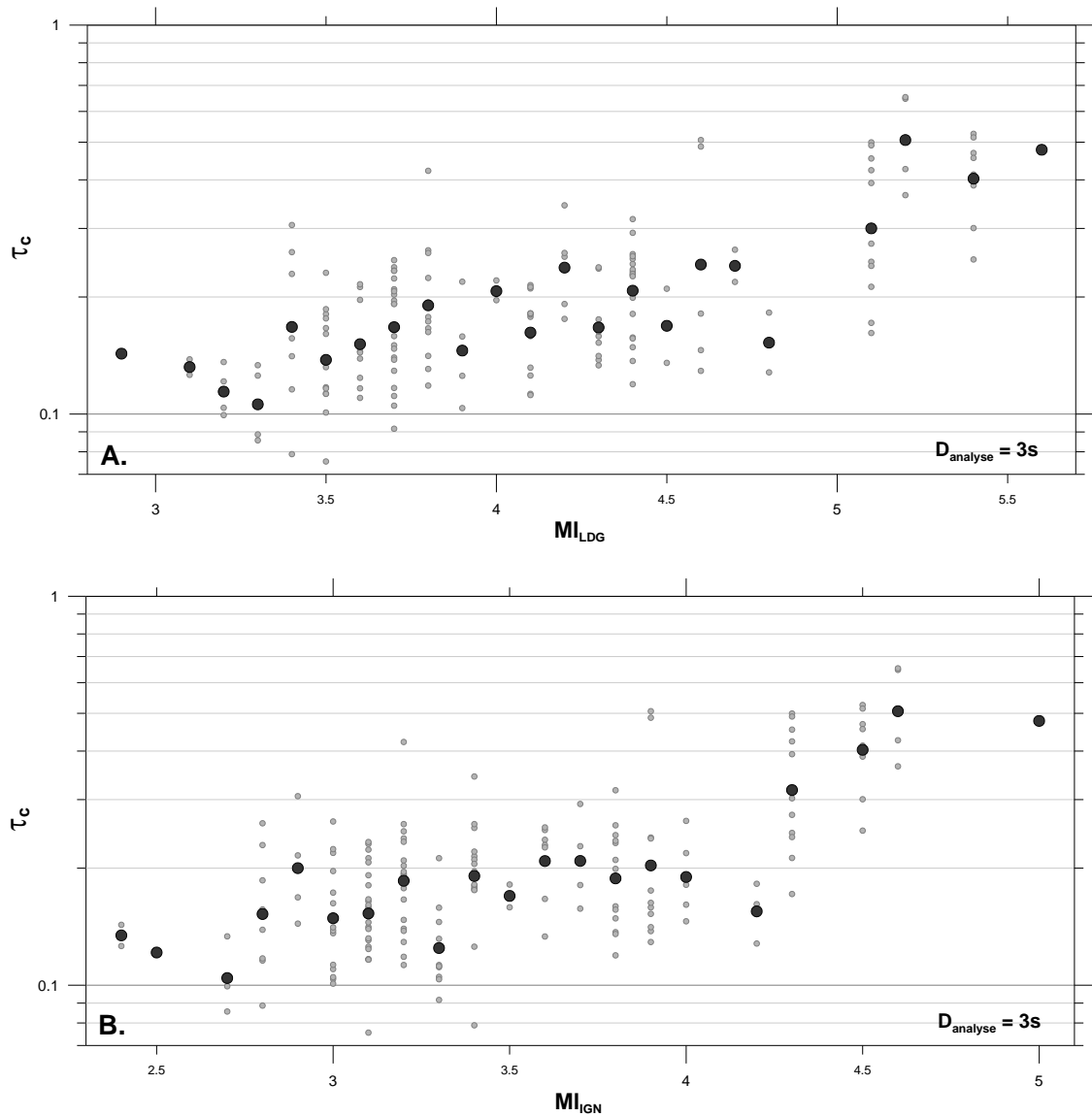


Figure 51 – A comparison between parameter τ_c and local magnitude calculated by LDG (A) and IGN (B) for Pyrenean earthquakes. The grey dots represent values of the parameter τ_c calculated in each station (analysis interval set at 3 s), which are averaged by 0.1 magnitude intervals (black dots).

The empirical linear relations linking τ_c with local magnitude determined from 73 events for the LDG and IGN magnitudes, on the basis of an analysis of the first three seconds of the P wave are as follows (cf. Equation 16, Equation 17 and Figure 52):

$$\log(\tau_c) = 0.2063 (\pm 0.0270) \times MI_{LDG} - 1.5653 (\pm 0.1139) \quad \text{Equation 16}$$

$$\log(\tau_c) = 0.2198 (\pm 0.0319) \times MI_{IGN} - 1.4870 (\pm 0.1154) \quad \text{Equation 17}$$

Used reciprocally to determine the magnitude from τ_c , these relations indicate corrected standard errors⁹ in magnitude of ± 0.46 of a unit of both M_{LDG} and M_{IGN} . These results would seem to show that the parameter τ_c does statistically represent a relatively good real-time estimator for magnitude.

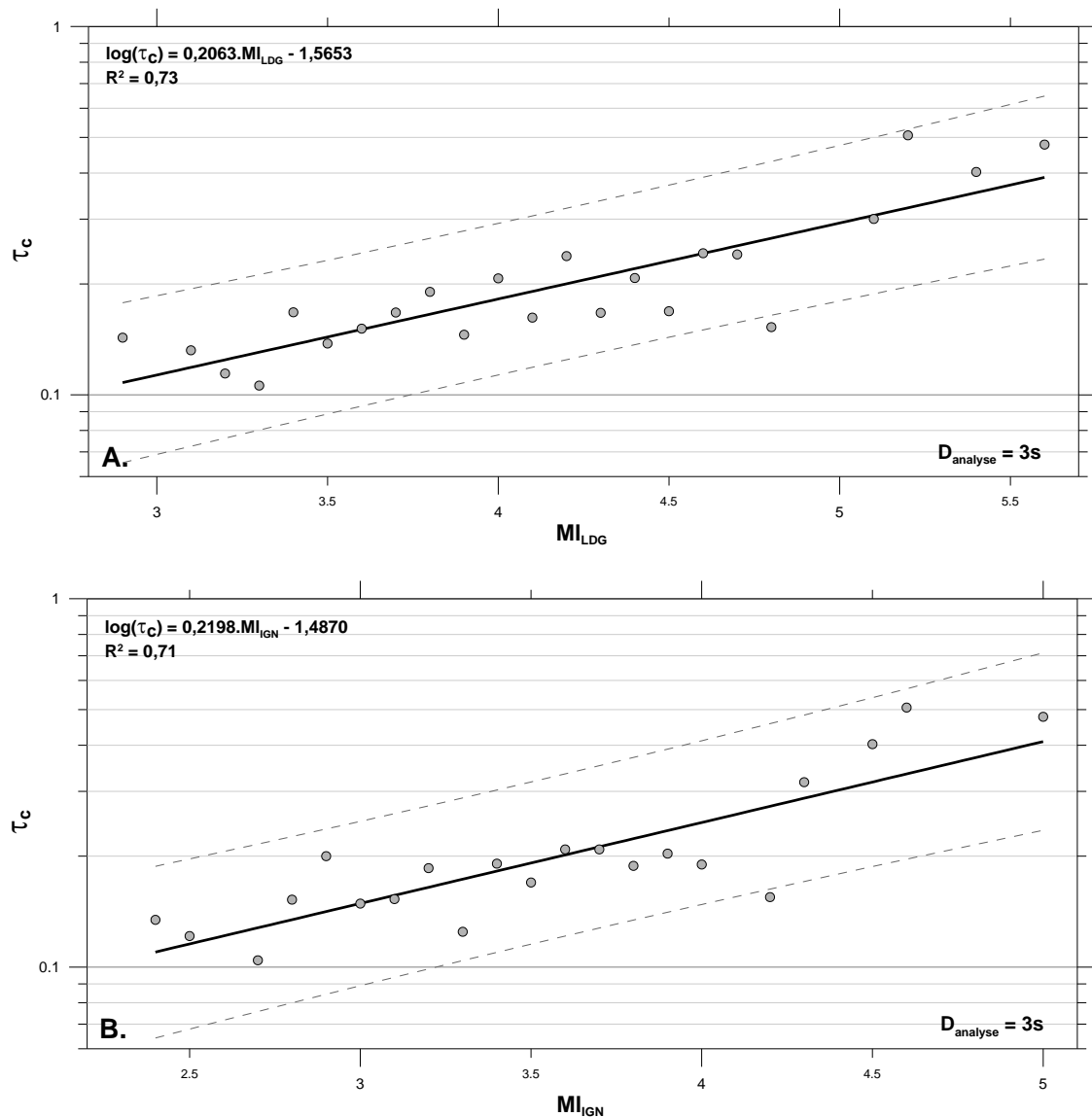


Figure 52 – Empirical relations linking the parameter τ_c (mean per event) with local magnitude calculated by LDG (A) and IGN (B) for Pyrenean earthquakes. Calculations carried out on the traces of the catalogue that satisfy the selection criteria (analysis

⁹ Corrected standard error (ES_c): the square root of the quotient of the sum of the residuals in magnitude per degree of freedom of the system.

interval set at 3 s). The straight line obtained by linear regression is shown in black, while the grey dashed lines indicate the confidence interval at 95 % for a new observation.

6.1.2. The τ_p method

The values of parameter τ_p^{max} computed on the traces that satisfy the selection criteria defined in chapter 6.2 (cf.5.4) are depicted on Figure 52 versus magnitude (M_{LDG} et M_{IGN}). The mean values for each event are indicated by dark grey dots.

An examination of the means for each event reveals a clear correlation between the parameter τ_p^{max} and magnitude (cf. Figure 53).

The empirical linear relations linking τ_p^{max} with local magnitude determined respectively from 105 events for the LDG and IGN magnitudes, on the basis of an analysis of the first three seconds of the P wave are as follows (cf. Equation 18, Equation 19 and Figure 54):

$$\log(\tau_p^{max}) = 0.1313 (\pm 0.0159) \times M_{LDG} - 1.1648 (\pm 0.0641) \quad \text{Equation 18}$$

$$\log(\tau_p^{max}) = 0.1413 (\pm 0.0164) \times M_{IGN} - 1.1286 (\pm 0.0564) \quad \text{Equation 19}$$

Used reciprocally to determine the magnitude from τ_c , these relations indicate corrected standard errors in magnitude of ± 0.52 of a unit of M_{LDG} and ± 0.46 of a unit of M_{IGN} . These results would seem to indicate that the parameter τ_p^{max} does statistically represent a relatively good real-time estimator for magnitude.

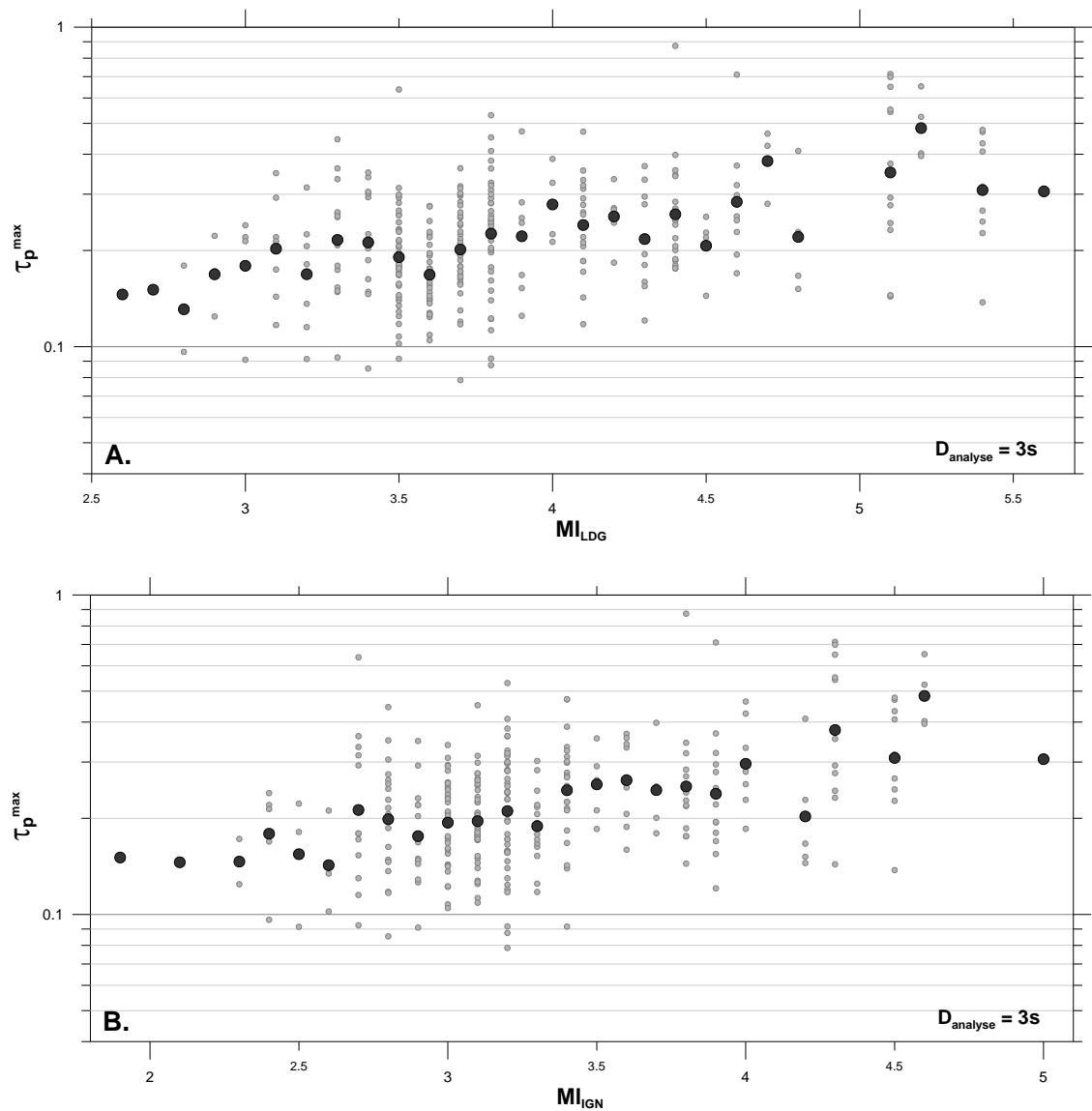


Figure 53 – A comparison between parameter τ_p^{\max} and local magnitude calculated by LDG (A) and IGN (B) for Pyrenean earthquakes. The grey dots represent values of the parameter τ_p^{\max} calculated in each station (analysis interval set at 3 s), which are averaged by 0.1 magnitude intervals (black dots).

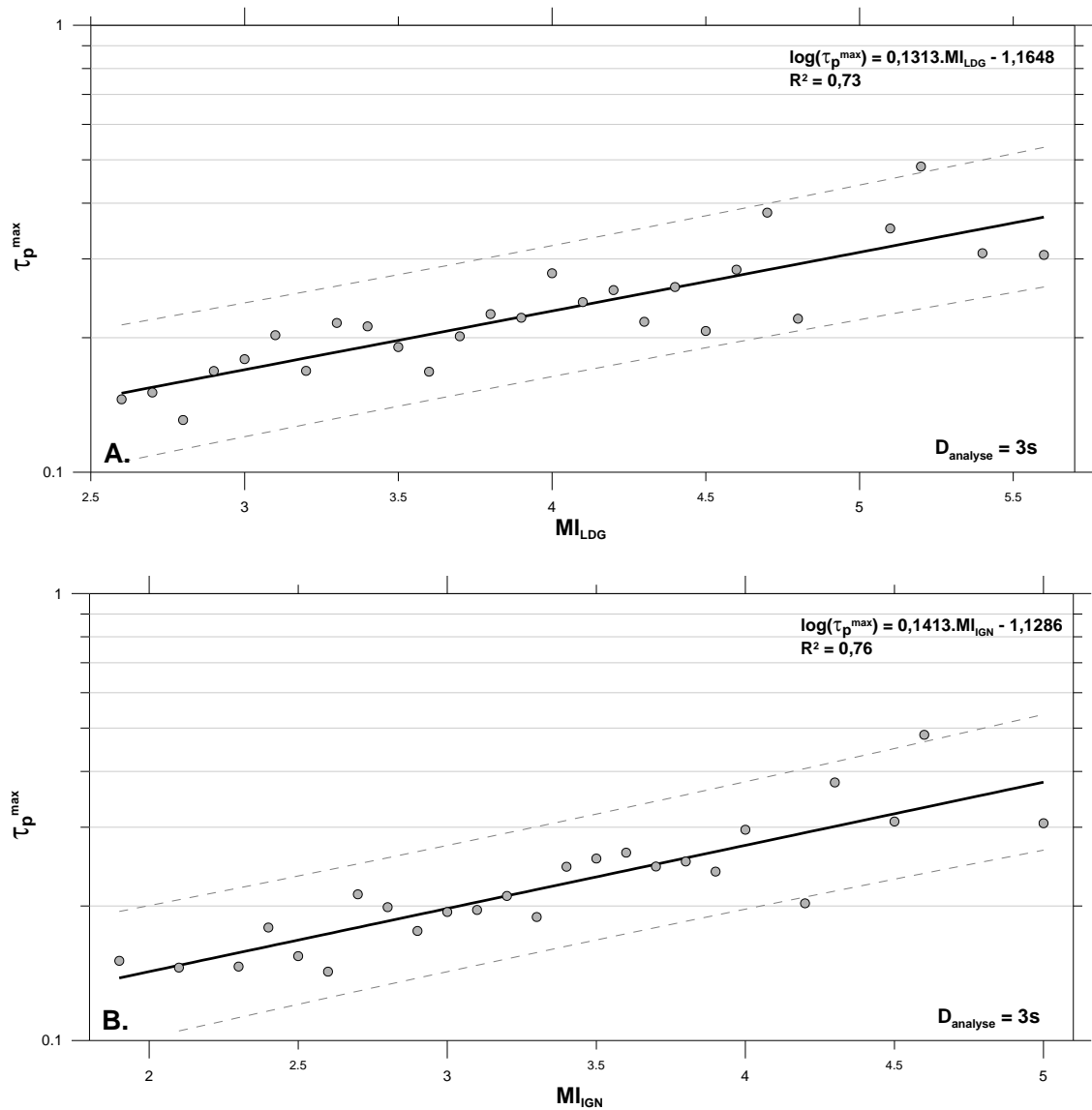


Figure 54 – Empirical relations linking the parameter τ_p^{\max} (mean per event) with local magnitude calculated by LDG (A) and IGN (B) for Pyrenean earthquakes. Calculations carried out on the traces of the catalogue that satisfy the selection criteria (analysis interval set at 3 s). The straight line obtained by linear regression is shown in black, while the grey dashed lines indicate the confidence interval at 95 % for a new observation.

6.1.3. Results for the P_d and P_v methods

As to the parameters τ_c and τ_p^{\max} , we have also sought to link the parameters P_d and P_v empirically with magnitude. Because the signal amplitude is dependent upon not only magnitude but also epicentral distance, however, it is not possible to apply the same methodology as in the previous case. Thus the

coefficients A , B and C of the following logarithmic equation must be determined:

$$\log(P_{d,v}) = A + B.M + C.\log(R) \quad \text{Equation 20}$$

In order to dispense with distance dependency, Zollo *et al.* (2006) suggest scaling the peak P_d and P_v values to a 10-km reference distance. To do so, and after having determined coefficients A , B and C of Equation 20, the scaling procedure is as follows:

$$\log(P_{d,v}^{10}) = \log(P_{d,v}^R) - C.\log(R/10) \quad \text{Equation 21}$$

Once the scaling has been accomplished, it is then possible to apply the methodology used previously for parameters τ_c and τ_p^{max} by determining coefficients A' and B' of the following log-linear equation:

$$\log(P_{d,v}^{10}) = A' + B'.M \quad \text{Equation 22}$$

i. The P_d method

The empirical linear relations linking P_d to local magnitude (LDG and IGN) and epicentral distance determined from 556 traces appertaining to 144 events on the basis of an analysis of the first three seconds of the P wave are as follows (cf. Equation 23, Equation 24 and Figure 55):

$$\log(P_d) = 0.7128 (\pm 0.0284) \times M_{LDG} - 1.3346 (\pm 0.0963) \times \log(D_{epi}) - 6.8858 (\pm 0.1896) \quad \text{Equation 23}$$

$$\log(P_d) = 0.7534 (\pm 0.0319) \times M_{IGN} - 1.3257 (\pm 0.0993) \times \log(D_{epi}) - 6.6251 (\pm 0.1918) \quad \text{Equation 24}$$

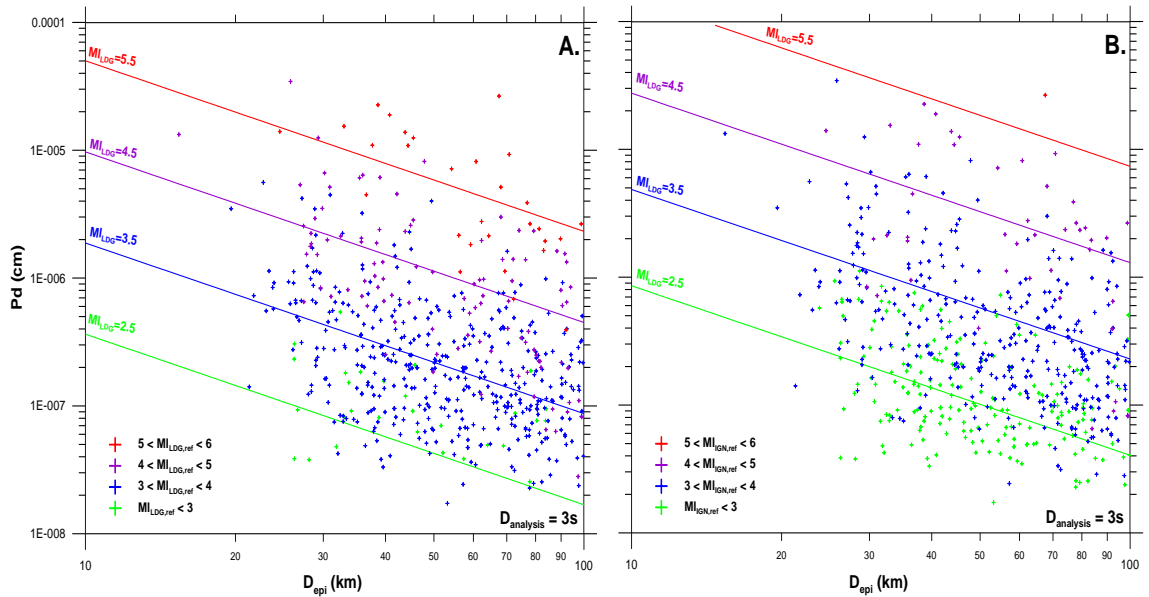


Figure 55 – Relation between P_d parameter and earthquake magnitude (LDG magnitude on fig. A and IGN magnitude on fig. B) and epicentral distance for Pyrenean records.

Once the parameter P_d^{10} has been scaled to an epicentral distance of 10 km, it can be represented versus magnitude (MI_{LDG} and MI_{IGN}) – cf. Figure 56. The mean for each event is indicated by dark grey dots.

An examination of the means for each event reveals a clear correlation between the parameter P_d^{10} and magnitude over all levels of magnitude (cf. Figure 57), unlike the frequency parameter τ_c for which this correlation emerges only above a certain magnitude.

The empirical linear relations linking P_d^{10} with local magnitude determined respectively from 144 events on the basis of an analysis of the first three seconds of the P wave are as follows (cf. Equation 25, Equation 26 and Figure 57):

$$\log(P_d^{10,LDG}) = 0.8169 (\pm 0.0424) \times MI_{LDG} - 8.6033 (\pm 0.1708) \quad \text{Equation 25}$$

$$\log(P_d^{10,IGN}) = 0.9049 (\pm 0.0527) \times MI_{IGN} - 8.4182 (\pm 0.1831) \quad \text{Equation 26}$$

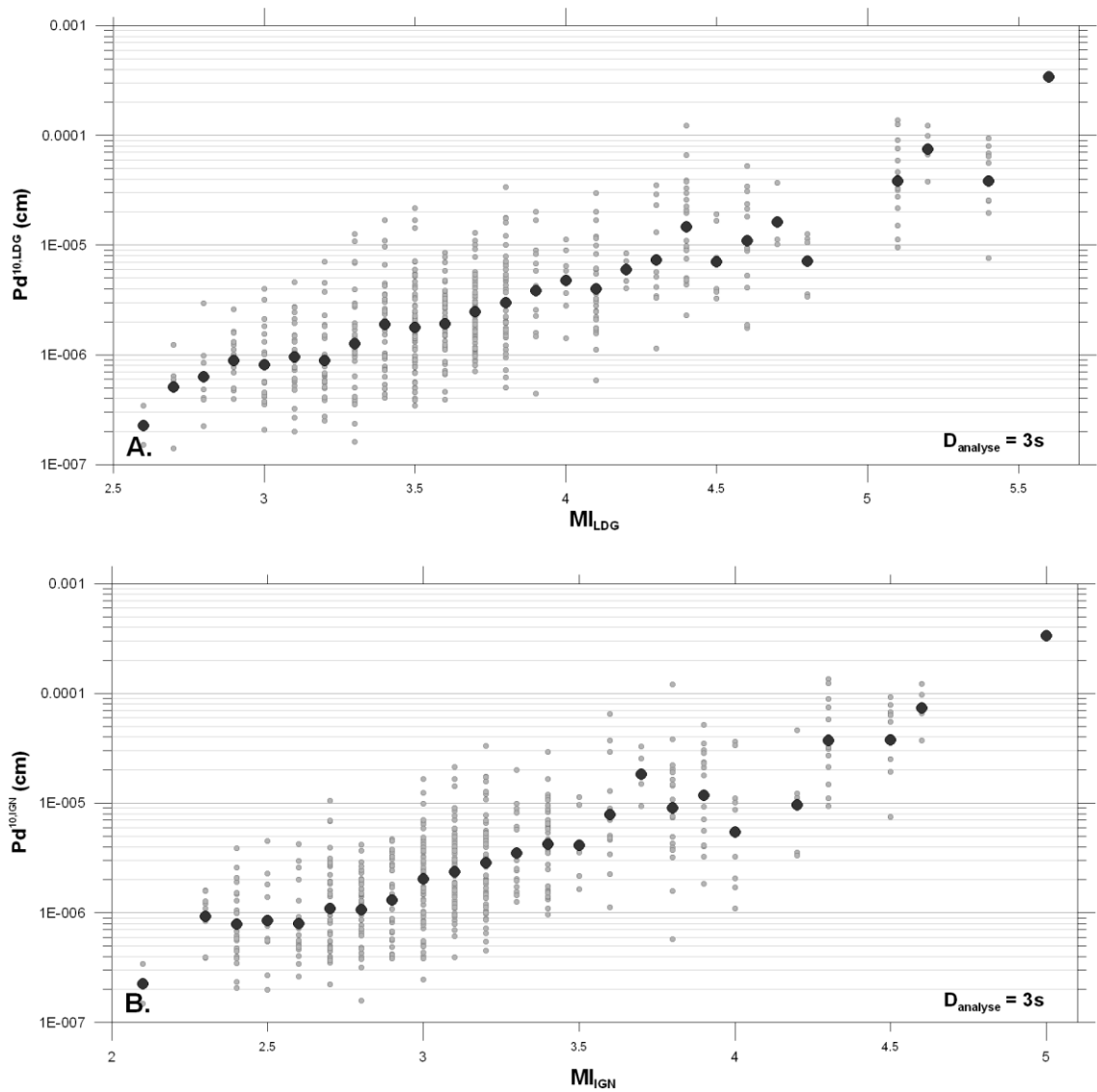


Figure 56 – A comparison between parameter P_d^{10} and local magnitude calculated by LDG (A) and IGN (B) for Pyrenean earthquakes. The grey dots represent values of the parameter P_d^{10} calculated in each station (analysis interval set at 3 s), which are averaged by 0.1 magnitude intervals (black dots).

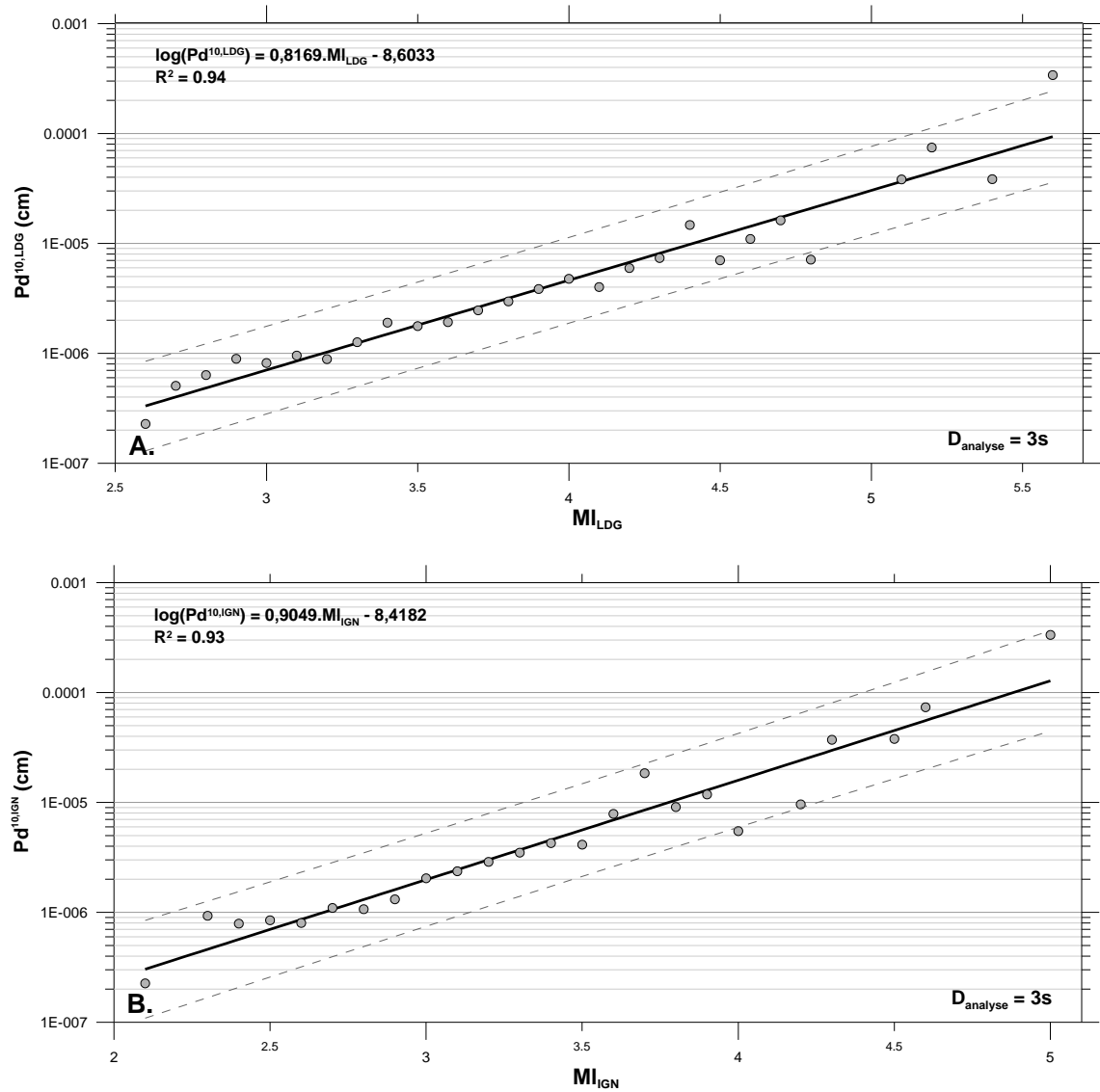


Figure 57 – Empirical relations linking the parameter P_d^{10} (mean per event) with local magnitude calculated by LDG (A) and IGN (B) for Pyrenean earthquakes. Calculations carried out on the traces of the catalogue that satisfy the selection criteria (analysis interval set at 3 s). The straight line obtained by linear regression is shown in black, while the grey dashed lines indicate the confidence interval at 95 % for a new observation.

Used reciprocally to determine the magnitude from P_d^{10} , these relations indicate corrected standard errors in magnitude of ± 0.21 of a unit of both MI_{LDG} and MI_{IGN} . These results would seem to indicate that the parameter P_d^{10} does statistically represent a very good real-time estimator for magnitude.

ii. The P_v method

As mentioned earlier in chapter 3.3.2.ii, the use of the parameter P_v may turn out to be preferable to that of P_d when working with acceleration signals because it avoids performing a double integration which is a potential source of noise. Unfortunately, the waveform catalogue used in the framework of this study does not contain enough signals that satisfy all our selection criteria to support determining an empirical relation specific to accelerometric records. Accordingly, we have calculated the P_v parameter here by including velocimetric data in such a way as to its potential as a magnitude “estimator”, as was done for τ_c , τ_p^{max} and P_d/P_d^{10} .

The empirical linear relations linking P_v with local magnitude (LDG et IGN) and epicentral distance, determined from 556 traces appertaining to 144 events on the basis of an analysis of the first three seconds of the P wave, are as follows (cf. Equation 27, Equation 28 and Figure 58):

$$\log(P_v) = 0.6010 (\pm 0.0280) \times M_{LDG} - 1.4577 (\pm 0.0947) \times \log(D_{epi}) - 4.6547 (\pm 0.1865) \quad \text{Equation 27}$$

$$\log(P_v) = 0.6489 (\pm 0.0306) \times M_{IGN} - 1.4533 (\pm 0.0953) \times \log(D_{epi}) - 4.4724 (\pm 0.1840) \quad \text{Equation 28}$$

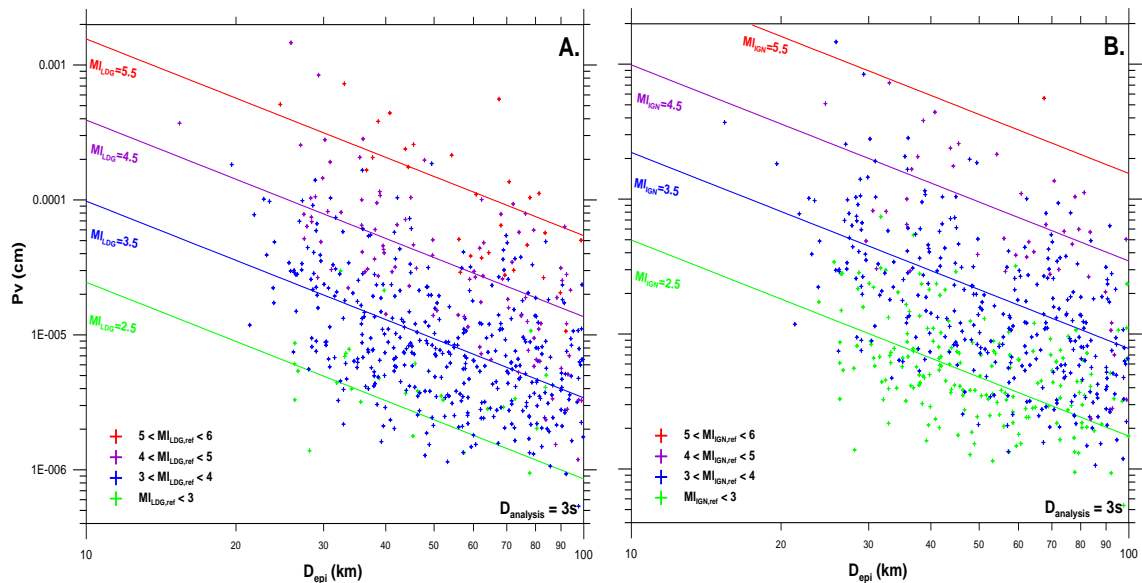


Figure 58 – Relation between P_v parameter and earthquake magnitude (LDG magnitude on fig. A and IGN magnitude on fig. B) and epicentral distance for Pyrenean records.

Once the parameter P_v^{10} has been scaled to an epicentral distance of 10 km, it can be represented versus magnitude (M_{LDG} and M_{IGN}) – cf. Figure 59. The mean for each event is indicated by dark grey dots.

An examination of the means for each event reveals a clear correlation between the parameter P_v^{10} and magnitude over all levels of magnitude (cf. Figure 60), unlike the frequency parameters for which this correlation emerges only above a certain magnitude.

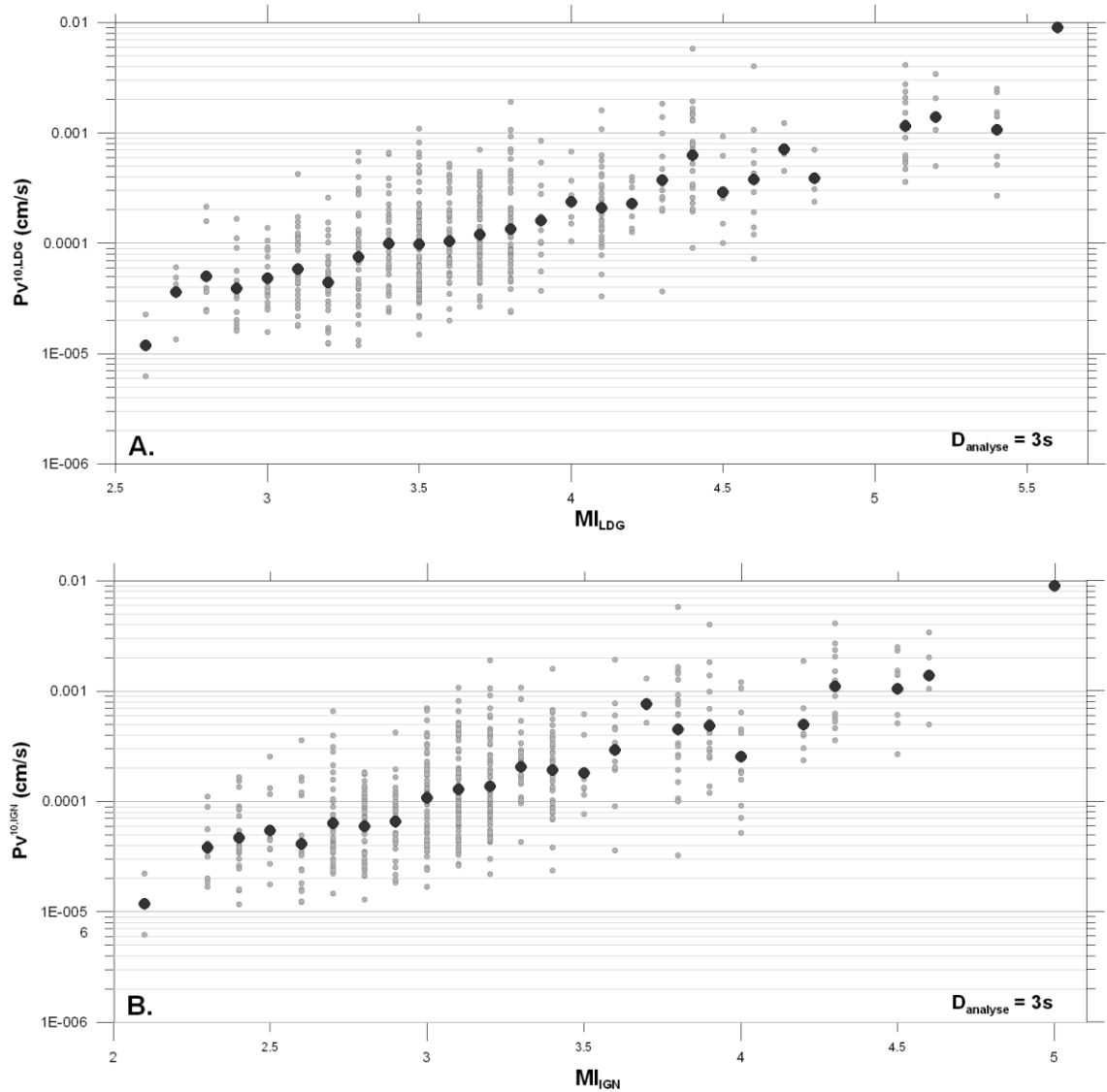


Figure 59 – A comparison between parameter P_v^{10} and local magnitude calculated by LDG (A) and IGN (B) for Pyrenean earthquakes. The grey dots represent values of the parameter P_v^{10} calculated in each station (analysis interval set at 3 s), which are averaged by 0.1 magnitude intervals (black dots).

The empirical linear relations linking P_v^{10} with local magnitudes determined from 144 events on the basis of an analysis of the first three seconds of the P wave are as follows (cf. Equation 29, Equation 30 and Figure 60):

$$\log(P_v^{10,LDG}) = 0.6895 (\pm 0.0392) \times MI_{LDG} - 6.4427 (\pm 0.1580) \quad \text{Equation 29}$$

$$\log(P_v^{10,IGN}) = 0.7821 (\pm 0.0455) \times MI_{IGN} - 6.3537 (\pm 0.1582) \quad \text{Equation 30}$$

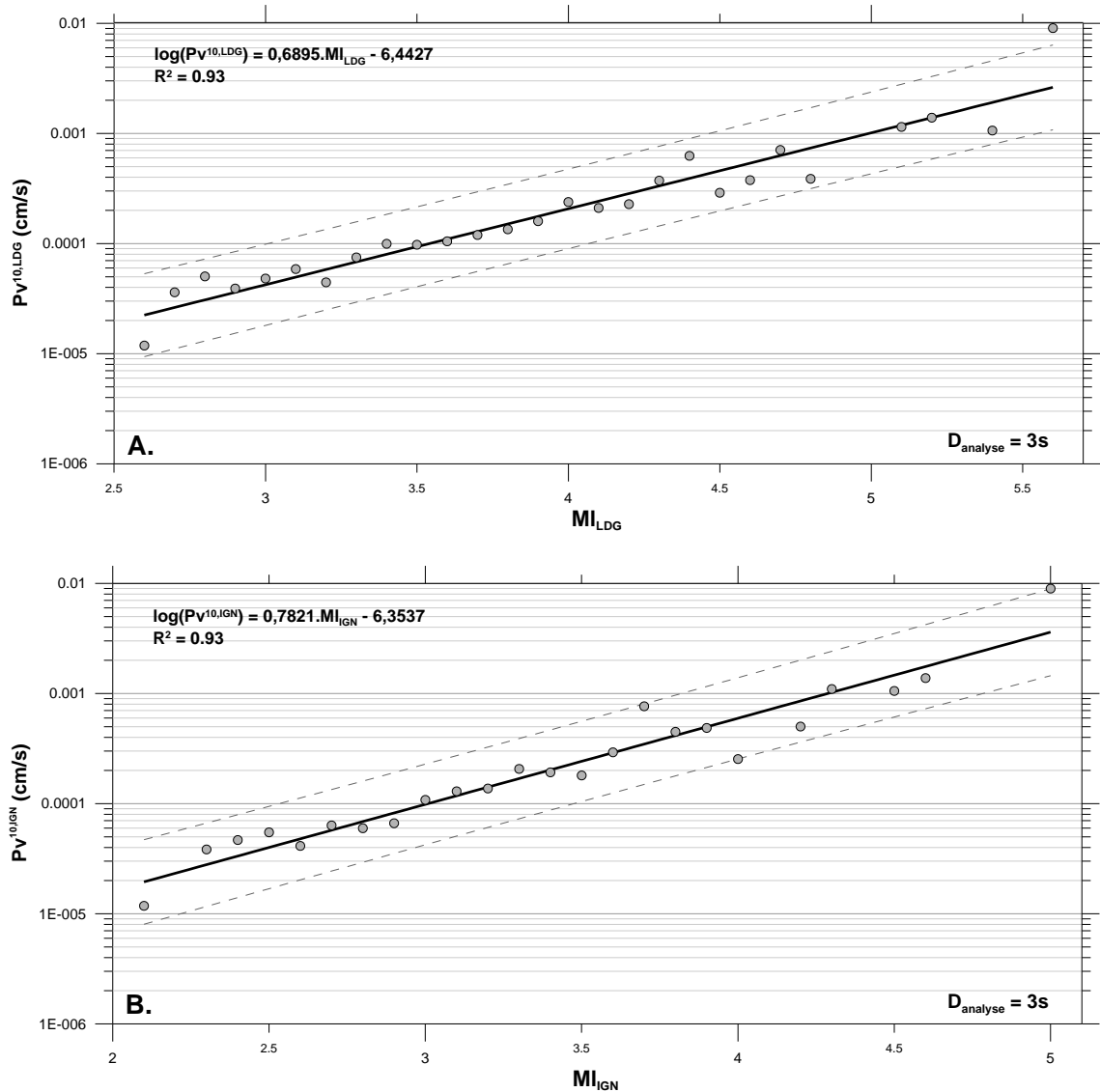


Figure 60 – Empirical relations linking the parameter P_v^{10} (mean per event) with local magnitude calculated by LDG (A) and IGN (B) for Pyrenean earthquakes. Calculations carried out on the traces of the catalogue that satisfy the selection criteria (analysis interval set at 3 s). The straight line obtained by linear regression is shown in black, while the grey dashed lines indicate the confidence interval at 95 % for a new observation.

Used reciprocally to determine the magnitude from P_v^{10} , these relations indicate corrected standard errors in magnitude of ± 0.22 of a unit of both M_{LDG} and M_{IGN} . These results would seem to indicate that the parameter P_v^{10} does statistically represent a very good real-time estimator for magnitude.

iii. Attempt to improve distance dependency of P_d/P_v parameters

As to improve distance dependency of P_d/P_v parameters, the same approach as the one previously detailed on paragraph 2.3.2 has been conducted considering relocations of Pyrenean earthquakes performed in the frame of module 3. Unfortunately, new epicentral distances calculated from these relocations show bad correlations with P_d/P_v parameters, while OMP original locations show relatively strong correlations as described on paragraphs 6.1.3.i and 6.1.3.i.ii.

6.2. *The influence of variations in the analysis time-length*

Although the parameters τ_c , τ_p^{max} , P_d^{10} and P_v^{10} appear to be relatively robust proxies for determining the magnitude of an earthquake from the first three seconds of recordings acquired in the epicentral zone, the specific context of the Pyrenees (cf. chapter 4) incites us to look into the effect that decreasing the time spent on analyzing the P wave could have on the magnitude estimate. Therefore the data analysis conducted in the preceding paragraphs is being extended to a P-wave analysis interval of 1 to 4 seconds. The results obtained from this work are summarized in Table 21 and Table 22, below, respectively for LDG and IGN-type magnitudes.

Due to the limited range of magnitudes considered in our analysis, it is not surprising that we should observe good correlation coefficients for analysis intervals shortened to 1 s (cf. Table 21 and Table 22), for the events considered correspond to relatively short rupture times. In other words, the portion of the signal being analyzed, however short it may be, bears the signature of most if not all the rupture, and accordingly of the magnitude. A study by Murphy and Nielsen (2009) showed that a 1-second analysis was long enough to assess moment magnitudes smaller than 6.0 ($2s \rightarrow M < 6.5$; $3s \rightarrow M < 7.0$). At larger magnitudes, the authors observe a saturation of the proxy being used (P_d). Theoretically, and taking into consideration a probable maximum magnitude of 6.5 for earthquakes in the Pyrenees, a 2-second analysis of the P wave would appear to suffice for determining the magnitude of Pyrenean events in real time.

Linear Relation: $\log_{10} y = a + b.MI_{LDG}$										
y	Analysis time-length	a			b			SE_c	SE_c (unit mag.)	R^2
τ_c	1 sec	-1.6965	±	0.0814	0.2422	±	0.0198	0.08	0.32	0.87
	2 sec	-1.6370	±	0.0917	0.2250	±	0.0220	0.08	0.36	0.83
	3 sec	-1.5653	±	0.1139	0.2063	±	0.0270	0.09	0.46	0.73
	4 sec	-1.6242	±	0.1222	0.2214	±	0.0287	0.09	0.42	0.75
τ_p^{\max}	1 sec	-1.1764	±	0.0581	0.1260	±	0.0144	0.06	0.49	0.75
	2 sec	-1.1286	±	0.0600	0.1198	±	0.0149	0.06	0.53	0.72
	3 sec	-1.1648	±	0.0641	0.1313	±	0.0159	0.07	0.52	0.73
	4 sec	-1.2196	±	0.0947	0.1449	±	0.0230	0.09	0.61	0.63
$P_d^{10,LDG}$	1 sec	-8.8150	±	0.1590	0.8272	±	0.0394	0.17	0.21	0.95
	2 sec	-8.8310	±	0.1741	0.8623	±	0.0432	0.00	0.00	0.94
	3 sec	-8.6033	±	0.1708	0.8169	±	0.0424	0.18	0.21	0.94
	4 sec	-8.5717	±	0.1871	0.7910	±	0.0459	0.19	0.24	0.93
$P_v^{10,LDG}$	1 sec	-6.5502	±	0.1518	0.6792	±	0.0377	0.16	0.24	0.93
	2 sec	-6.6694	±	0.1531	0.7284	±	0.0380	0.00	0.00	0.94
	3 sec	-6.4427	±	0.1580	0.6895	±	0.0392	0.17	0.22	0.93
	4 sec	-6.3868	±	0.1718	0.6459	±	0.0422	0.17	0.23	0.91

Table 21 – Summary of the empirical relations obtained for each parameter that was studied and for different analysis intervals, with a local magnitude LDG.

Considering a given set of waveforms, an increase in the analysis interval of the P wave results qualitatively in an improvement in the correlations between the various proxy parameters being considered and magnitude. In our case, in order to constrain each of the empirical relations as much as possible, we have nevertheless opted for always considering all the traces available, which are all the more numerous as we decrease the analysis interval and that the selection criterion on the time differential between the onsets of P and S waves is made less restrictive (cf. Table 23). Thus, since these two effects act simultaneously, Table 21 and Table 22 do not reflect a systematic connection the analysis interval and the quality of the linear relation. In other words, although as estimators they are in essence not as powerful, the parameters determined on the basis of a short analysis are paired with empirical relations versus magnitude that are better constrained than the parameters determined on the basis of a longer analysis.

Linear Relation: $\log_{10} y = a + b.MI_{IGN}$										
y	Analysis time-length	a			b			SE_c	SE_c (unit mag.)	R^2
τ_c	1 sec	-1.6014	±	0.0689	0.2566	±	0.0198	0.07	0.29	0.88
	2 sec	-1.5267	±	0.0896	0.2326	±	0.0254	0.09	0.38	0.80
	3 sec	-1.4870	±	0.1154	0.2198	±	0.0319	0.10	0.46	0.71
	4 sec	-1.4899	±	0.1142	0.2230	±	0.0316	0.10	0.44	0.72
τ_p^{\max}	1 sec	-1.1360	±	0.0611	0.1354	±	0.0178	0.07	0.52	0.72
	2 sec	-1.0750	±	0.0577	0.1246	±	0.0168	0.07	0.53	0.70
	3 sec	-1.1286	±	0.0564	0.1413	±	0.0164	0.07	0.46	0.76
	4 sec	-1.2291	±	0.0875	0.1691	±	0.0248	0.09	0.51	0.69
$P_d^{10,IGN}$	1 sec	-8.6609	±	0.1726	0.9279	±	0.0509	0.21	0.22	0.93
	2 sec	-8.7822	±	0.2049	1.0007	±	0.0604	0.00	0.00	0.92
	3 sec	-8.4182	±	0.1831	0.9049	±	0.0527	0.19	0.21	0.93
	4 sec	-8.4070	±	0.2175	0.8861	±	0.0617	0.21	0.24	0.91
$P_v^{10,IGN}$	1 sec	-6.5038	±	0.1803	0.7849	±	0.0531	0.22	0.28	0.90
	2 sec	-6.6589	±	0.1766	0.8536	±	0.0521	0.00	0.00	0.92
	3 sec	-6.3537	±	0.1582	0.7821	±	0.0455	0.17	0.22	0.93
	4 sec	-6.3027	±	0.1737	0.7377	±	0.0493	0.17	0.23	0.91

Table 22 – Summary of the empirical relations obtained for each parameter that was studied and for different analysis intervals, with a local magnitude IGN.

From a more qualitative standpoint, examining Table 21 and Table 22 allows us to emphasize that initial magnitude estimates seem to be able to be derived from a very short analysis interval, which can subsequently be refined in the framework of an evolving approach. For example, shortening the analysis interval from three to two seconds in the instance of a single station situated at the epicenter comes down to decreasing the blind-zone by about 5 km.

<i>Proxy</i>	<i>Analysis time-length</i>	<i>Nb. seismic traces (nb. earthquakes)</i>	<i>Range of Validity</i>
τ_c	1 s.	293 (109)	$2.6 \leq M_{LDG} \leq 5.6$
			$2.0 \leq M_{IGN} \leq 5.0$
	2 s.	221 (83)	$2.9 \leq M_{LDG} \leq 5.6$
			$2.3 \leq M_{IGN} \leq 5.0$
	3 s.	171 (73)	$2.9 \leq M_{LDG} \leq 5.6$
			$2.4 \leq M_{IGN} \leq 5.0$
	4 s.	121 (56)	$3.1 \leq M_{LDG} \leq 5.6$
			$2.4 \leq M_{IGN} \leq 5.0$
τ_p^{max}	1 s.	447 (133)	$2.6 \leq M_{LDG} \leq 5.6$
			$2.0 \leq M_{IGN} \leq 5.0$
	2 s.	389 (118)	$2.6 \leq M_{LDG} \leq 5.6$
			$2.0 \leq M_{IGN} \leq 5.0$
	3 s.	312 (105)	$2.6 \leq M_{LDG} \leq 5.6$
			$2.0 \leq M_{IGN} \leq 5.0$
	4 s.	240 (88)	$2.8 \leq M_{LDG} \leq 5.6$
			$2.3 \leq M_{IGN} \leq 5.0$
P_d^{10} & P_v^{10}	1 s.	701 (155)	$2.6 \leq M_{LDG} \leq 5.6$
			$2.0 \leq M_{IGN} \leq 5.0$
	2 s.	634 (152)	$2.6 \leq M_{LDG} \leq 5.6$
			$2.0 \leq M_{IGN} \leq 5.0$
	3 s.	556 (144)	$2.6 \leq M_{LDG} \leq 5.6$
			$2.1 \leq M_{IGN} \leq 5.0$
	4 s.	460 (130)	$2.7 \leq M_{LDG} \leq 5.6$
			$2.3 \leq M_{IGN} \leq 5.0$

Table 23 – Table summarizing the data used in establishing the correlations presented in Table 21 and Table 22, and the associated ranges of validity in magnitude.

Furthermore, it is seen that although each of the parameters τ_c , τ_p^{max} , P_d^{10} and P_v^{10} would seem individually to be closely correlated with earthquake magnitude, some appear to be better proxies than others. Thus, from a statistical standpoint, the most satisfactory proxies are, in order, P_d^{10} and P_v^{10} (which are very similar by nature and cannot be considered as independent parameters), the frequency parameter τ_c , and lastly the frequency parameter τ_p^{max} . However, these different parameters can, to a certain extent, be considered as complementary. Thus, by averaging different magnitude

estimations such as one coming from a frequency parameter and another one coming from an amplitude parameter, a better estimate of magnitude is obtained with a smaller standard deviation. For example, in the instance of a 3-second analysis interval with a 60 SNR threshold (so as to be able to estimate for each proxy parameter), the standard error associated with the determination of a mean magnitude of τ_c^{10} and $P_{d,10}$ estimates is 0.41 for both LDG and IGN local magnitudes (cf. Figure 61). These results are slightly less good than the ones got with the $P_{d,10}/P_{v,10}$ parameters, but should be more robust.

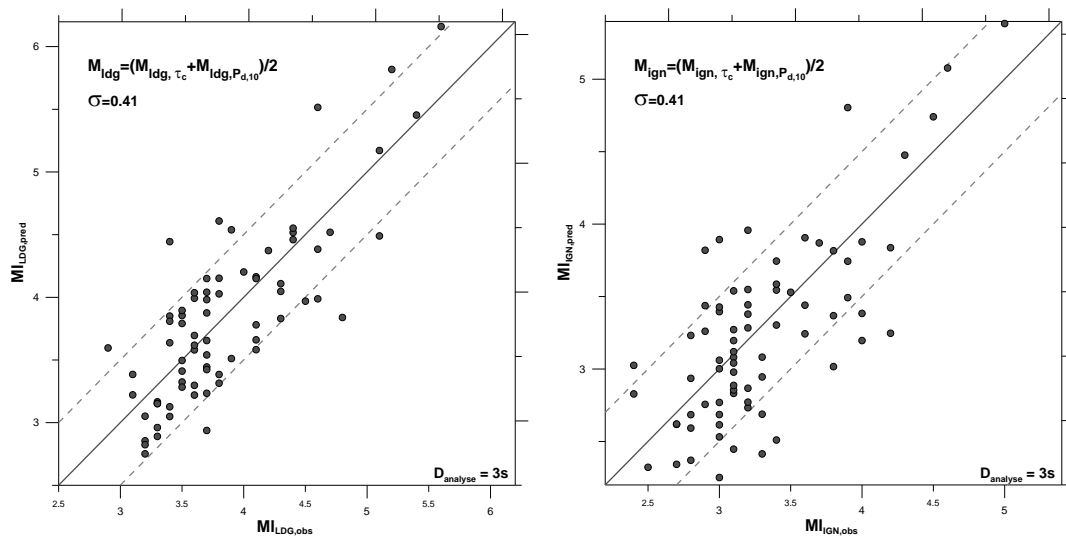


Figure 61 – Comparison between observations and predictions of $M_{LDG,IGN}$, using both τ_c and $P_{d,10}$ proxy parameters (SNR=60, analysis time-length = 3s). Each dot is associated to a single earthquake. Grey dashed lines indicate the ± 0.5 magnitude prediction domain.

Highlight:

It is very noticeable to point out from Table 21 and Table 22 the quasi unitary slope between magnitude and $P_{d,10}/P_{v,10}$ parameters got from correlations for all the considered calculation configurations. Far to be a surprise, that unity slope comes from the fact that the expression of the relation linking P_d/P_v parameters (thereafter normalized to 10 km) with local magnitude is similar to the local

¹⁰ τ_c is favoured to τ_p^{max} since 1) it exhibits sensibly best results in Pyrenean data and 2) it is considered by many authors as less influenced than τ_p^{max} by the filter parameters and pre-event noise (e.g. Shieh et al., 2008 ; Zollo et al., 2010).

magnitude definition itself¹¹. Working on a portion of the P-wave and none on the whole signal, we consequently calculate a pseudo local magnitude which reveals to be very close to the one calculated classically.

6.3. *A comparison with previously established relations*

As we have already pointed out, the values of the different proxy parameters used in this study depend strongly upon the parameters of the calculation, and notably on the filtering, making it difficult to compare different studies with each other. Be that as it may, it is nevertheless interesting to situate the relations obtained in the present report globally with respect to others established earlier by other authors in contexts that were significantly different.

Because most of the pre-existing relations favor moment magnitude over local magnitude, we will focus on IGN magnitude related relations since IGN local magnitude is close to moment magnitude¹².

The first assessment that could be done looking Figure 62, Figure 64 and Figure 65 is that the range of validity in magnitude for our relations is lower than the one in other relations. This comes from the fact that these latter were obtained in countries characterized by a considerably higher level of seismicity than that in the Pyrenees.

With regard to parameters τ_c and τ_p^{max} , relations obtained in the framework of this study (from IGN-type magnitudes – afterwards called “SISPy relations”) are globally coherent with the other available relations, notably in terms of slope of the log-linear relation, although SISPy relations remains on the bottom part of the whole relations (Figure 62 and Figure 64). That relatively stable slope confirmed that τ_c , and in a lesser measure τ_p^{max} , are quite stable proxy parameters to predict magnitude – even for low magnitudes, while the shift between relations comes probably from differences of both frequency band considered for calculations and reference magnitudes used to establish correlations.

The stability of τ_c parameter could also be illustrated by Figure 63 comparing estimations of that parameter on data related to Pyrenean and worldwide

¹¹ Local magnitude is got measuring maximal amplitude of seismic waves on relatively close-field stations, applying a distance correction, and for a relatively high frequency as a rule close to 1 Hz.

¹² Indeed, as shown by Braunmiller et al. (2005), LDG local magnitude exhibits a nearly-systematic discrepancy of +0.6 compared with moment magnitude, as it is the case with IGN local magnitude (cf. paragraph 4.2). Thus M_{IGN} and M_w could be globally considered as equivalent in first approximation.

earthquakes: it can be seen that both dots clouds are mixed up on their common magnitude range.

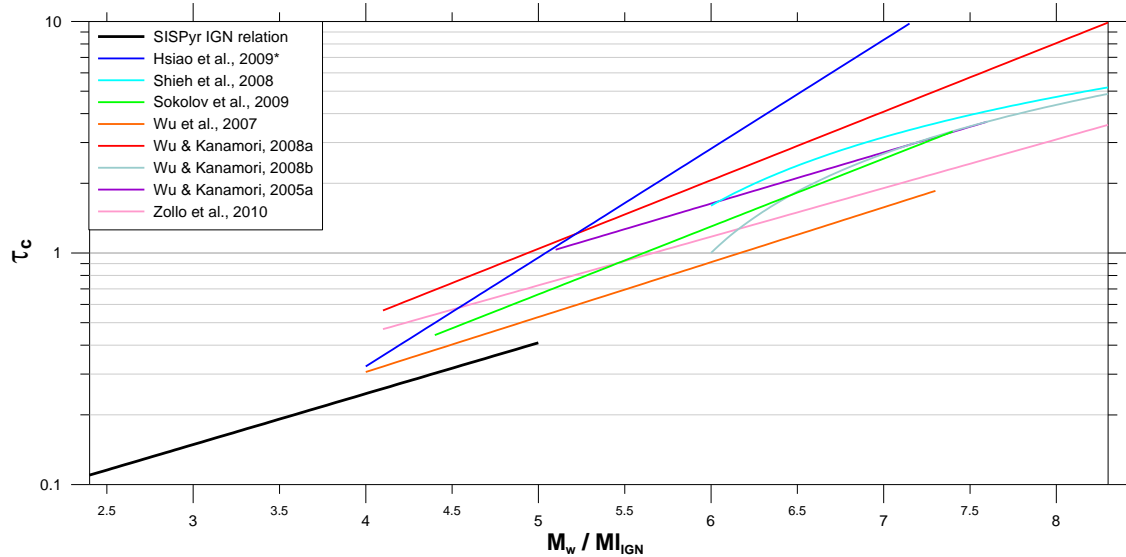


Figure 62 – A comparison between the empirical relation linking the parameter τ_c with the magnitude determined in the framework of this study (M_{IGN} – analysis interval 3 s) with other relations published in the literature. Relations mentioned with an asterisk symbol are related to a local magnitude definition.

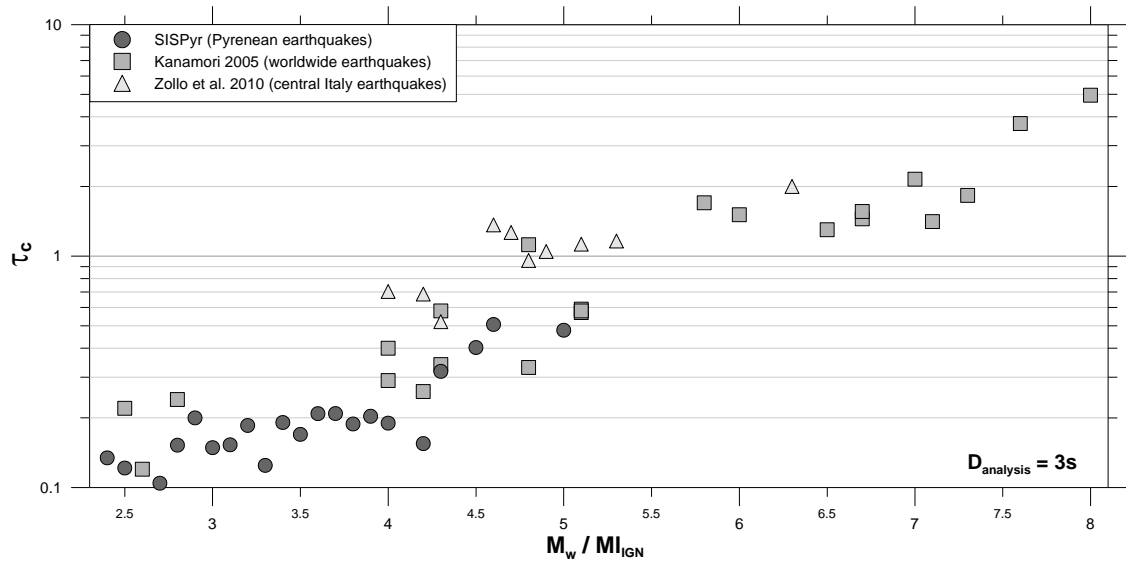


Figure 63 – Comparison between τ_c estimations from Pyrenean data (this study) and worldwide data (Kanamori, 2005).

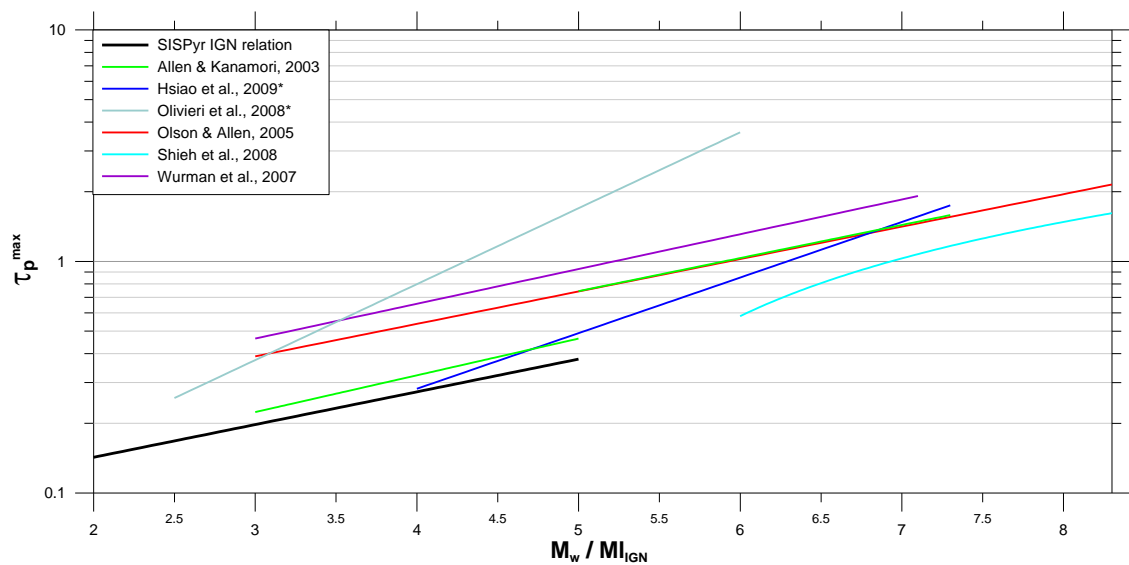


Figure 64 – A comparison between the empirical relation linking the parameter τ_p^{max} with the magnitude determined in the framework of this study ($M_{I_{DG}}$ converted into M_w using the relation in Drouet (2005) – analysis interval 3 s) with other relations published in the literature. Relations mentioned with an asterisk symbol are related to a local magnitude definition.

As to the comparison of relations that involve the amplitude parameters P_d and P_v , we have only presented here the example of P_d^{10} insofar as, to the best of our knowledge, the parameter P_v^{10} has not been dealt with so far in published relations. It would thus appear that, although the SISPyR relations does predict values that are lower than the other relations represented, the different curves are still coherent (cf. Figure 65). The observed differences probably result from the different frequency band considered in our study which is shorter than the one used in other ones.

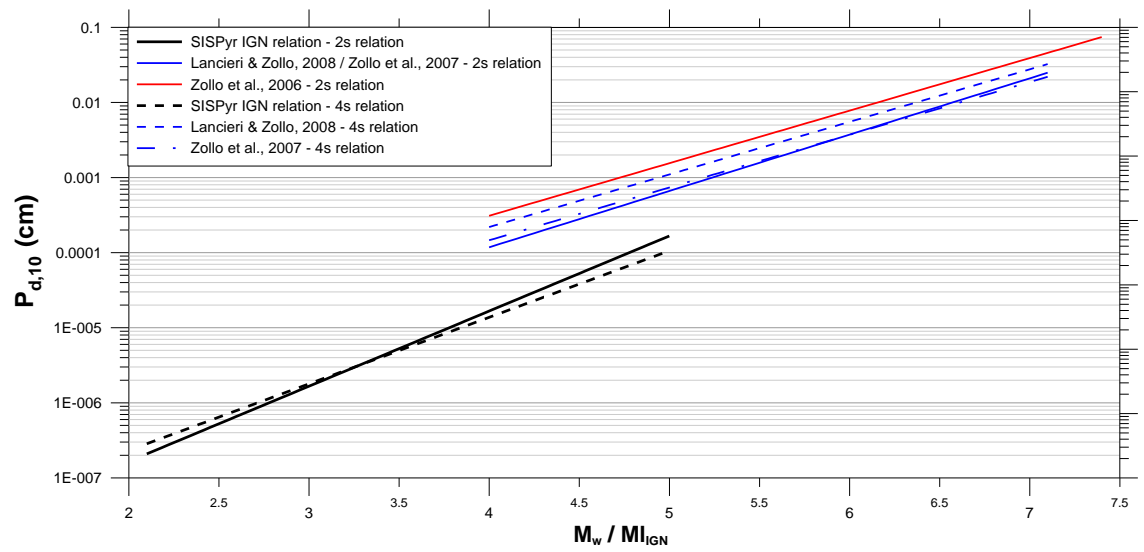


Figure 65 – A comparison between the empirical relation linking the parameter P_d^{10} with the magnitude determined in the framework of this study (M_{IGN} – analysis interval 2/4 s) with other relations published in the literature.

7. Towards extending the range of validity of the reference relations

The empirical relations established in chapter 7 between different indicators for seismic ground motion and magnitude remain limited by their range of validity, which is restricted with respect to magnitude ($\sim 2.6 \leq M_{LDG} \leq \sim 5.6$ and $\sim 2.0 \leq M_{IGN} \leq 5.0$), as are the contents of the waveform catalogue (cf. chapter 0).

Clearly, while it is important to be able to distinguish in real time between small earthquakes and more powerful ones and, to this effect, have access to relations that are valid for small events, the principle of early warning is mainly pertinent for large, potentially damaging, magnitudes. As to the Pyrenean massif, the seismotectonic context thus raises the possibility of major earthquakes with magnitudes that could reach 6.5. Accordingly, we need to look into a way to extend the range of validity in magnitude of the relations established earlier.

Two solutions can at first glance be considered in order to proceed to extend the catalogue to cover stronger magnitudes:

- Using empirical relations already published that are based on worldwide data;
- Extending the catalogue by integrating signals not from the Pyrenees recorded for stronger earthquakes in regions characterized by seismotectonic contexts comparable to that in the Pyrenees, or by creating synthetic signals for the desired magnitude range.

7.1. *On using relations from other regions for Pyrenean earthquakes*

Recent work published in 2010 by Zollo *et al.* indicates that empirical relations linking parameters τ_c and P_d with magnitude depend little on the local context and can be considered as “global” relations usable by all EWSs. In fact, these authors show notably that differences in earthquake mechanism are reflected solely in the limits of uncertainty associated with the relations.

Since also Zollo *et al.* (2010) propose in their article a simplified methodology for EWS based notably on a test using the 6 April 2009 l’Aquila earthquake ($M_w=6.3$), we decided to test the applicability of their relations on the Pyrenean context. To do so, we applied their procedure for calculating the indicators τ_c and P_d to our Pyrenean data in order to compare the results obtained with their relations, with a high-pass filter with a cut-off frequency at 0.075 Hz.

It stands out from that comparison that the 0.075 Hz high-pass filter is not suitable to our data-set because the majority of records correspond to small magnitudes, that results in a significant degree of scatter of our results (see light grey dots on Figure 57). Raising the cut-off frequency of the high-pass filter to higher values (e.g. 0.3 Hz), we may observe a drop-off of scattering and a relatively good agreement between pyrenean τ_c values and the empirical relation established by Zollo *et al.* (2010) based on worldwide data (cf. Figure 66). The same comparison with our reference τ_c [1-50] Hz band-pass filter also shows a good fit with the Zollo *et al.* relation, with an even lowest scatter: even though our results seem to be slightly shifted downward compared to the reference relation, they remain in the overall dots cloud of Zollo *et al.* Moreover, Italian data used by Zollo *et al.* are on the contrary shifted upward.

This would appear to confirm the authors' hypothesis according to which the relation between τ_c and magnitude is relatively independent of the seismotectonic context under consideration, and supports the possibility to apply their relation to the Pyrenees.

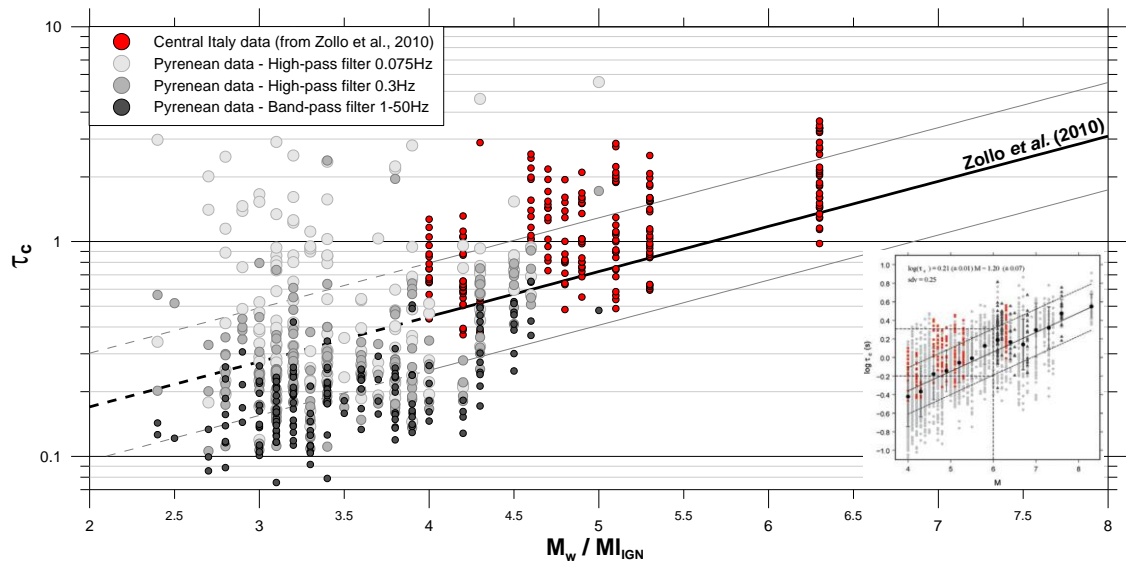


Figure 66 – Comparison between the results obtained for parameter τ_c from Pyrenean data with the relation established by Zollo *et al.* (2010) using worldwide data linking the parameter τ_c to magnitude. Grey dots indicated different results got for Pyrenean data making use of different filters, while red dots represents data from central Italy, which belong to the data set used by Zollo *et al.* (2010) to establish their correlation (see insert down-right).

8. Application to the April 2010 earthquake

Next, we sought to test the pertinence of the relations that we have succeeded in establishing by conducting a “blind” test on an actual example: the recent Bigorre event on 1 April 2010, having a local LDG magnitude of 4.4 (cf. Figure 67). The acceleration and velocity time histories (ACC and BB) recorded in the Pyrenean stations accordingly were processed and used. There are 21 vertical-component traces available in acceleration and 14 in velocity, hence a catalogue of 35 signals.

We are depicting the evolution of magnitude estimation in the stations having an epicentral distance of less than 100 km and satisfying the selection criteria using the parameters τ_c , τ_p^{max} , P_d^{10} and P_v^{10} . In the context of real-time estimation, we accept to use stations presenting at least a one-second interval between the P and the S-wave onsets. Thus ten stations provide vertical traces that satisfy the criteria defined above ($SNR \geq 60$ as to be able to properly calculate each proxy, $\Delta t_{P,S} \geq 1$ s., $d_{epi} \leq 100$ km) (cf. Table 24).

The first estimate of magnitude is made once one second of signal has been recorded in the first station that detected the event, using the log-linear relation established corresponding to the analysis interval. Initially, we calculate the magnitude estimations independently for each parameter. Thus, we use the different relations established relative to the analysis intervals of 1, 2, 3 and 4 seconds according to the length of the analysis window available for each station when the update takes place. This process continues until four seconds of signal become available on the last station to have triggered (PYAT). At the same time and at each instant, a mean magnitude is calculated by averaging the estimates made using the four indicators τ_c , τ_p^{max} , $P_{d,10}$, $P_{v,10}$ as well a mixed indicator resulting from average between τ_c and $P_{d,10}$ magnitude estimations.

	P-wave onset / origin time (s)	Epicentral distance (km)
FMON	3.4	15.9
PYCA	3.4	9.3
PYBB	3.7	13.9
PYLS	5.4	25.8
PYLU	6.1	33.6
PYAS	6.6	43.1
PYTB	7.1	33.7
PYAD	10.5	58.3
PYPC	12.1	63.6
PYAT	14.2	81.0

Table 24 – List of the different recordings available for estimating the magnitude for the Bigorre earthquake on 1 April 2010.

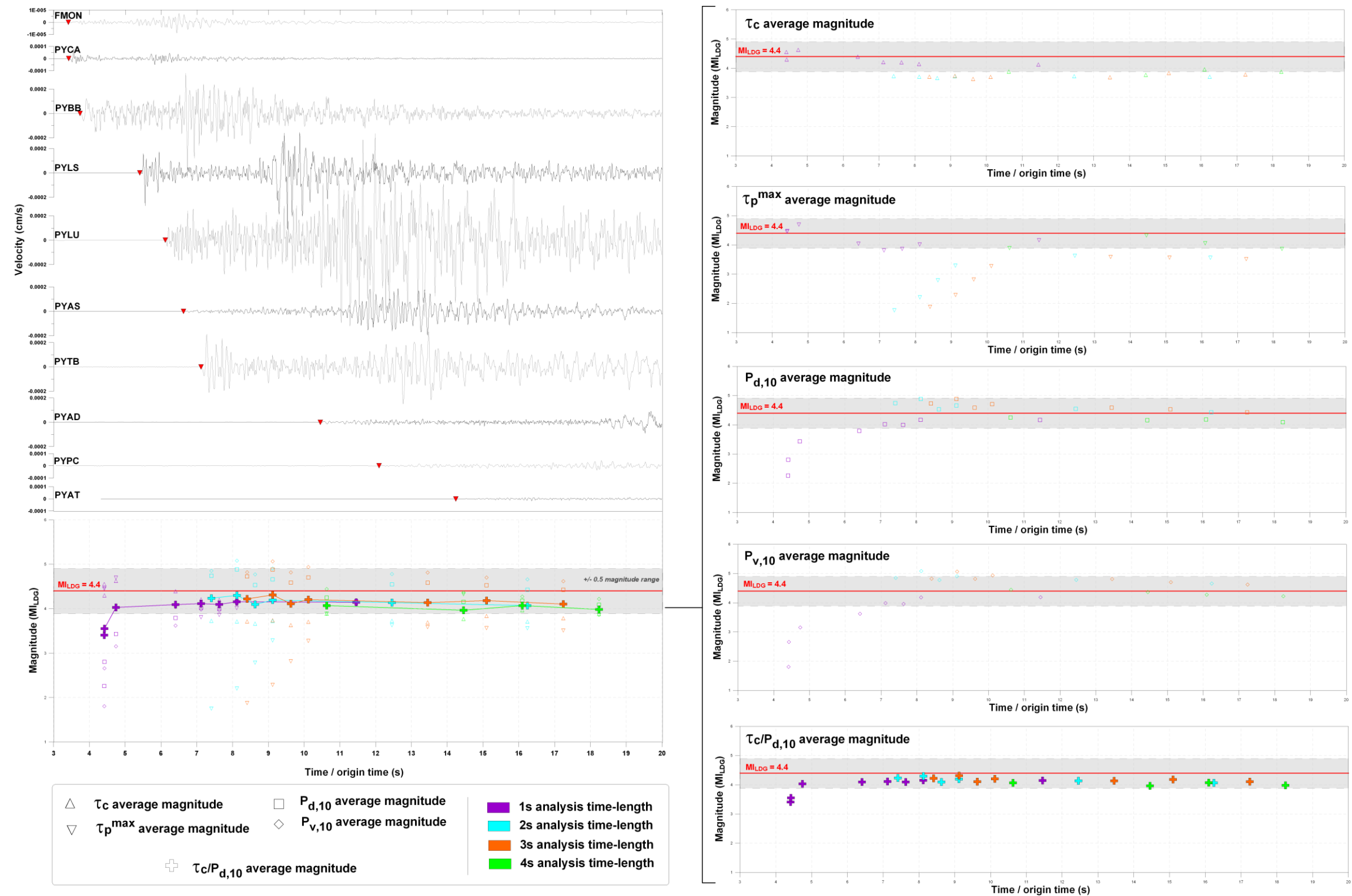


Figure 67 – Seismic traces for the 1 April 2010 earthquake that satisfied the selection criteria and real-time evolution of the magnitude estimated by means of the different methods that have been examined versus the reference LDG magnitude (red line). The P-wave onset pick is marked by a red triangle.

The estimates obtained are globally relatively satisfactory insofar as they appear to quickly converge over time towards final values for the event which are very close to the true one (cf. Figure 67), even though some of the predictions notably misestimate the magnitude.

The first observation that could be done from these results is that the combined estimator $\tau_c / P_{d,10}$ allows to get a best estimation of magnitude that from each proxy parameter considered individually. In particular, as it seems that the amplitude-based methods slightly overestimate the magnitude while the ones relying on the frequency content of the signal underestimate it, this alternative estimator looks more reliable. Another very interesting remark is that the time length window considered for the analysis of the P-wave does not influence strongly the assessed values of magnitude confirming that for low magnitudes the first second of the P-wave give information about the final size of the earthquake. Thus, final estimates performed from analysis of 1, 2, 3 and 4 seconds of the P wave are respectively 4.1, 4.1, 4.1 and 4.0, for a reference LDG magnitude of 4.4. Moreover, disregarding time-transmission of the data from each station to the system center, we can observe in this test a stable estimate of magnitude equal to 4.0, 4.7 s only after the origin time of the earthquake. In the same time, making use of the relation of Zollo et al. (2010) conduct to clear under-estimation of magnitude with an estimation of M_{LDG} around 3.0 (considering that $M_{LDG} \sim M_w + 0.6$).

9. Utility of a Pyrenean EWS

Early-warning should not be considered as an end in itself and its utility has to be deemed with regard to effective use that can be done of it. Indeed EWS may be divided into two essential components which are the scientific analysis and the diffusion/use of early-warning (Nigg, 1995). Then, as early and reliable that an alert can be, if it is not relayed in a satisfactory way or if addressees do not take appropriate actions in response to its reception, a EWS could be considered as ineffective with reason.

Nevertheless, end-user aspects are very often neglected during conception and setting up of EWS, all the efforts being concentrated on technical questions allowing emitting alerts. As an example, Mexican system SAS which is operating since 1991 and is able to provide nearly 1 minute alerts in Mexico, is often finger-pointed for the absence of strategy in identification of end-users and their needs: this absence of strategy is judged as being the main limiting factor of the efficiency of the system (Suárez *et al.*, 2009).

Then it is indispensable not only to identify potential end-users of a Pyrenean EWS, but also to evaluate their perception of the system, their needs as well as their envisaging actions in response to an early-warning. According Suárez *et al.* (2009), this step must also allow to hierarchy recipients of the alert considering as well amount of stake that they represent and their vulnerability, as their capability to react in an appropriate way.

Away from being disconnected from the more technical phase consisting to analyse seismic data, this reflexion is necessary to the conception of the system, from the choice of methods used for the data analysis to the definition of type(s) of alerts and the way to diffuse them.

9.1. *Using seismic early warning*¹³

Potential impacts of strong natural hazards on urban societies may be reduced by quick and adapted actions Example of tsunami that occurred on 26th December 2001 in Indian Ocean is particularly explicit about importance to dispose of adapted measures to take in case of alert. Indeed, in spite of the existence of an operational tsunami early warning system at that time, a bad-adapted decision and dissemination chain did not allowed to reduce impact of the tsunami.

¹³ From Auclair et Bertil, 2009.

In the case of seismic hazard, available time to protect from an earthquake once it has occurred is extremely short. Thus EWS generally provide few seconds to few ten of seconds to take measurements able to minimize the impact of strong motions. With such short times, decision taking must be as automatized as possible, even though in some cases individual actions can also be taken.

9.1.1. Automatic actions

Most of the EWS – being “regional” or “specific” – are associated to automatic actions which present the great advantage to be not dependent to time-costly human actions. Choice of automatic actions to take in case of early-warning reception mostly depends on adequacy between lead times and the time necessary for the considered system's safety stop.

For information purposes, here is a list of existing automatic actions:

- Power shut-down of high-speed trains to slow down them in order to avoid their passage into the epicentral area where the line is potentially damaged (ex. West Japan Railway Company) – cf. Nakamura (1989);
- Critical systems cessation (nuclear plants, chemical reactor, etc.) – cf. Wieland et al. (2000) and Wieland (2001);
- Traffic stop and shut-down of sensible transportation networks (ex. turning to red of traffic lights on the Lions Gate Bridge at Vancouver) ;
- Closure of sensible energy networks (oil and gas pipelines and distribution networks – ex. Tokyo gas network : http://www.tokyo-gas.co.jp/techno/stp/97c1_e.html);
- Stopping elevators at security positions in order to prevent people from being trapped;
- Stopping of sensible informatics systems and saving of important data;
- “Semi-active” control of building: rapid change of buildings' dynamic properties.

9.1.2. Semi-automatic actions

When lead times reach a ten of seconds, additional measures needing human interventions can also be put in place. The enforcement of these measures still implies automatic alert processes, but relies on a human decision.

For information purposes, here is a list of existing semi-automatic actions:

- Warning of the airports in order to avoid landing;

- Warning of crisis management centres and rescue teams in order to let a better organisation of crisis management thanks to anticipation;
- Warning of hospitals in order to suspend activity of surgical units during strong motions.

9.1.3. Population warning

When lead time is important enough, the alert can be send to the population in order to evacuate the most exposed places and to enable behaviours of personal protection.

9.2. ***End-users survey***

EWS are intended to reduce impacts of earthquakes by means of issuing few seconds early-warnings, in order that preventive measures could be quickly done before arrival of destructive strong motions. Being only a tool for the management of seismic hazard, thus it presents usefulness only when it is properly used by end-users. By its conception, it is consequently imperative that a EWS could answer to demands of these end-users in such a way to be adapted to their needs, and not the contrary as it is often the case. Indeed, many EWS (seismic or not) have been developed in total disconnection with this notion of “need”, requiring their end-users to adapt themselves to the systems...

Henceforth, approach of consultation of potential end-users is necessary so as to better understand their own problematic, their expectations (or conversely their absence of expectations), as well as their needs in terms of early warning. To that end, it has been decided to carry out a survey in the French side of the SISPyR's area. Despite that surveys are broadly used, realization of enquiry questionnaires still remains a critical step that has to be considered with care, since it conditions the outreach of the survey itself. Five steps are usually recommended for this work:

- Formulation of survey's objectives;
- Determination of the public targeted by the survey;
- Definition of information that need to be collected and choice of variables;
- Formulation of questions;
- Structuration of the questionnaire (gathering and linking questions, questionnaire length, etc.).

9.2.1. Survey's objectives

The final objective of the survey is to make available answer elements about opportunity to endow Pyrenees with a EWS. If need be, collected information should allow to give directions for the conception of the EWS based on the SISPYR's network, in order to offer a system fully adapted to end-users' needs and expectations.

Collected information in the frame of this survey must notably provide key elements to answer to the question "*Does it exist a need to dispose of a Pyrenean EWS?*". In function of answers given to that question, if the response is yes, it will be advisable to explicit this need and to confront it with results of the technical feasibility analysis performed on chapters 3 and 6. If the response is not, it will be advisable to possible proven needs for other types of seismic risk managing tools (pseudo onsite EWS: i.e. automatic shutdown systems relying on threshold exceedance of parameters such as PGA, Rapid Response Systems –RSS- such as the one develop during the ISARD Interreg project, etc.).

9.2.2. Targeted public

In function of conditions specific to each situation (earthquake characteristics, expected ground motions' amplitude, lead time, EWS reliability, sensitisation of involved actors to seismic risk, etc.), number and type of EWS's end-users may vary drastically. Thus, question of addressees of the survey designated under general denomination of "end-users" must be considered with care. That implies to identify potential end-users of the system in a way as exhaustive and realistic as possible, crossing information dealing with 1) stakes in presence and with their management, 2) conceivable actions in response to reception of an early warning, and 3) orders of magnitude of expected leading times in Pyrenees (cf. chapter 3).

Joint examination of points 2 and 3 leads us in a first time to rule out possibility of a broad diffusion of the early warning at destination of population, Pyrenean context obviously not allowing to get lead times important enough to envisage population alerts. Indeed, preliminary analysis performed on chapter 3 suggests lead times ranging between 0 and a ten of seconds in average in sinister areas (around 20 seconds in best case with hypothesis of major earthquakes). That moves us to consider in priority organisations for which setting up of fully automatic or semi-automatic actions is conceivable. In addition, and as suggested by the survey realized in the frame of the TriNet project dealing with the setting up of a EWS in California, it seems to be possible to associate the education sector (Riopelle et al., 2001 a and b). Indeed, contrary to general public, educational environment is generally easily sensitizable and then in position to answer to a warning, should it be "early", relatively quickly in an

appropriate way. Then, putting student in security position under their tables could, by means of regular exercises, take only few seconds as it is the case in Japan.

List of French Pyrenean stakes that could use seismic early warnings

On the basis of actions that could be taken in response to early warnings presented on chapter 9.1, we propose the following list of French Pyrenean stakes that seem to be identified as potential end-users of a EWS:

- **High-stake facilities**
 - Oil and gas pipelines;
 - ICPE (French classification that qualifies industrial facilities that present a risk for environment) and SEVESO facilities (European guideline that qualifies industrial facilities that present risk of major accidents).
- **Others**
 - High-speed rail networks ;
 - Highways ;
 - Airports ;
 - Hospitals (in particular those who dispose of surgery units).
- **Restricted public alerts**

In hypothesis of major earthquake occurring in well monitored area, it is possible that the lead time would be enough in some remote areas to envisage alerts that could be followed by non-automatic measures such as voluntary self-protection behaviours.

- **Legal beneficiaries**

In complement of the list of potential end-users of a Pyrenean EWS proposed here before in the basis of a presumed need, one should also identify potential addressees of early warnings having not necessary the possibility to use it in few seconds, but who may be considered as “legal beneficiaries” and/or who may take advantage of the knowledge of the early warning. These legal beneficiaries could be:

- Emergency centres such as SDIS;
- Civil protection at its several levels of management: ministerial level (SIDPC), zonal and departmental levels (COZ and COD), and possibly national level (DGSC and COGIC);

- Prefectures;
- Local administrations such as municipalities.

Survey's addressees

Rather than conducting our inquiry in an “open” way addressing to the whole of potential end-users previously identified, we favour to focalize on actors still well accustomed to crisis management and to the taking of preventive measures (often automatic or semi-automatic actions), represented by the industrial world and the managers of critical networks. Indeed, these actors are likely to be seeker of seismic early warnings and the most apt to act in consequence. In addition, it is important to notice that the operational declension of a EWS is generally mainly conditioned by criticality of exposed elements. Lastly, this choice has also been motivated by the will to do not risk arousing a large need until now inexistent and for what we are not sure to be able to answer.

As a result, our survey focalizes on a limited number of industrials and managers of critical networks and dams. Selection of targeted industrials and dams managers was done with the help of concerned French regional directions in charge of environment (DREAL), considering in priority facilities at risks (SEVESO facilities and biggest dam sites). In addition, list of addressees elaborated with the help of DREALs has been completed by BRGM with administrators of electric, gas and high-speed train networks.

Given the limited number of identified addressees (around fifty), it has been favoured to mailed-questionnaires a survey based on telephonic interviews.

Searched information

In order to answer to the objective of the enquiry, interviews have to be able to identify companies established in Pyrenees which could be interested in use of a EWS, actions that these potential end-users could put in place in response to early warnings, as well as the limits of their use of the system.

We draw up herein a list of information to collect, with in some cases the way in which we want to deal with:

- Characteristics of targeted entities / Organization type:
 - Type of company / site (SEVESO or ICPE sites);
 - Type of activity (petrochemical industry, hydrocarbon storage, transportation activities, etc.).
- Positioning in relation to seismic risk:
 - Knowledge (qualitative);

- Perception (qualitative);
- Experience in taking into account for seismic risk (qualitative).
- Expectations in terms of seismic early warning:
 - Lead times (quantitative);
 - Reliability (false alerts / missed alerts) – (qualitative);
 - Sensitisation to principle of EWS (quantitative);
 - In case of absence of need of EWS, possible alternative needs (qualitative).
- Possible use of seismic early warning:
 - Conceivable measures (quantitative/qualitative);
 - Barriers to application of these measures (qualitative);
 - Expected gain of these measures (qualitative).
- Toward a potential Pyrenean EWS:
 - Interest in participating in a potential pilot study.

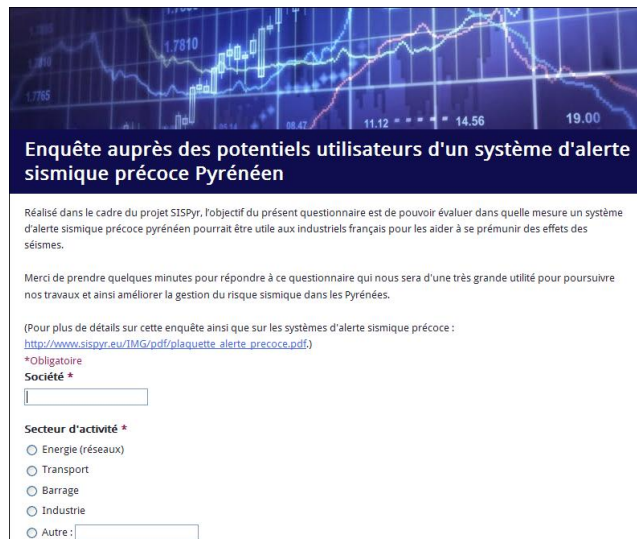
In order to avoid pitfalls met by the survey performed in the frame of the TriNet project (too-long questionnaire, irksome questions sometimes perceived as market research, etc.), some questions will be voluntary disregarded as for example questions dealing with the willingness to pay for a EWS.

In addition, interview should insist on the fact that the hypothesis of a Pyrenean EWS is not purely theoretical, and that on the contrary it lies on a study of technical feasibility and on an existing seismic network.

9.2.3. Questionnaire

It is important to notice that interviews must be done in such a way that collected information be comparable each other. Then it is important to precisely define formulation of questions and to order them in a questionnaire, as well as to have recourse whenever it is possible to “closed” questions which facilitate comparison of results.

Thus a questionnaire (in French) of about twenty questions has been developed and implemented on the *GoogleDocs* online platform in order to facilitate its sharing as well as the compilation of results (cf. Figure 68). Translated version of this questionnaire (in English) is shown on Table 26 of Appendix B.



Enquête auprès des potentiels utilisateurs d'un système d'alerte sismique précoce Pyrénéen

Réalisé dans le cadre du projet SISPYR, l'objectif du présent questionnaire est de pouvoir évaluer dans quelle mesure un système d'alerte sismique précoce pyrénéen pourrait être utile aux industriels français pour les aider à se prémunir des effets des séismes.

Merci de prendre quelques minutes pour répondre à ce questionnaire qui nous sera d'une très grande utilité pour poursuivre nos travaux et ainsi améliorer la gestion du risque sismique dans les Pyrénées.

(Pour plus de détails sur cette enquête ainsi que sur les systèmes d'alerte sismique précoce : http://www.sispyr.eu/IMG/pdf/plaquette_alerte_precoce.pdf)

*Obligatoire

Société *

Secteur d'activité *

☐ Energie (réseaux)

☐ Transport

☐ Barrage

☐ Industrie

☐ Autre :

Figure 68 – Screen-shot of the online questionnaire (in French) in which lies the SISPYR EWS survey

9.2.4. Survey teaching aid

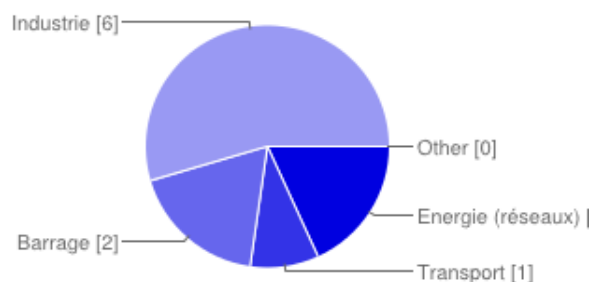
Thematic of seismic risk in general and of EWs in particular being bad known in metropolitan France, it seems to be necessary to make available from participants a teaching aid showing in a simple way main principles of seismic early warning, as well as objectives of works done into the SISPYR project.

Then we developed a brochure dedicated to the module 5 of the SISPYR project that has been sent to each participant to the survey before its interview. This brochure is shown on Appendix C.

9.2.5. Results of the survey

Company

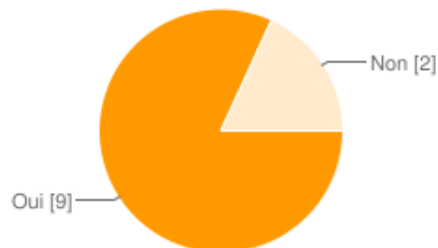
- Line of business**



Line of business	Nb.	Perc.
Energy (network)	2	18%
Transportation	1	9%
Dam	2	18%
Industry	6	55%

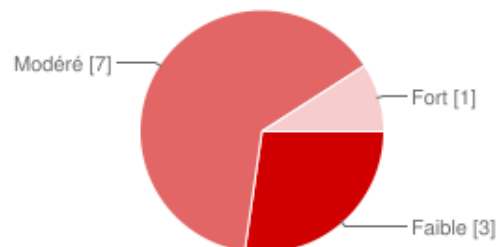
Perception of seismic risk

- 1) Do you feel concern by seismic risk?



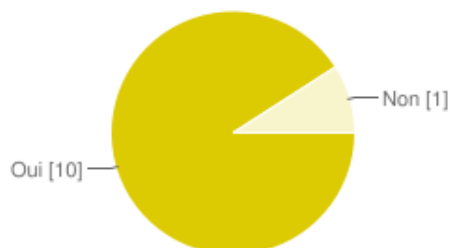
Answ.	Nb.	Perc.
Yes	9	82%
No	2	18%

- 2) How do you estimate the level of seismic hazard in your region?



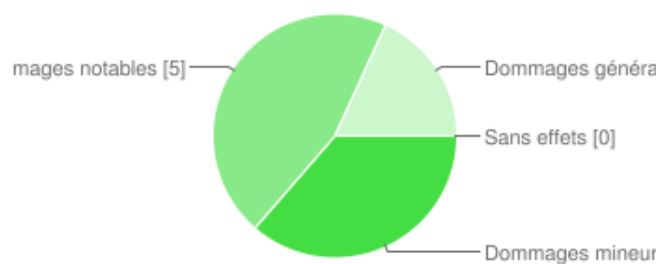
Answ.	Nb.	Perc.
Low	3	27%
Moderate	7	64%
High	1	9%

- 3) Do you think that your installations are exposed to seismic risk?



Answ.	Nb.	Perc.
Yes	10	91%
No	1	9%

- 4) In your opinion, what could be maximal consequences of a major regional earthquake on your installations?



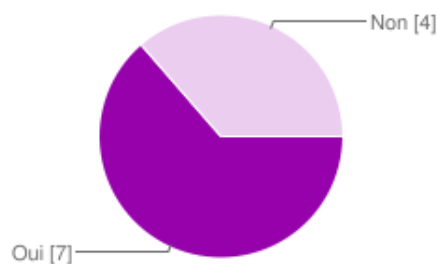
Answ.	Nb.	Perc.
Without effects	0	0%
Minor damages	4	36%
Notable damages	5	45%
Generalised damages	2	18%

- **4') What kind of consequences do you expect?**

- Energy (networks): damaging of building rather than networks themselves, risk of over-accidents threatening security of peoples and possessions, financial consequences, etc.;
- Transportation: train derailment;
- Dam: cracking of concrete elements, deformation of talus, gate breaking, and even whole dam breaking;
- Industry: building and installations (pipes) structural and non-structural damages, roof collapsing, problems with the anchorage of equipment, risk of tank break-down and massive spreading of chemicals, etc.

Management of seismic risk

- **5) Are security measures envisaged in your installations in case of strong earthquake?**

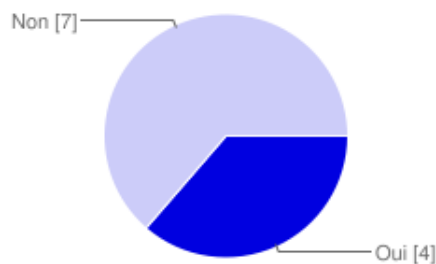


Answ.	Nb.	Perc.
Yes	7	64%
No	4	36%

- **5') If yes, what kind of measure?**

- Follow-up inspection of installations and test of security organs:
 - in case of exceedance of an acceleration threshold (threshold of 0.025g for some industrial facilities).
 - in case of exceedance of a magnitude threshold according to LDG alerts.
- Targeted emergency semi-automatic stopping of industrial critical processes (chemistry and petrochemical activities): ex. stopping of chemical reactions in order to reduce pressure and temperature of installations;

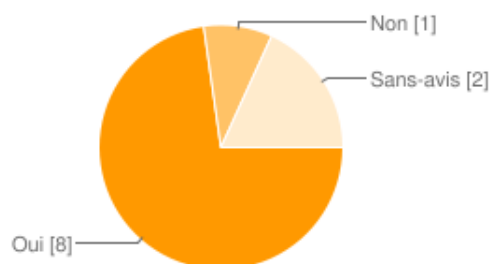
- Closing of energy-networks in order to isolate its critical portions;
- Etc.
- **6) Before being solicited to participate to this study, have you ever heard about principle of seismic early warning?**



Answ.	Nb.	Perc.
Yes	4	36%
No	7	64%

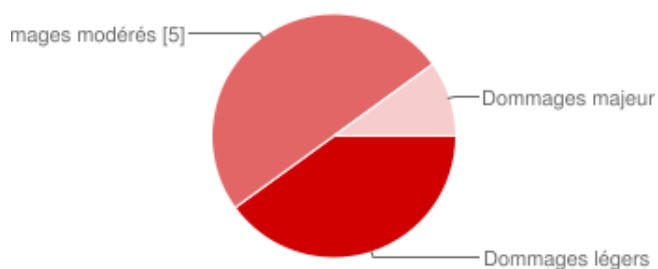
Perception of potential EWS usefulness

- **7) Does an early warning announcing coming destructive strong motions seem to you useful for your company?**



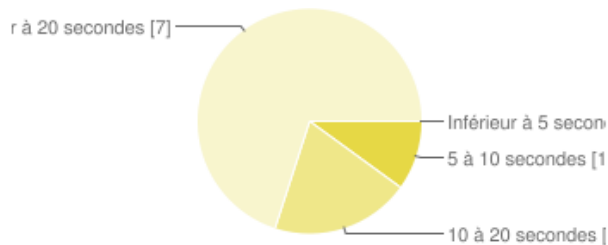
Answ.	Nb.	Perc.
Yes	8	73%
No	1	9%
Without opinion	2	18%

- **7') If yes, from what level of expected effects do you need to be alerted?**



Answ.	Nb.	Perc.
Slight damages	4	36%
Moderate damages	5	45%
Major damages	1	9%

- **8) Could you precise minimum lead time that you think to be enough to take automatic actions to put in security your installations?**



Answ.	Nb.	Perc.
Lower than 5s	0	0%
5 to 10 s	1	9%
10 to 20 s	2	18%
More than 20 s	7	64%

- **9) What kind of action does seem to you conceivable for your installations with a lead time of 5 seconds?**

Only chemical industry seems to be able to take preventive actions with a lead-time of 5 seconds: they will mainly consist in stopping critical chemical reactions by introduction of security bars, and stopping circulation of chemicals fluids.

- **9') With a lead time of 10 seconds?**

With 10 seconds of lead-time, additional actions are proposed by Pyrenean industrials:

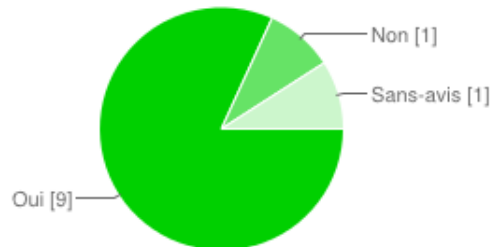
- Dam: isolating of upstream water by mean of automatic closing of front gates, and stopping of production sets (semi-automatic actions);
- Petrochemical industry and gas storage: depressurization of (surface) installations and closing of wells.

- **9'') With a longer lead time (specify that lead time)?**

According to industrials, many other preventive actions are conceivable from lead times of around 20 seconds:

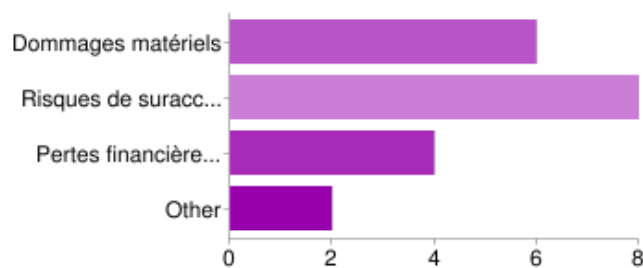
- Energy (networks): semi-automatic targeted local closing of networks;
- Transportation: warning of the traffic control centre in order to get under way semi-automatic stop of high-speed trains;
- Industry: closure of valves, and warning of the staff in order to move away from critical installations/processes.

- 10) In your opinion, could consequences of strong earthquake be reduced thanks to the use of a EWS?



Answ.	Nb.	Perc.
Yes	9	82%
No	1	9%
Without opinion	1	9%

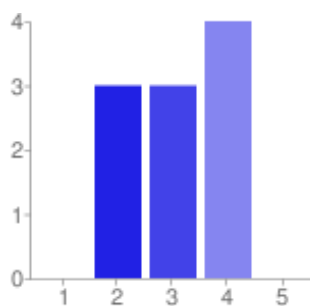
- 10') If yes, for what kind of consequences?



Answ.	Nb.	Perc.
Material damages	6	60%
Risk of over accident	8	80%
Financial loss (due to activity stop, loss of data, etc.)	4	40%
Other	2	20%

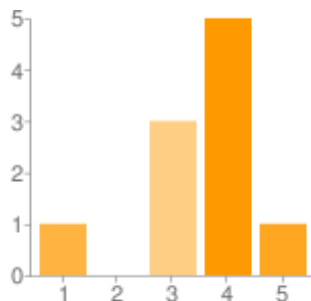
Demands on EWS reliability

- 11) If your company adhered to a EWS, at which point would it be important to notice a reduction of consequences in case of earthquake?



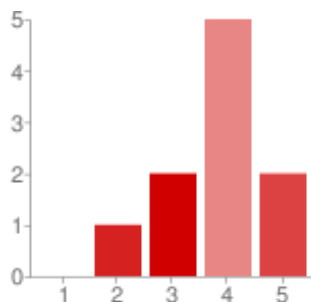
Answ.	Nb.	Perc.
1	0	0%
2	3	27%
3	3	27%
4	4	36%
5	0	0%

- 12) In your opinion, what would be the impact of a false alert for your company?



1	2	3	4	5
Answ.				
No Impact				
↓				
Major impact				
Nb.		Perc.		
1		9%		
0		0%		
3		27%		
5		45%		
1		9%		

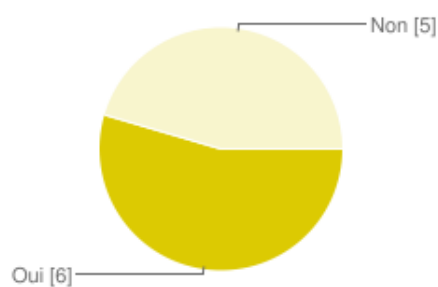
- 13) In your opinion, what would be the impact of a missed alert for your company?



1	2	3	4	5
Answ.				
No Impact				
↓				
Major impact				
Nb.		Perc.		
0		0%		
1		9%		
2		18%		
5		45%		
2		18%		

Toward a potential Pyrenean EWS

- 14) Would your company be interested in participate in a potential coming pilot study?



1	2	3
Answ.		
Yes		
No		
Nb.		Perc.
6		55%
5		45%

- 15) Free comments

Among industrials' free comments, some are particularly interesting insofar as they allow to precise existing needs about seismic risk managing tools, linked to early warning or not:

- Industrial are globally favourable to principle of EWS, but some of them underline that they could involve themselves in such a system only if other industrials expressed their own interest on the system;
- Whatever be the kind of alerts (early-warning alerts, rapid-response alerts, etc.), industrial insist on the fact that – contrary to LDG alerts – they should be personalised for each recipient (for example with an estimation of intensity/damages/PGA/etc. at the site);
- Even if a EWS seems to be potentially useful for Pyrenean industrials, other kind of tools could efficiently help them on the management of seismic risk, such as rapid-response-systems (RSS) as the one developed in the frame of the ISARD Interreg project.

9.2.6. Discussion

Participants

Even though one can think that they are not numerous (11), participants to this enquiry cover an important part of “industrial” (in the broad sense of the word) stakes identified on paragraph 9.2.2. Then, main managers of energy-networks (electricity and gas) have answered to the enquiry, as well as main regional actors of high-speed railway transport. Moreover, the two participants intervening on field of dam security constituted the two main managers of dams in the French Pyrenean area, representing together nearly 40 dams. Otherwise, because of their low participation to the enquiry, real industrial actors are those who are comparatively the less well represented since theirs six participants represent only 20% of targeted industrials.

In addition, it has to be pointed out that most of participants are in charge of security of targeted sites/facilities.

Perception of seismic risk

It is very interesting to notice that participant to the enquiry seem to have a good perception of Pyrenean seismic risk. That conclusion comes from the joint analysis of answers to questions 1 to 4 that shows in a first-hand strong coherence ones according to others (from determination of seismic risk to estimation of potential damages), and in a second hand a good agreement with both French seismic hazard zonation and effects of historical regional earthquakes. This is important because having a good knowledge of their installations, the fact that they are also well sensitized to seismic risk let us think that their answers are fully representative and thus can help to estimate if a EWS could be useful for them.

Perception of EWS principle

It has been somehow surprising to note such a favourable welcome of the idea to endow Pyrenees with a EWS. Thus, only one participant thinks that a EWS would be of no help for its company. Indeed, even though in most of cases many conceivable preventive actions are likely to need more time than the available lead-times (time necessary for automatic or semi-automatic actions is generally greater than 20 seconds, while 20 seconds roughly corresponds to probable greater lead time - cf. paragraph 3.3), industrials tend to want to be early warned of the occurrence of earthquakes in order to initiate security actions as soon as possible. Indeed, even if these actions are fully efficient only some seconds before arrival of destructive strong motions, they can drastically reduce the risk of over-accident as well as minimize economic losses. That reduction of consequences thanks to the use of a EWS is expected by most of participants (cf. question 10) but does not constitute a necessary condition to this use, since the early warning seems to be perceived as a precious information in itself.

Potential use of a Pyrenean EWS

Envisaged actions mentioned by participants are in majority fully pertinent and seem to be in position to reduce to some extent consequences of strong earthquakes as previously discussed. Nevertheless, realization of telephonic interviews has allowed realizing that generally speaking, participants are inclined to systematically disregard fully automatic-actions because they are not used of it. Indeed, except in the case of seismic early warning, available times to take preventive actions are generally long enough to consider non-automatic actions or semi-automatic actions which are preferred to automatic actions since specific human decisions are considered as more adapted than predefined thresholds. Nevertheless, discussing with each of these participants let us think that additional automatic actions (currently non-existing) could be conceivable by means of a shared stage of reflexion requiring their accompaniment by specialists of early warning.

EWS reliability

Another aspect that can be pointed out from this survey is that – not surprisingly – potential end-users of a Pyrenean EWS express a relatively strong demand of reliability of the system. Nevertheless a lesson can be learned from questions 12 and 13 that priority is generally given to security since missed alert are judged to be slightly more impacting than false alerts: that observation comes essentially from companies with a line of business identified as “industry”, for which this trend is particularly well marked (for these participants, impact of missed alerts are in average one level higher than the one of false alerts).

Indeed, an uncertainty being inevitably associated to each early warning, EWS end-users have necessarily to define their own level of acceptability: does an addressee of an early-warning prefer to be warned in a secure sense at the risk of taking useless (costly) prevention actions in case of false alert, or does he prefer to be warned in a certainty sense at the risk to miss relevant alerts associated to high uncertainty. It is usually qualitatively considered that the more effects of damages on a stake have a strong impact (socio-economic, environmental, etc.), the lowest acceptability of the situation is, what in terms of early warning is traduced by favouring false alerts rather than missed alerts. It is then not surprising that so-called “industrial” be notably in the way of security as they are all classified as “SEVESO” sites, which in France are associated with a very low society-acceptance of risk.

This requirement of reliability of early warnings implies the necessity for a potential EWS to qualify the reliability of each alert, for example by means of conditional probabilities of exceedance of PGA threshold values as it is done in PSHA (probabilistic seismic hazard assessments). That kind of approach is currently done by EWS through Bayesian approaches.

Additional needs

As previously shown on question 15 (cf. paragraph 9.2.5), EWS does not constitute the only way to answer to the needs of Pyrenean industrials, and it seems that a RSS such as the one of ISARD would be very helpful.

10. Conclusion

Thanks to improvements realized through the SISPyR project on the seismic monitoring of Pyrenees that allows pooling of real-time seismic data, it is now possible to test the feasibility of an EWS covering the Massif in order to emit early warnings few seconds before destructive seismic waves in case of major earthquake in Pyrenees like the 1967 Arette event.

Even though regional EWS usually rely on dedicated seismic networks, an analysis of the SISPyR real-time network shows that the existing stations may be used for early warning purposes. However, operational setting up of this type of innovative tool in Pyrenees technically faces to important barriers due to 1) the moderate seismicity context of Pyrenees implicating strong attenuation of destruction effects with distance that implies that the EWS should be effective at short epicentral distances, and to 2) the current limited coverage of the real-time network as well as to the time-latency of the existing system. Consequently, a possible approach to bypass these issues would be to consider a “hybrid” system that would initially conduct an “onsite” analysis (from a single station) and then make the warning gradually more substantive by means of a regional approach (using several stations). In addition, network improvements would be necessary in order to make it safer, for example implementing redundant systems.

The exploration of an important set of Pyrenean seismic data gathered in the frame of the SISPyR project has also shown that the main real-time magnitude assessment methodologies dedicated to EWS are fully adapted to the Pyrenean context. Thus, it has been possible to establish some reference relations linking empirically different proxy parameters calculated in real-time (so called τ_c , τ_p^{max} , P_d and P_v parameters) to magnitude. Unfortunately, these empirical relations remain limited by their range of validity, which is restricted with respect to magnitude as a consequence of the instrumental data available in Pyrenees. Consequently, even though they exhibit interesting results for moderate events such as the one of Bigorre of 1st April 2010, they cannot be used as is in case of strong earthquakes as they should. Indeed, while it is important to be able to distinguish in real time between small earthquakes and more powerful ones and, to this effect, have access to relations that are valid for small events, the principle of early warning is only pertinent for large, potentially damaging, magnitudes. As to the Pyrenean massif, the seismotectonic context thus raises the possibility of major earthquakes with magnitudes that could reach 6.5. Accordingly, we need to look into a way to extend the range of validity in magnitude of the relations established earlier.

One solution would be to use empirical relations already published that are based on worldwide data after having checked that they are consistent with Pyrenean data. Such a comparison has been undertaken and suggests that this option should be considered using relations such as those defined by Zollo and others (2010) and linking τ_c with magnitude. Indeed, while specific filtering parameters allow to minimize scattering of Pyrenean data and thus to establish dedicated but limited empirical relations, a test performed with a smaller high-pass cut-off frequency value of 0.3 Hz allows to show that an extension of the Zollo and others' relation is possible for Pyrenees, but implies a greater scattering. One other solution would be to establish broader relations dedicated to Pyrenees based on a synthetic waveform catalogue. Nevertheless, this option is not an easy way as high-frequencies strong-motions simulation is still a difficult scientific challenge.

In the other hand, a very important issue on the evaluation of the feasibility of an EWS in Pyrenees deals with the question of the end-users in order to assess if such a system could answer to an existing need or not. In particular, the question of "How usefully use an early warning for earthquakes associated to high return periods?" is preponderant and strongly linked to the potential end-users' seismic hazard perception. This aspect has been studied through the carrying-out of a survey bound to Pyrenean potential end-users in order to evaluate their wishes in terms of earthquake early warning. Results of this survey show a very favourable and enthusiast welcome of the principle of EWS by the Pyrenean industrials, which seem to be likely to have use of early-warning even in case of moderate earthquakes. This survey also reminds us that for potential end-users such a system could be useful on condition that it provides reliable warnings associated to long enough warning-times.

11. Acknowledgements

Many thanks to Maria Lancieri (IRSN) for its very interesting comments that greatly helped us during this study, as well as for its nice welcome of a SISPy's student.

Thanks to Prof. Richard Allen (Berkeley University) who took time to answer to our question about calculation of τ_p^{max} .

And a special thank you to Julie Baron who have spent her engineering training-course working on the technical feasibility of a Pyrenean EWS.

12. Bibliography

- Allen R.M., H. Kanamori** (2003). The potential for earthquake early warning in southern California. *Science* 300, 786–789.
- Allen R.M.** (2007). The ElarmS Earthquake Early Warning Methodology and Application across California. In *Earthquake Early Warning Systems*, ed. P. Gasparini et al., 21-41. Berlin: Springer.
- Allen R.M., P. Gasparini, O. Kamigaichi, M. Böse** (2009). The Status of Earthquake Early Warning around the World: An Introductory Overview ; *Seismological Research Letters* .vol 80(5).
- Auclair S., Bertil D.** (2009). Systèmes d'alerte sismique : principes et faisabilité aux Antilles françaises. Rapport final. BRGM/RP-56663-FR, 87 p., 37 fig., 3 tabl., 1 ann.
- Bakun W.H., Scotti O.** (2006). Regional intensity attenuation models for France and the estimation of magnitude and location of historical earthquakes. *Geophys. J. Int.* 164, 596-610.
- Böse M.** (2006). Earthquake Early Warning for Istanbul using Artificial Neural Network. Thesis.
- Böse M., F.Wenzel, M. Erdik** (2008). PreSEIS: a neural network based approach to earthquake early warning for finite faults, *Bull. Seismol. Soc. Am.* 98, no. 1, 366–382.
- Böse M., E. Hauksson, K. Solanki, H. Kanamori, T. H. Heaton** (2009). Real-time testing of the on-site warning algorithm in southern California and its performance during the July 29, 2008 Mw 5.4 Chino Hills earthquake. *Geophysical Research Letters* 36, L00B03.
- Cua G.** (2005). Creating the Virtual Seismologist: Developments in Ground Motion Characterization and Seismic Early Warning. Ph. D. Thesis: California Institute of Technology.
- Cua G., T. Heaton** (2007). The Virtual Seismologist (VS) method: A Bayesian approach to earthquake early warning. In *Earthquake Early Warning Systems*, ed. P. Gasparini, G. Manfredi, and J. Zschau, 97–132. Berlin and Heidelberg: Springer.
- Drouet S., Chevrot, S., Cotton, F., Souriau, A.** (2008). Simultaneous inversion of source spectra, attenuation parameters, and site responses: application to the data of the French accelerometric network. *Bull. seism. Soc. Am.*, 98(1).
- Glangaud J.L., F. Coppens** (1997). Traitement du signal pour géologues et géophysiciens. Ed. Technip.
- Hsiao N.-C., Y.-M. Wu, L. Zhao, D.-Y. Chen, W.-T. Huang, K.-H. Kuo, T.-C. Shin, P.-L. Leu** (2010) - A new prototype system for earthquake early warning in Taiwan. *Soil Dyn Earthquake Eng.*

- Hsiao N.-C., Y.-M. Wu, T.-C. Shin, L. Zhao, T.-L. Teng** (2009). Development of earthquake early warning system in Taiwan. *Geophysical Research Letters* 36, L00B02.
- Jara J.A.** (2010). Earthquake Early Warning System (EWS) - Short note about: "SISPyR Seismic Network applicability as a EWS", GEOCAT.
- Kamigaichi O.** (2004). JMA earthquake early warning. *Journal of the Japan Association for Earthquake Engineering* 4, 134–137.
- Kanamori H.** (2005). Real-time seismology and earthquake damage mitigation. *Annual Review of Earth and Planetary Sciences* 33, 195–214.
- Lancieri M., and A. Zollo** (2008). A Bayesian approach to the realtime estimation of magnitude from the early P and S wave displacement peaks. *Journal of Geophysical Research* 113, B12302.
- Lockman A., R.M. Allen** (2007). Magnitude-period scaling relations for Japan and the Pacific Northwest: Implications for earthquake early warning. *Bulletin of the Seismological Society of America*, 97, 140–150.
- Murphy, S., and S. Nielsen** (2009). Estimating earthquake magnitude with early arrivals: A test using dynamic and kinematic models. *Bulletin of the Seismological Society of America*, 99, 1–23.
- Nakamura, Y.** (1989). Earthquake alarm system for Japan railways, *Jpn. Railway Eng.*, 28(4), 3–7.
- Nakamura Y.** (1988). On the urgent earthquake detection and alarm system (UrEDAS). Presented at Ninth World Conf. Earthq. Eng., Tokyo.
- Nigg J.M.** 1995. Risk communication and warning systems. In Hortlick-Jones T., A. Amendola and R. Casale (eds.). *Naturale Risk and Civil Protection*. London : E & FN Spon. Pp. 369-382.
- Odaka T., K. Ashiya, S. Tsukada, S. Sato, K. Ohtake, D. Nozaka** (2003). A new method of quickly estimating epicentral distance and magnitude from a single seismic record. *Bulletin of the Seismological Society of America* 93, 526–532.
- Olivera C., E. Redondo, J. Lambert, A. Riera Melis and A. Roca** (2006). Els terratrèmols dels segles XIV i XV a Catalunya, Institut Cartogràfic de Catalunya.
- Olivieri M., R. M. Allen, G. Wurman** (2008). The Potential for Earthquake Early Warning in Italy Using ElarmS. *Bulletin of the Seismological Society of America*, vol. 98, No. 1.
- Olivieri M., J. Schweitzer** (2007). An empirical procedure for rapid magnitude estimate in Italy, *Bull. Seismol. Soc. Am.*,
- Olson E. L. R. M. Allen** (2005). The deterministic nature of earthquake rupture. *Nature* 438, 212-215.

- Riopelle D.R., Bourque L.B., Shoaf K.I.** (2001a). "Survey of Potential Early Warning System Users." (Task 1 Report for the TriNet Policy Studies and Planning Activities in Real-Time Earthquake Early Warning). University of California, Los Angeles, Center for Public Health and Disaster Relief.
- Riopelle D.R., Flores P.F., Shoaf K.I., Seligson H.A.** (2001b). "TriNet Studies & Planning Activities in Real-Time Earthquake Early Warning, Task 3 Report, ABS Consulting, Center for Advanced Planning and Research.
- Shieh J.T., Wu Y.M., Allen R.M.** (2008). A comparison of t_c and t_{pmax} for magnitude estimation in earthquake early warning, *Geophys. Res. Lett.*, 35, L20301.
- Simons F.J., B.D.E. Dando, R.M. Allen** (2006). Automatic detection and rapid determination of earthquake magnitude by wavelet multiscale analysis of the primary arrival. *Earth and Planetary Science Letters*, 250, 214–223.
- Sokolov V., F. Wenzel, T. Fururama** (2009). On estimation of earthquake magnitudes in Earthquake Early Warning systems. *Earth Planets Space*, 61 1275-1285.
- Souriau A. H. Pauchet** (1998). A new synthesis of Pyrenean seismicity and its tectonic implications. *Tectonophysics*, 290, 221-244.
- Sponheuer, W.** (1960). Methoden zur Herdtiefenbestimmung in der Makroseismik, Freib. Forschungsh. C88, 117 pp.
- Suárez, G., D. Novelo, and E. Mansilla** (2009). Performance evaluation of the seismic alert system (SAS) in Mexico City: A seismological and a social perspective. *Seism. Res. Lett.* 80 (5), 707–714.
- Susagna T., Roca A., Goula X., Batlló, J.** (1994). Analysis of macroseismic and instrumental data for the study of the November 19, 19-23 earthquake in the Aran Valley (Central Pyrenees). *Natural Hazard* vol.10, 7-17.
- Weber E., G. Iannaccone, A. Zollo, A. Bobbio, L. Cantore, M. Corciulo, V. Convertito, M. Di Crosta, L. Elia, A. Emolo, C. Martino, A. Romeo, C. Satriano** (2007). Development and testing of an advanced monitoring infrastructure (ISNET) for seismic early warning applications in the Campania region of southern Italy. In *Earthquake Early Warning Systems*, ed. P. Gasparini, G. Manfredi, and J. Zschau, 325–341. Berlin and Heidelberg: Springer.
- Wieland M.** (2001). Earthquake Alarm, Rapid Response and Early Warning Systems: Low Cost Systems for Seismic Risk Reduction. International Workshop on Disaster Reduction. Reston, VA. August 19-22, 2001.
- Wieland M., Griesser L., Kuendig C.** (2000). Seismic Early Warning System for a Nuclear Power Plant. Proc. 12th World Conf. on Earthquake Engineering, Auckland, New Zealand, Jan. 31-Feb. 4, 2000.

- Wu Y.-M., H. Kanamori** (2005b). Rapid assessment of damage potential of earthquakes in Taiwan from the beginning of P waves. *Bulletin of the Seismological Society of America* 95, 1,181–1,185.
- Wu Y.-M., H. Kanamori** (2008). Development of an Earthquake Early Warning System Using Real-Time Strong Motion Signals. *Sensors* 8, 1–9. ISSN 1424-8220
- Wu Y.-M., T.-L. Teng** (2002). A virtual subnetwork approach to earthquake early warning. *Bulletin of the Seismological Society of America* 92, 2,008–2,018.
- Wu Y.-M., H. Kanamori, R. M. Allen, E. Hauksson** (2007). Determination of earthquake early warning parameters, Tc and Pd, for southern California. *Geophys. J. Int.*
- Wu Y.-M., L. Zhao** (2006). Magnitude estimation using the first three seconds P-wave amplitude in earthquake early warning, *Geophys. Res. Lett.*, 33, L16312.
- Wurman G., R. M. Allen, P. Lombard** (2007). Toward earthquake early warning in northern California. *Journal of Geophysical Research* 112.
- Zollo A., M. Lancieri, S. Nielsen** (2006). Earthquake magnitude estimation from peak amplitudes of very early seismic signals on strong motion records. *Geophysical Research Letters* 33, L23312.
- Zollo A., M. Lancieri, S. Nielsen** (2007). Reply to comment by P.Rydelek et al. on "Earthquake magnitude estimation from peak amplitudes of very early seismic signals on strong motion records". *Geophysical Research Letters* L20303.
- Zollo A., O. Amoroso, M. Lancieri, Y.-M. Wu, H. Kanamori** (2010). A threshold-based earthquake early warning using dense accelerometer networks. *Geophys. J. Int.*, 183, 963–974.

APPENDIX A

CONSTITUTION OF THE WAVEFORM CATALOGUE

Id	Day	Month	Year	M_ILDG	M_IIGN	Number of records
1	4	6	2001	3.6	3.2	8
2	1	8	2001	3.7	3.3	8
3	7	10	2001	3.2	3	10
4	12	12	2001	3.3	2.8	8
5	14	12	2001	3.5	3.1	9
6	16	5	2002	4.4	3.7	22
7	16	5	2002	4.8	4.2	19
8	19	5	2002	3.8	3.1	23
9	11	6	2002	3.3	2.7	6
10	13	6	2002	3.5	3.4	15
11	21	6	2002	4.1	3.4	19
12	8	7	2002	3.3	2.7	11
13	16	7	2002	3.1	2.5	5
14	16	7	2002	3.2	2.8	8
15	21	8	2002	3.2	3	7
16	5	9	2002	4.1	3.8	15
17	28	11	2002	3.3	2.7	10
18	9	12	2002	3.7	3.1	13
19	11	12	2002	4.3	3.6	12
20	12	12	2002	4.7	4	18
21	13	12	2002	3.3	3.1	12
22	21	1	2003	4.6	4	20
23	26	2	2003	4.4	3.8	25
24	10	3	2003	3.1	3	15
25	18	4	2003	3.6	3	14
26	27	6	2003	3.3	2.7	9
27	2	7	2003	3.3	2.7	14
28	7	7	2003	3	2.4	5
29	30	8	2003	3.4	2.8	13
30	30	9	2003	3.4	2.9	16
31	3	10	2003	3.5	3	24
32	26	10	2003	3	2.4	10
33	31	10	2003	3.4	3.1	5
34	9	1	2004	3.2	2.7	17
35	12	1	2004	3	2.9	15
36	3	2	2004	3.7	3.2	23
37	1	6	2004	4.2	3.4	15
38	4	6	2004	3.5	3.1	22

Id	Day	Month	Year	M_I LDG	M_I IGN	Number of records
39	4	6	2004	3.4	2.8	9
40	17	6	2004	3.3	2.4	17
41	18	7	2004	3.8	3.2	22
42	15	8	2004	2.8	2.2	12
43	18	9	2004	5.2	4.6	25
44	18	9	2004	3.2	2.6	11
45	21	9	2004	5.1	4.3	30
46	23	9	2004	3.5	2.9	16
47	23	9	2004	4	3.4	20
48	23	9	2004	3.2	2.6	8
49	30	9	2004	4.6	3.9	19
50	3	10	2004	3.2	2.8	16
51	4	10	2004	3.6	3	15
52	7	10	2004	3.9	3.4	15
53	27	11	2004	3.7	3.1	19
54	2	12	2004	3.2	2.6	14
55	5	12	2004	3.2	2.6	13
56	21	12	2004	3.4	2.9	12
57	24	12	2004	3.4	2.7	12
58	15	1	2005	3.6	3.1	26
59	9	2	2005	3.6	3	20
60	15	2	2005	3.3	2.9	21
61	26	2	2005	3.7	3.2	31
62	20	4	2005	3.4	2.6	16
63	15	6	2005	3.5	3.2	16
64	17	6	2005	3.3	2.7	20
65	16	7	2005	3.5	2.7	17
66	23	10	2005	2.9	2.5	16
67	5	11	2005	3.7	3.3	23
68	17	11	2005	3.2	2.5	14
69	27	12	2005	3.8	3.4	26
70	28	1	2006	3.2	2.6	13
71	7	2	2006	3.7	3.2	25
72	21	3	2006	3.3	2.7	13
73	29	3	2006	3.4	3	18
74	4	5	2006	3.3	3	12
75	4	5	2006	3.4	3.4	23
76	8	5	2006	3.6	3.1	17

Id	Day	Month	Year	M_ILDG	M_IIGN	Number of records
77	20	5	2006	3.7	3.1	15
78	20	5	2006	3.7	3.1	10
79	2	6	2006	3.5	2.6	22
80	12	6	2006	3.3	2.6	7
81	3	8	2006	3.3	2.6	5
82	24	10	2006	3.6	2.9	14
83	25	10	2006	3.4	2.8	12
84	4	11	2006	3.8	3.2	14
85	14	11	2006	3.2	2.9	24
86	17	11	2006	5.4	4.5	45
87	18	11	2006	3.6	2.9	14
88	18	11	2006	3.3	2.7	14
89	19	11	2006	3.5	2.9	9
90	19	11	2006	3.5	2.9	6
91	19	11	2006	3.2	2.6	5
92	20	11	2006	3.2	2.7	14
93	2	12	2006	3.3	2.6	4
94	16	12	2006	4.1	3.3	31
95	22	12	2006	3.5	2.8	12
96	13	1	2007	2.9	2.3	26
97	16	2	2007	3.9	3	24
98	28	3	2007	3.5	3.1	29
99	9	4	2007	3.4	2.8	21
100	11	4	2007	3.3	2.9	8
101	3	5	2007	3.2	2.5	28
102	22	6	2007	3.1	2.9	30
103	13	7	2007	3.8	3	32
104	8	8	2007	4.1	3.5	34
105	11	9	2007	3.6	2.8	31
106	19	9	2007	3.2	2.6	21
107	11	10	2007	3.7	3.1	26
108	15	10	2007	3.3	2.8	25
109	15	11	2007	4.5	3.8	35
110	22	11	2007	3.2	2.3	10
111	24	11	2007	3.7	3.2	30
112	19	1	2008	3.2	2.6	20
113	15	2	2008	3.8	3.2	31
114	22	2	2008	3.1	2.4	23

Id	Day	Month	Year	M_I LDG	M_I IGN	Number of records
115	3	5	2008	4.1	4	27
116	18	5	2008	4.6	3.9	32
117	26	5	2008	3.2	2.6	1
118	22	6	2008	3.7	3.1	25
119	25	6	2008	3.5	2.8	24
120	16	7	2008	4.4	3.6	31
121	21	7	2008	3.4	2.8	22
122	23	7	2008	2.9	2.3	19
123	23	7	2008	3	2.4	19
124	25	7	2008	3.2	2.7	13
125	27	8	2008	3.2	2.6	17
126	16	9	2008	3.1	2.8	8
127	18	9	2008	3.9	3.3	24
128	28	9	2008	3.1	2.4	16
129	12	10	2008	3	2.7	9
130	12	3	2002	3	2.4	1
131	18	3	2002	4.1	3.3	1
132	23	4	2002	2.9	2.3	2
133	2	5	2002	3	2.4	1
134	20	5	2002	2.6	2	1
135	7	11	2002	3.4	3	1
136	10	11	2002	3.9	3.4	2
137	16	12	2002	3.3	2.7	3
138	4	4	2003	3.2	2.6	1
139	27	8	2003	3	2.4	2
140	13	10	2003	4	3.3	2
141	13	1	2004	3.8	3.1	2
142	16	1	2004	3.2	2.6	4
143	22	7	2004	3	2.6	4
144	16	9	2004	3.7	3.2	2
145	17	9	2004	3.5	3	2
146	18	9	2004	3.5	3.1	3
147	21	9	2004	3	2.4	5
148	20	10	2004	3.7	2.7	2
149	24	3	2006	3.5	2.9	5
150	25	7	2006	2.9	2.3	3
151	4	9	2006	2.9	2.6	2
152	7	10	2006	3.5	2.4	3

Id	Day	Month	Year	M_ILDG	M_IIGN	Number of records
153	2	4	2007	3.5	3	2
154	19	4	2007			1
155	7	7	2007	3.1	2.5	2
156	7	7	2007	3.2	2.7	2
157	29	8	2007	3.8	3.1	2
158	6	2	2008	2.6	2.1	3
159	13	4	2008	2.7	2.2	2
160	20	4	2008	2.6	2	2
161	16	5	2008	2.7	1.5	5
162	18	5	2008	3.3	2.8	5
163	30	6	2008	2.6	2	1
164	19	7	2008	2.7	1.8	1
165	22	7	2008	0	-0.6	4
166	4	1	2009	3	2.7	1
167	21	1	2009	3.3	2.9	1
168	5	2	2009	2.7	1.9	2
169	9	2	2009	4.3	3.6	4
170	12	2	2009	2.5	2	1
171	21	2	2009	2.6	2.1	2
172	28	2	2009	3	2.7	5
173	8	3	2009	2.9	2.3	1
174	23	3	2009	3	2.6	4
175	1	4	2009	2.8	2.4	5
176	5	4	2009	3	2.5	2
177	10	4	2009	2.9	2.6	2
178	3	5	2009	2.5	1.8	1
179	5	5	2009	2.7	2.4	3
180	17	5	2009	2.6	1.9	1
181	11	6	2009	3.2	2.6	4
182	19	6	2009	2.9	2.4	2
183	20	6	2009	2.8	2.2	3
184	27	6	2009	2.8	2.7	4
185	30	6	2009	2.9	2.4	3
186	5	8	2009	2.6	2.3	2
187	6	8	2009	3.4	2.8	3
188	15	9	2009	3.1	2.6	3
189	16	11	2009	3	2.3	1
190	17	11	2009	3.1	2.8	4

Id	Day	Month	Year	M_I LDG	M_I IGN	Number of records
191	18	2	1996	5.6	5	1
192	4	10	1999	5.1	4.2	1
240	1	4	2010	4.3	3.9	37
Total	-	-	-	-	-	2429

Table 25 – List of earthquakes included in the study catalogue.

APPENDIX B

QUESTIONNAIRE OF THE END-USERS SURVEY

Id.	Question	Possible answers	Compulsory answer
-	Company	Free answer	Yes
-	Line of business	Energy / Transportation / Dam / Industry / Other : free answer	Yes
-	Participant's function	Free answer	Yes
1	Do you feel concern by seismic risk?	Yes / No	Yes
2	How do you estimate the level of seismic hazard in your region?	Low / Moderate / High	Yes
3	Do you think that your installations are exposed to seismic risk?	Yes / No	Yes
4	In your opinion, what could be maximal consequences of a major regional earthquake on your installations?	Without effect / Minor damages / Notable damages / Generalised damages	Yes
4'	What kind of consequences do you expect?	Free answer	No
5	Are security measures envisaged in your installations in case of strong earthquake?	Yes / No	Yes
5'	If yes, what kind of measure?	Free answer	No
6	Before being solicited to participate to this study, have you ever heard about principle of seismic early warning?	Yes / No	Yes
7	Does an early warning announcing coming destructive strong motions seem to you useful for your company?	Yes / No / Without opinion	Yes
7'	If yes, from what level of expected effects do you need to be alerted?	Slight damages / Moderate damages / Major damages	No
8	Could you precise minimum lead time that you think to be enough to take automatic actions to put in security your installations?	Lower than 5s / 5 to 10 s / 10 to 20 s / More than 20 s	No
9	What kind of action does seem to you conceivable for your installations with a lead time of 5 seconds?	Free answer	No
9'	With a lead time of 10 seconds?	Free answer	No
9''	With a longer lead time (specify that lead time)?	Free answer	No
10	In your opinion, could consequences of strong earthquake be reduced thanks to the use of a EWS?	Yes / No / Without opinion	Yes
10'	If yes, for what kind of consequences?	Material damages / Risk of over accident / Financial loss (due to activity stop, loss of data, etc.) / Other	No

Id.	Question	Possible answers	Compulsory answer
11	If your company adhered to a EWS, at which point would it be important to notice a reduction of consequences in case of earthquake?	From 1 (not important at all) to 5 (extremely important)	No
12	In your opinion, what would be the impact of a false alert for your company?	From 1 (no impact) to 5 (major impact)	No
13	In your opinion, what would be the impact of a missed alert for your company?	From 1 (no impact) to 5 (major impact)	No
14	Would your company be interested in participate in a potential coming pilot study?	Yes / No	Yes
15	Free comments	Free answer	No

Table 26 – Questions of the questionnaire in which lies the SISPyR EWS survey

APPENDIX C

SURVEY TEACHING AID: BROCHURE



CONTEXTE : LE PROJET SISPYR

Les Pyrénées constituent l'une des régions de France métropolitaine et d'Espagne où l'aléa sismique est le plus important. Ceci a motivé le développement progressif de réseaux de surveillance sismologique du massif pyrénéen. Dans ce contexte, le projet transfrontalier SISPYR (www.sispvr.eu) a pour principal objectif de permettre la mise en commun des données acquises à travers les Pyrénées tout en y favorisant la modernisation des réseaux sismologiques.

SISPYR fait suite au projet ISARD finalisé en mars 2008 et qui avait rencontré l'adhésion des acteurs de la gestion de crise en France et en Catalogne. Ainsi, en Catalogne, la mise en place progressive du programme SISMICAT, protocoles de gestion de crise sismique à l'échelle régionale, intègre d'ores et déjà les résultats du programme ISARD, alors qu'en France une réflexion est menée afin de valoriser les développements du projet ISARD en appui à la gestion de crise sismique.

UNE ENQUETE, POURQUOI ?

Faute de prévision possible des séismes à ce jour, la communauté scientifique a conçu un outil d'analyse en temps-réel des signaux sismiques permettant de fournir une alerte dès les premières secondes suivant un séisme de manière à pouvoir mettre en œuvre des procédures permettant de minimiser les dommages. Cet outil, appelé système d'alerte sismique précoce (ou 'Early Warning System' dans sa dénomination anglo-saxonne), est déjà opérationnel dans certains pays parmi les plus sismiques tels que le Japon ou le Mexique, et est également en phase de test dans des pays à sismicité plus modérée comme en Italie.

Au sein du projet SISPYR, le BRGM coordonne un module consacré à la faisabilité d'un tel système à l'échelle des Pyrénées valorisant le réseau de surveillance sismique existant. L'objectif de cette action est de montrer la faisabilité technique d'un tel outil d'une part, et d'autre part de justifier de son intérêt pour l'amélioration de la gestion de crise dans le contexte pyrénéen.

Il est en effet indispensable de pouvoir évaluer la perception d'un tel outil par les utilisateurs potentiels d'un système d'alerte sismique précoce pyrénéen. Les membres du projet SISPYR ont donc souhaité engager une démarche active de consultation des potentiels utilisateurs afin de comprendre leurs problématiques propres, leurs attentes ainsi que leurs besoins. Pour ce faire, il a été décidé de réaliser une enquête qui sera dans un premier temps menée du côté français de la frontière.

SYSTEME D'ALERTE SISMIQUE PRECOCE : GRANDS PRINCIPES

PRINCIPE

En cas de séisme, les ondes P (« P » comme Premières) – non destructrices – libérées au niveau de la faille, se propagent dans le sol près de 2 fois plus rapidement que les ondes S (« S » comme Secondes) qui sont responsables d'une grande partie des dommages.

Les systèmes d'alerte sismique précoce sont pour la plupart basés sur l'analyse des premières secondes des ondes P enregistrées par quelques stations sismologiques situées à proximité de l'épicentre, puis sur l'émission d'alertes. La diffusion de cette alerte s'effectuant à une vitesse proche de celle de la lumière, il est possible d'informer en quelques secondes des zones non encore atteintes par les ondes S : par conséquent, plus vous êtes éloigné de

Partenaires :



Programme soutenu par :



1



l'épicentre¹ et plus l'intervalle de temps séparant l'arrivée de l'alerte et celle des ondes S est importante, vous laissant ainsi plus de temps pour réagir.



UTILISATION DE L'ALERTE

Afin de mettre à profit l'alerte précoce, il est important de mettre en place des procédures de réponse appropriées. L'exemple du tsunami du 26 décembre 2004 dans l'Océan Indien est ainsi particulièrement explicite quant à l'importance de disposer de mesures adaptées à prendre en cas d'alerte. En effet, bien qu'un système d'alerte précoce de tsunamis était alors opérationnel et avait pu détecter le séisme, une chaîne de prise de décision et de communication de l'information mal adaptée n'a pas permis de réduire l'impact du tsunami. Les utilisateurs doivent donc être placés au cœur de la démarche de l'alerte précoce !

Dans le cas de l'aléa sismique, le temps disponible pour se prémunir d'un séisme une fois que celui-ci a eu lieu est extrêmement court. Ainsi, les systèmes d'alerte précoce sismique ne permettent généralement de disposer que de quelques secondes à quelques dizaines de secondes pour prendre des mesures à même de minimiser les impacts du séisme. En des temps aussi réduits, la prise de décision doit être autant que possible automatisée, alors que dans certains cas, des mesures individuelles peuvent également être prises.

Coupures de systèmes dangereux et de systèmes critiques, arrêt de l'alimentation de trains, fermeture de réseaux énergétiques ou arrêt de systèmes informatiques sensibles et mise en sécurité des données sont autant d'actions efficaces qui peuvent être mise en œuvre automatiquement suite à la réception d'une alerte sismique précoce.



MERCI DE VOTRE PARTICIPATION !

Merci de consacrer quelques minutes de votre temps pour répondre à notre questionnaire d'enquête : cela nous sera d'une grande aide afin d'élaborer les outils dont vous avez besoin pour une meilleure gestion du risque sismique dans les Pyrénées !

[ACCES AU FORMULAIRE D'ENQUETE](#)

Contact : s.auclair@brgm.fr

¹ Epicentre : localisation du séisme en surface

Partenaires :



Programme soutenu par :

